Contributions of Fibronectin and Cells to Elastogenic Protein Expression and Deposition in Tissue-engineered Blood Vessel Constructs and Wound Healing

Joseph Di Paolo

Department of Anatomy and Cell Biology, Faculty of Medicine

McGill University

Montréal, Québec, Canada

August, 2018

A thesis submitted to McGill University in partial fulfillment of the requirements of the degree of Master of Science

TABLE OF CONTENTS

TABLE OF FIGURES

LIST OF TABLES

ACKNOWLEDGEMENTS

First and foremost, I would like to acknowledge my supervisor, Dr. Dieter P. Reinhardt. I am grateful for having been given the opportunity to conduct scientific research in his lab, to learn the many techniques necessary for cell biology research, and for his comments and critiques of my work. I also thank him for giving me the great experience of attending several scientific conferences, where I presented my work and discussed ideas with other scientists in the field.

Next, I would like to thank all current members of the Reinhardt laboratory who were a constant source of friendly conversation and scientific advice. Heena Kumra, a current Ph.D. candidate, introduced me to my projects, taught me all the relevant techniques necessary for me to work on my projects, and helped me deal with issues relating to both research and personal events. Chae Syng Lee, the current lab manager and a former M.Sc. student, kept the lab organized, made sure materials were always stocked and instruments were always functioning, and helped me learn to use some lab equipment. Rongmo Zhang, Muthu Lakshmi, Hana Hakami, and Valentin Nelea, and Ian Costas (of the Rouiller lab) who all were good friends and helped me with useful advice for all aspects of my Master's. I also thank Dr. Maya Ayach (of the Ortega lab) for her invaluable help with the French translations of my abstracts.

I would also like to thank Dr. Daniele Pezzoli for his work on this collaborative project. Without him, I would not have had the necessary materials to do my research, and his help with planning experiments was vital to the progression of the project.

I thank my committee members, Dr. Anie Phillip, Dr. Lisbet Haglund, and Dr. Craig Mandato, for their time during my committee meeting, which greatly helped me and guided my project. I would like to give special thanks to my mentor Dr. Mandato, for always being available to help me with my work and for helping me learn to deal with difficult interpersonal situations.

I would also like to thank my family, who helped me deal with the stresses of pursuing my Master's degree in science with kind conversation, words of encouragement, and delicious meals. I especially thank my father, Libero Antonio Di Paolo, for his advice and invaluable guidance and criticisms which helped me with every aspect of my Master's and personal life. I would also like to thank my father for his help with the French translation of my project abstracts.

Last but not least, I would like to thank McGill University and the Department of Anatomy and Cell Biology for providing me with the opportunity to do research and for providing me with the facilities required to conduct my work. I give special thanks to Joseph Dubé, who helped me through tough times by being a good listener whenever I needed someone to talk to.

CONTRIBUTIONS

I planned and performed all the experiments and data analysis included in this thesis, with the exceptions listed below.

Dr. Dieter Reinhardt, Dr. Daniele Pezzoli, and Heena Kumra guided this project. They contributed in providing ideas for experiments, trouble-shooting, and discussions. Dr. Dieter Reinhardt also developed the methods used for quantification of elastic fibers in immunofluorescence images.

Dr. Daniele Pezzoli fabricated all of the engineered tissues used in the experiments below, fixed and sectioned the tissues for analysis, and provided the porcine aortic smooth muscle cells used in immunofluorescence experiments.

Heena Kumra provided the mouse skin for use in the cellular fibronectin deletion experiments, including raising the mice, euthanasia, and dissection. She also provided figure 5.

Chae Syng Lee produced figures 6 and 7, Hana Hakami produced figure 4, and Rongmo Zhang produced figure 22.

The results of chapter 1 were published in the journal Biomaterials (Pezzoli, D., Di Paolo, J., Kumra, H., Fois, G., Candiani, G., Reinhardt, D.P., and Mantovani, D. (2018). Fibronectin promotes elastin deposition, elasticity and mechanical strength in cellularised collagen-based scaffolds. Biomaterials).

ABBREVIATIONS

A – alanine

AEC - 3-amino-9-ethylcarbazole

BiEC - two-layered construct containing endothelial and smooth muscle cells

BiFB - two-layered construct containing smooth muscle cells and fibroblasts

CABG - coronary artery bypass graft

CAD - coronary artery disease

CD - cluster of differentiation

cDNA - complementary deoxyribonucleic acid

cFN - cellular fibronectin

D - aspartic acid

DAPI - 4',6-diamidino-2-phenylindole

DMEM - Dulbecco's modified Eagle's medium

DNA - deoxyribonucleic acid

EC - endothelial cell

ECM - extracellular matrix

EDA - extra domain A of fibronectin

EDB - extra domain B of fibronectin

ELN - Elastin

EPC - endothelial progenitor cell

FA - focal adhesion

FB - fibroblast

FBLN - fibulin

FBN - fibrillin

FBS - fetal bovine serum

FN - fibronectin

$FNIII_8$-EDA_RGA - fibronectin fragment containing FNIII domain 8 to EDA domain, RGA

$FNIII_8$-EDA_RGD - fibronectin fragment containing FNIII domain 8 to EDA domain, RGD

HEPES - 4-(2-hydroxyethyl)-1-1-piperazineethanesulfonic acid

HRP - horseradish peroxidase

IF - immunofluorescence

IgG - immunoglobulin G

IHC - immunohistochemistry

IL - interleukin

kDa - kilo Dalton

LOX - lysyl oxidase

LOXL - lysyl oxidase like protein

LTBP - latent TGF-β binding protein

Mono - single layer construct containing smooth muscle cells

mRNA - messenger ribonucleic acid

MSC - mesenchymal stem cell

PAoSMC - porcine aortic smooth muscle cell

PBS - phosphate-buffered saline

PCI - percutaneous intervention

PCR - polymerase chain reaction

pFN - plasm fibronectin

PS - penicillin-streptomycin

PSG - penicillin-streptomycin-glutamate

qPCR - real-time polymerase chain reaction

RGA - arginine glycine alanine

RGD - arginine glycine aspartic acid

RT-PCR - reverse transcription polymerase chain reaction

SMC - smooth muscle cell

TBS - tris-buffered saline

TE - tropoelastin

TEBV - tissue engineered blood vessel

TGF-β - transforming growth factor β

Tri - three layered construct containing fibroblasts, smooth muscle, and endothelial cells

V - variable domain of fibronectin

WT - wild-type

1 ABSTRACT AND RÉSUMÉ: CHAPTER 1

1.1 Abstract

In the western world, coronary artery disease is responsible for more than half of all cardiovascular disease-related deaths. One of the most pressing clinical problems of the field is the need for small diameter vascular grafts for coronary bypass surgery. Tissue engineered blood vessels (TEBVs) have been proposed as arterial substitutes but, despite the many advancements in the field, further work is required to address one of the biggest issues toward their clinical application, the lack of strength and elasticity caused by limited elastic fiber formation.

The primary objective of this project is to improve elastic fiber formation in TEBV equivalents. The hypothesis is that: i) exogenously provided fibronectin (FN), which is a known organizer of several extracellular matrix (ECM) fiber systems, can be utilized to improve elastogenesis in TEBV equivalents, and ii) that blood vessel cells act together in promoting elastogenesis in these constructs. The secondary objective is to determine the effect different FN fragments have on elastogenesis in planar, collagen gel-based, human SMC-seeded engineered tissues. The hypothesis is that exogenously added FN fragments will have a similar effect compared to full length FN due to the presence of the RGD sequence.

For this study, our collaborators at the University of Laval prepared two types of 3D TEBVs. The first construct is based on collagen gels cellularized with porcine aortic smooth muscle cells (SMCs) and supplemented with human plasma fibronectin. The second more complex construct is based on collagen gels cellularized with all three relevant human blood vessel cell types, smooth muscle cells, fibroblasts (FBs), and endothelial cells (ECs) organized in concentric layers to mimic the physiological vessel anatomy. To understand the role of fibronectin and of cell organization, the maturation of the constructs over time was investigated in terms of production and deposition (immunohistochemistry) of relevant elastogenic proteins. To investigate the function of FN over time on elastic fiber assembly, a 2D cell culture system with SMC was established and analyzed by immunofluorescence analysis and 3D constructs were analyzed by autofluorescence.

Our collaborators also prepared planar, collagen-gel based constructs seeded with human SMCs and supplemented with different fragments of cellular FN (EDA FN). To investigate the difference between the fragments in terms of elastic fiber-related protein production and deposition by SMCs, immunohistochemical analysis was employed.

Results with the SMC-only 3D TEBV equivalent demonstrate that supplementation with FN increased the production and deposition of tropoelastin, fibrillin-1, lysyl oxidase, and latent TGF-β binding protein 4, with the largest increases in protein production and deposition at later time points (7 d). The 2D SMC approach additionally showed that exogenously added FN increases all relevant and analyzed elastic fiber associated proteins. The multi-cell layered constructs containing either FBs+SMCs or FBs+SMCs+ECs showed an increase in production and deposition by SMCs of fibrillin-1 at day 7 and tropoelastin, lysyl oxidase, and latent TGF-β binding protein 4 at day 7 and day 14. Results with the planar constructs supplemented with various EDA FN fragments demonstrated that short EDA FN fragments and full length EDA FN are equally capable of increasing the production and deposition of elastogenic proteins such as fibrillin-1, tropoelastin, and LOX.

1.2 Résumé

Dans les pays occidentaux, la maladie coronarienne est la manifestation la plus frequente des maladies cardiovasculaires et represente a elle seule la moitie des morts dus aux maladies cardiovasculaires. Il existe un besoin clinique pour des protheses vasculaires de faible diametre pour realiser des pontages vasculaires.. Les vaisseaux sanguins generes par ingenierie tissulaire ont été proposés comme substituts artériels. malgré les nombreux progrès dans le domaine, la manque de force et d'élasticité causé par la formation limitée des fibres élastiques reste un des problèmes essentiels dans l'application clinique de ces vaisseaux.

L'objectif principal de ce projet étant d'améliorer la formation des fibres élastiques dans les vaisseaux sanguins issus de l'ingénierie tissulaire. En effet, notre hypothèse de travail est que i) la fibronectine (FN) exogène, un organisateur connu de plusieurs systèmes de fibres de la matrice extracellulaire (ME), peut être utilisée pour améliorer l'élasticité dans ces vaisseaux, et que ii) les cellules des vaisseaux sanguins agissent ensemble pour promouvoir l'élasticité dans ces modèles. Quant a l'objectif secondaire, il consiste a déterminer l'effet de différents fragments de la protéine FN sur l'élasticité dans des modèles de gel constitué de collagéne planaires et inséminés de FML. L'hypothèse pour cet objectif est que les fragments de FN exogènes auront un effet réduit en comparaison avec la protéine entière de fibronectine.

Pour cette étude, nos collaborateurs de l'Université de Laval ont préparé deux types de modèles 3D de vaisseaux sanguins par ingénierie tissulaire. Le premier modèle est basé sur des gels de collagène cellularisés à partir de FML porcines d'origine aortique et supplémentés de fibronectine humaine plasmique. Le second modèle, plus complexe, est basé sur des gels de collagène cellularisés à partir des trois types de fibres vasculaires humaines : fibres musculaires lisses, fibroblastes (FB), et cellules endothéliales (CE) organisés en couches concentriques pour répliquer l'anatomie physiologique des vaisseaux. Pour comprendre les rôles de la fibronectine ainsi que l'organisation cellulaire, nous avons étudié la maturation de ces modèles au cours du temps et ceci en regardant particulièrement la production et la déposition de protéines élastiques d'intérêt (immunohistochimie). Pour étudier l'effet de la FN sur la formation des fibres élastiques au cours

du temps, un système de culture cellulaire 2D a été établi à partir de FML et analysé par immunofluorescence ainsi que des modèles 3D qui eux, ont ete analysés par autofluorescence.

Nos collaborateurs ont également préparé des modèles de gel en collagène planaires inséminés de FML et supplémentés de fragments variés de FB cellulaire (FN EDA). Dans le but de comprendre la différence entre les fragments et particulièrement la production des cellules élastiques et leur agencement par FML , l'analyse immunohistochimique a été utilisée.

Les résultats obtenus avec les vaisseaux sanguins équivalents produit par ingénierie tissulaire en 3D et qui sont faits uniquement de FML démontrent que l'ajout de FN augmente la production et la déposition de tropoélastine, fibrilline-1, lysyl oxidase, et latent TGF-β binding protein 4. L'optimale de la production et la déposition de protéines est observée tardivement au bout de 7 jours. En ce qui concerne le modèle FML 2D, l'addition de FN exogène augmente la production de toutes les protéines élastiques.

Les modèles à couches multi-cellulaires contenant soit FB+FML ou FB+FML+CE quant á eux, ils démontraient une augmentation de la production et de la déposition de fibrilline-1 au Jour 7, et de tropoélastine, lysyl oxidase, et latent TGF-β binding protein 4 aux Jour 7 et Jour 14 par les FML. Et enfin, les résultats obtenus avec les modèles planaires supplémentés de différents fragments FN EDA ont révélé que les fragments FN EDA courts ainsi que la protéine entière sont tous les deux capables de façon similaire d'accroitre la production et la déposition de protéines élastiques comme la fibrilline-1, la tropolastine, et le LOX.

2 LITERATURE REVIEW AND INTRODUCTION: CHAPTER 1

2.1 Coronary Artery Disease

2.1.1 Incidence, Pathogenesis, and Complications

Coronary artery disease (CAD) is the most common type of cardiovascular disease and the most common cause of death globally, accounting for 15.9% of all deaths (Wang et al., 2016). In 2015 alone, CAD affected 110 million people and killed 8.9 million people globally (Vos et al., 2016; Wang et al., 2016). CAD has several known risk factors, including smoking, excessive alcohol consumption, sedentary lifestyle, obesity, diabetes, depression, hypercholesterolemia, and hypertension. CAD is most often caused by a significant reduction of blood flow and oxygen to cardiac tissues, most typically caused by coronary artery obstruction due to atherosclerosis, or the buildup of subendothelial degenerative material (Torpy et al., 2009). Symptoms of the disease are episodic in nature, most often occurring during exercise or periods of emotional stress and resolving themselves after rest. The most common symptoms of CAD are shortness of breath and pain or discomfort in the chest, though the location can vary. Complications of CAD include cardiac dysrhythmia, myocardial infarction, cardiac failure, and death (NHLBI, 2014).

2.1.2 Treatments

Although prevention is the best method to reduce the risk of complications associated with CAD, several methods of treatment exist for patients diagnosed with the disease. For those with early stage CAD, simple lifestyle changes such as eating a healthier diet, getting regular exercise, and quitting smoking or drinking may be enough (Torpy et al., 2009). In cases where these treatments are not enough, medications such as anticoagulants, statins, nitroglycerin, and beta blockers may be added. In the worst cases, however, more drastic intervention may be required (Centre, 2018; NHLBI, 2014).

If a coronary artery occluded enough to obstruct blood flow, characterized by a cross-sectional stenosis of at least 50%, percutaneous coronary intervention (PCI) may be employed (Figure 1). PCI is a non-surgical procedure wherein the bloodstream is accessed either via the radial artery or

femoral artery and a deflated balloon catheter is advanced to the atherosclerotic coronary artery. Once arrived at the atheromatous plaque, the balloon is inflated to relieve the narrowing caused by the plaque (called angioplasty). In order to keep the artery open, medical devices such as stents may be placed within the artery (Bittl, 1996).

If a coronary artery is 50% to 99% blocked, coronary artery bypass graft (CABG) surgery is undergone (Figure 1). There are two main approaches to CABG surgery. The first approach involves diversion of the left thoracic artery (also known as the internal mammary artery) to the left anterior descending branch of the coronary artery. The second approach involves the use of arterial grafts to bypass a blockage in a coronary artery, accomplished by attachment of one end of the graft to the aorta or one of the major aortic branches and the other end of the graft to the coronary artery just ahead of the blockage, returning the flow of blood to the myocardium (Figure 2). The most common arterial grafts used are autologous grafts, or grafts derived from the patient themselves. Most often, the great saphenous vein of the leg is removed and utilized to bypass the coronary occlusion, and less frequently the radial artery is removed (Barner, 2008; Hayward et al., 2007; Seifu et al., 2013).

Although CABG surgery is an effective treatment for CAD, there are several issues surrounding the use of autologous blood vessels, including the invasive nature of acquiring the blood vessels, the potential for surgical complications such as infection and excessive scarring, the patency of the grafts, and the need for multiple vessels for multiple bypass surgery and for future bypass surgeries. One potential solution for these pressing issues is the development and use of tissue engineered blood vessels, or TEBVs, in CABG surgery.

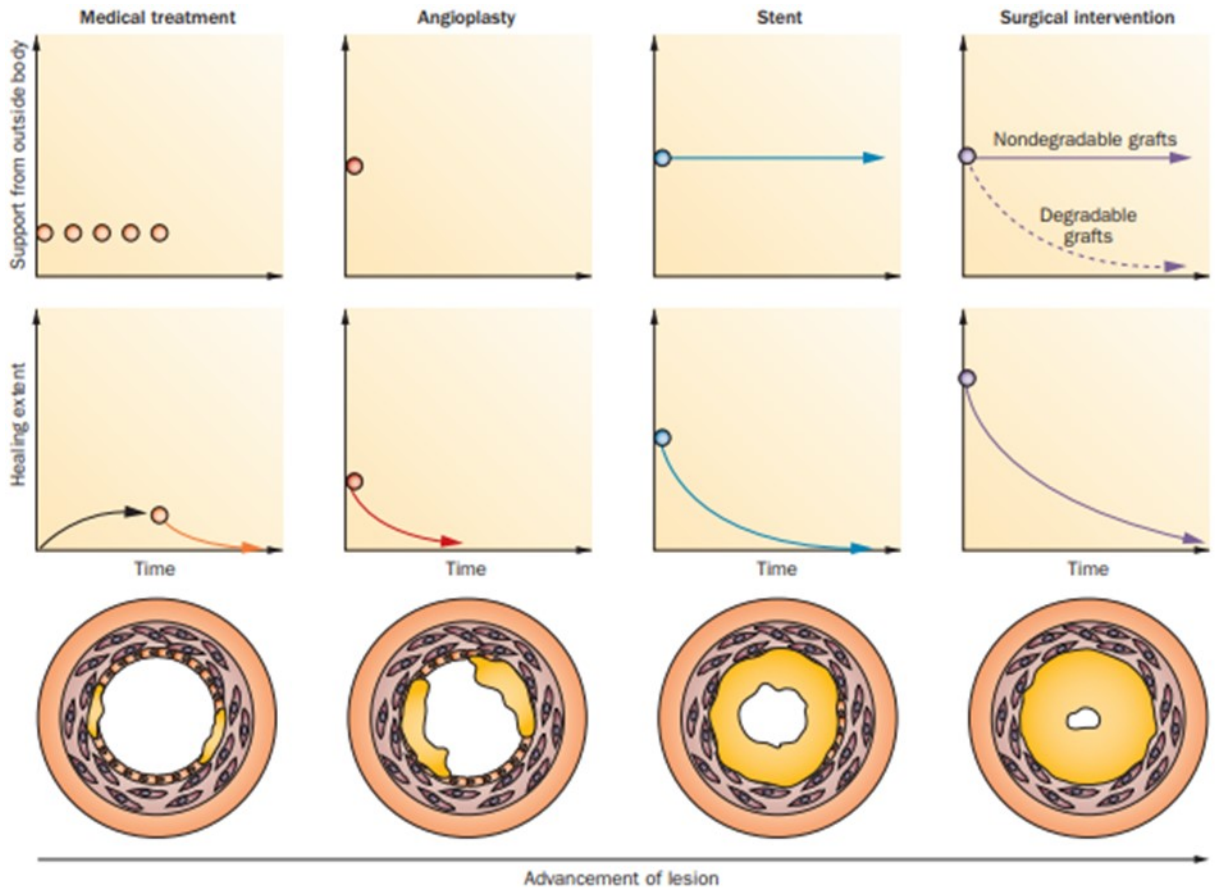

Figure 1. Stages of atherosclerosis within a coronary artery.

In the earliest stages of CAD, pharmaceutical compounds may be used to reverse the trend of plaque growth. As the atherosclerotic plaque grows, however, more drastic measures such as angioplasty must be taken to treat CAD. At later stages, a stent may be employed to reduce the plaque and heal the coronary artery. At the latest stages, surgical intervention becomes necessary. Figure reproduced from Seifu et al. 2013.

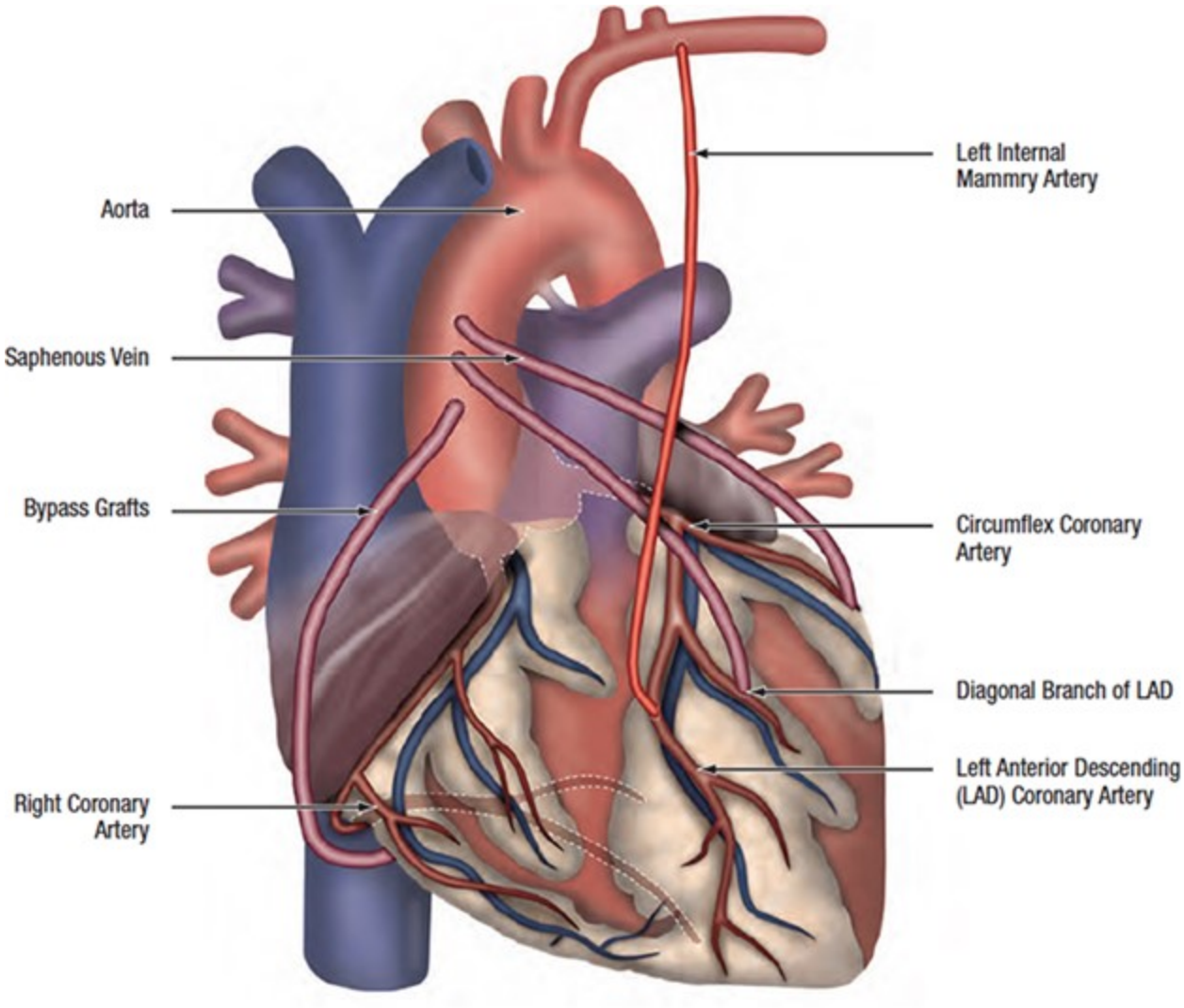

Figure 2. Heart anatomy and coronary artery bypass grafts.

The heart is responsible for supplying blood throughout the body via the circulatory system and to itself via the coronary arteries. Blockage of the coronary arteries by atherosclerotic plaques eventually leads to reduced blood flow to the cardiac muscle, resulting in ischemia and eventual death of cardiac tissue. To circumvent severe blockages in the coronary arteries, CABG surgery may be used, wherein autologous vessels are used as depicted above. Figure reproduced from the Ottawa Cardiovascular Center.

2.2 Vascular Tissue Engineering

2.2.1 Goals of Vascular Tissue Engineering

The main goal of vascular tissue engineering is the design of living vessels that are anatomically and physiologically similar to endogenous vascular tissues (Shin'oka et al., 2001). As such, engineered vascular tissues must have the following properties: nonthrombogenicity, biocompatibility, and mechanical strength and elasticity. To prevent the formation of blood clots within engineered vascular grafts, the grafts may be treated with anti-coagulants such as heparin or may be seeded with endothelial cells on the luminal surface (Li and Henry, 2011). To achieve biocompatibility, engineered vasculature must be nontoxic and incapable of triggering inflammation or immune rejection. To have proper mechanical properties, engineered blood vessels must have a burst pressure similar to the saphenous vein (≥1700mmHg), exhibit resistance to fatigue from prolonged cyclic strain (elastic recoil) with insignificant dilatation, and show fabrication consistency (L'heureux et al., 2007; Li et al., 2014).

Another goal of vascular tissue engineering is the reduction in fabrication and maturation time to permit for upscaling of tissue fabrication. Upscaling of vascular graft fabrication would permit for both on-demand use of grafts as well as commercialization.

2.2.2 Adult Cells for Engineered Vascular Tissue Engineering

As one main goal for vascular tissue engineering is mimicking the anatomy and physiology of native blood vessels, differentiated vascular tissue cells have been considered for use in graft fabrication, including endothelial cells, vascular smooth muscle cells, and fibroblasts (Rabkin and Schoen, 2002). These cells should preferably be sourced from the vasculature of patients to build their own personal vascular grafts, as these cells are easily sourced and their use prevents issues relating to immune system rejection and ensures that the cells maintain their physiological properties (Nerem and Seliktar, 2001; Platt and Nagayasu, 1999). Patient-derived cells have the issue of cell senescence, leading to limited cell proliferation and longer cell expansion times,

extending the production time of engineered vascular grafts and limiting the potential clinical use of such grafts (Rabkin and Schoen, 2002; Stegemann et al., 2007).

To mitigate the issue of limited proliferation rates, experiments have been conducted wherein the gene for human telomerase reverse transcriptase was ectopically expressed by gene transfection in adult vascular smooth muscle cells (McKee et al., 2003; Poh et al., 2005). Results showed a much improved cell proliferation rate, with vascular smooth muscle cells forming a thick vessel wall on the scaffold upon which they were seeded. Despite these encouraging results, several issues remain surrounding the use of this technique, including the risk of intimal hyperplasia, uncontrolled cell growth, and potential tumorigenesis (Kassem et al., 2004).

2.2.3 Stem Cells for Engineered Vascular Tissue Engineering

Considering the issues surrounding the use of terminally differentiated primary vascular cells for the fabrication of engineered vascular grafts, the use of progenitor cells and stem cells has been explored. The most studied stem cells for the fabrication of engineered vasculature are bone marrow-derived mesenchymal stem cells, although MSCs may be obtained from other sources including umbilical cord and adipose tissue (Bajpai and Andreadis, 2012). MSCs can differentiate into both smooth muscle cells and platelet activation-resistant endothelial cells, making them useful for vascular graft endothelialisation and as a source of rapidly-expanding smooth muscle cells (Hashi et al., 2007; Kurpinski et al., 2010). A clinical study conducted in 2012 showed success in a portal vein bypass using endothelial cells and smooth muscle cells derived from autologous bone marrow-derived MSCs to repopulate a decellularized vein (Olausson et al., 2012). Similar studies conducted in dogs showed that bone marrow derived MSCs seeded on vascular scaffolds could differentiate into smooth muscle cells and partly contribute to vessel endothelialisation. Furthermore, the engineered vessels maintained their patency throughout the 24 month investigation (Cho et al., 2005; Matsumura et al., 2003).

Another potential cell type for vascular tissue engineering is the endothelial progenitor cell. EPCs can be obtained from umbilical tissue, circulating blood, and bone marrow, and specific EPCs expressing endothelial cell markers (e.g. CD133, CD34, and VEGFR-2) can differentiate into endothelial cells when they attach onto extracellular matrix (Asahara et al., 1997; Prater et al., 2007). Despite their potential use in engineered vascular grafts, adult stem cells are not very well understood and thus require further study before they can be used for graft fabrication.

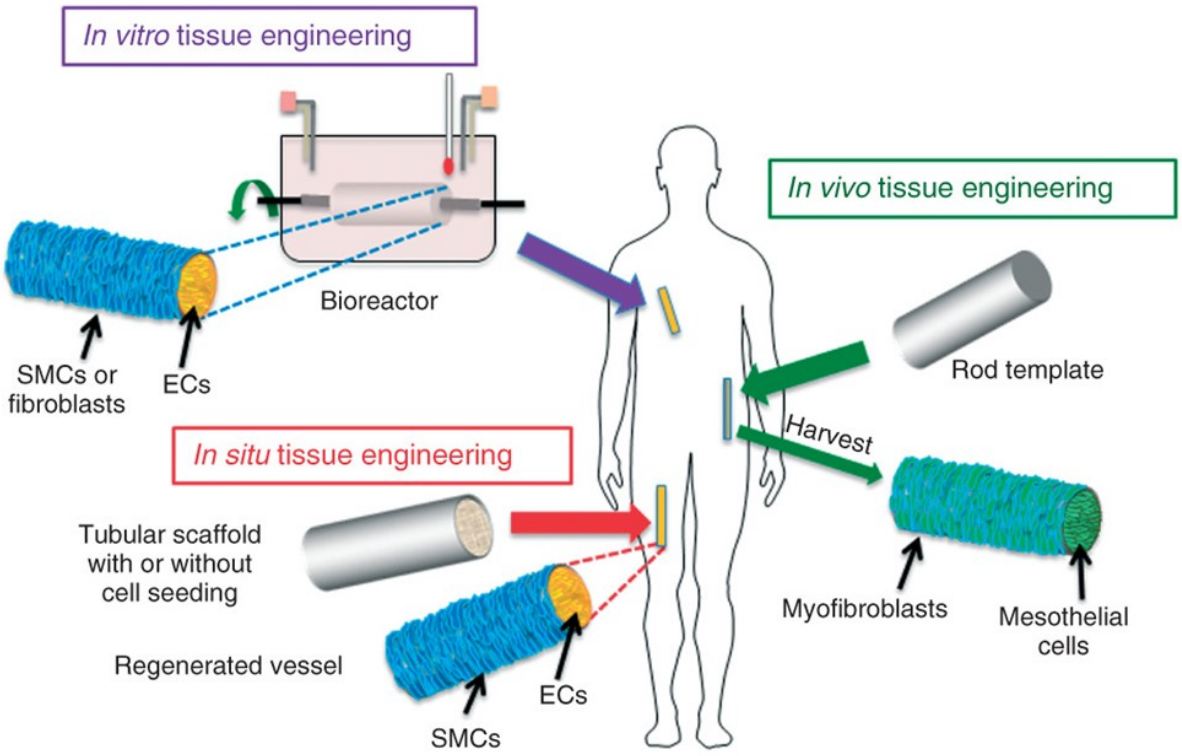

Figure 3. Vascular Engineering Techniques.

There are three major methods for the engineering of vascular tissue. In vitro vascular tissue engineering can be accomplished using such methods as rolled cell sheets and matured natural scaffolds seeded with vascular cells. In situ vascular tissue engineering can be accomplished using methods such as artificial polymer scaffolds (with or without cell seeding) and decellularized vessel grafts. In vivo vascular tissue engineering involves placement of a rod within the body cavity and harvesting the tissue which grows around it for use as a vascular graft. Figure adapted from Li et al. 2014.

2.2.4 Cell Sheets

Although cells are primarily used for seeding pre-made scaffolds, seminal research in 1998 challenged the use of scaffolds by showing engineered vascular grafts could be fabricated using cells only. In order to accomplish this, human umbilical vein smooth muscle cells and fibroblasts were separately cultured for 30 days in medium supplemented with ascorbic acid to induce production of type I collagen. After the maturation period, the organized cell sheets were molded into tubes by first manually peeling the sheets from their culture containers and subsequently rolling them into tubular structures using a mandrel. After molding, the constructs were further matured for another ≥8 weeks and subsequently endothelialized, resulting in a final engineered vessel mimicking native tissues, having an inner endothelial cell layer (intima), a middle layer of smooth muscle cells (media), and an outer layer of fibroblasts (adventitia) (L'Heureux et al., 2006; L'heureux et al., 1998).

Vascular constructs made from cell sheets are very similar to native tissues, having a similar ECM composed of collagen types I, III, and IV, chondroitin sulfate proteoglycans, laminins, and fibronectin (Figure 3). The constructs also exhibit adequate suture retention and have a burst pressure ≥2000mmHg, exceeding the burst pressure of the commonly used saphenous vein. Furthermore, the constructs have a functional, nonthrombogenic endothelium, and are capable of handling physiological blood flow (L'heureux et al., 1998). Clinical studies have shown success in using cell sheet-derived engineered vascular grafts, although these constructs have some drawbacks (Peck et al., 2011). Issues with separating the sheets from their culture containers can cause weak spots to form in the constructs, reducing physical strength and increasing the chance of bursting. These constructs also take an extremely long time to make, 3 months or longer, making them inadequate for use in patients requiring CABG surgery in the short-term (Peck et al., 2012).

2.2.5 Artificial Polymer-based Scaffolds

Considering their successful use in large-diameter vascular grafts, particularly Dacron and Teflon, artificial polymer-based scaffolds have been proposed for the fabrication of engineered vascular grafts and are currently being studied (Abbott et al., 1993). The most well-studied synthetic

polymers, including polyurethanes, polyesters of lactide and glycolide, and the co-polymers of those polyesters (polycaprolactone, polyglycolic acid, and poly-L-lactic acid) are good candidates for vascular engineering, as their properties, such as porosity, mechanical properties, and degradation rate, can be easily controlled and they can be produced with high consistency (Kim and Mooney, 1998; Tiwari et al., 2002). Furthermore, these synthetic polymers are affordable and readily available, allowing for the possibility of large-scale production of vessels fabricated from these compounds (Zhang et al., 2007). The first study to demonstrate the successful use of synthetic polymer-based scaffolds to produce functional vascular grafts was performed by Niklason et al in 1999. In this pioneering study, engineered vascular grafts were fabricated using polyglycolic acid seeded with smooth muscle cells and lined with endothelial cells in the lumen. The resulting engineered vessels were subsequently implanted in miniature pigs, and after 4 weeks showed 100% patency, burst pressures over 2,000mmHg, and contractile responses to pharmacological compounds (Niklason et al., 1999).

Despite their successful use in the fabrication of functional vascular grafts, synthetic polymer-based scaffolds have several issues. One such issue is the lack of bioactivity exhibited by these compounds (Yow et al., 2006). To address this common issue, peptides associated with cell-adhesion can be incorporated onto the surface of these synthetic polymers (Ye et al., 2000). Another issue with the use of synthetic polymer-based scaffolds is the compliance mismatch between the synthetic polymers and the host graft site. This mismatch can cause turbulence in blood flow through the grafted vessel, causing thrombus formation and eventually leading to intimal hyperplasia and reduced graft patency (Baguneid et al., 2011; Desmet et al., 1992). Considering this, patients who receive synthetic polymer-based grafts must remain on anticoagulants for longer periods of time compared to autologous graft recipients. Lastly, although these synthetic polymers are biocompatible, their degradation products are acidic and can cause local decreases in pH, which has been shown to induce vascular smooth muscle cells to switch from a contractile phenotype to a synthetic phenotype and cause a decrease in their mitosis rate (Higgins et al., 2003).

2.2.6 Decellularized Scaffolds

As blood vessels already have the requisite architecture to carry out their physiological functions, decellularized blood vessels have been suggested as a possible source of vascular grafts (Figure 3). Considering that the constituent ECM proteins of native blood vessels, mostly collagen and elastin, are nonimmunogenic, blood vessels could be obtained from donors or other animals and decellularized to remove any immunogenic cellular components (Quint et al., 2012; Quint et al., 2011). There are several methods which can be used to remove cells and their components from the tissues, including the use of various solvents, enzymes, and physical forces. The methods used depend on the tissues being used and the intended use of the decellularized matrix, as decellularization involves an inherent trade-off between preserving extracellular matrix integrity and removing as much cellular material as possible. Once the decellularization process is complete, decellularized scaffolds can be stored for future use by cryopreservation methods such as vitrification and freezing. Both methods require the use of a cryoprotectant, such as glycerol, to prevent matrix-damaging ice crystal formation (Keane et al., 2012). When the scaffolds are required for use, they must be thoroughly washed to remove the cryoprotectant solution and sterilized to prevent bacterial or fungal growth within the scaffolds. Finally, the decellularized vessels can be seeded with autologous vascular cells and matured into proper vascular grafts (Figure 3) (Wolfinbarger Jr et al., 2004).

Although decellularized vascular scaffolds are an attractive solution, they come with several issues. Firstly, there is considerable variation in the mechanical properties of the decellularized vessels, as these properties depend on many factors, including the age, sex, and species of the organism from which the blood vessels originated (Birchall and Hamilton, 2012). Secondly, these scaffolds have the potential of transmitting pathogens from one organism to another, which can be harmful for more than just the patient receiving the engineered blood vessel (Leyh et al., 2003). Lastly, the decellularization process utilized can have major impacts on the resulting scaffold; a process which completely eliminates all cellular components from a vessel may leave the matrix damaged, while a process leaving the matrix entirely intact may leave behind some immunogenic cellular debris (Wolfinbarger Jr et al., 2004).

2.2.7 Biological Polymer-based Scaffolds

Considering that naturally occurring polymers such as collagen and elastin are the main constituents of blood vessels, are responsible for the mechanical properties of blood vessels, and are nonimmunogenic and readily available, they have been thoroughly studied as potential scaffolds for engineering blood vessels (Seifu et al., 2013). The first attempt was conducted in 1986 by Weinberg and Bell, who demonstrated the feasibility of engineering vascular constructs using collagen gel tubes seeded with bovine aortic smooth muscle cells. Despite the properties of collagen, these collagen gel-based vascular constructs had poor mechanical strength and elasticity, due in part to the lack of elastic fibers within the constructs, and thus could not be used in clinical studies (Weinberg and Bell, 1986). Although all constructs fabricated using naturally occurring polymers are too weak for clinical applications, they have some important benefits. Autologous cells can be obtained and seeded directly in the gels during construct moulding, removing the requirement of porosity in the constructs for cell seeding (Boccafoschi et al., 2005).

In the decades following the Weinberg and Bell study, new methods have been developed to improve the fabrication and maturation of natural polymer-based scaffolds. For instance, the use of fibrin gels has been studied and shown to have no appreciable effect on the strength of the constructs, although fibrin is abundant in blood and easily obtainable from patients (Haisch et al., 2000). The development of bioreactors capable of pulsatile flow has helped increase the mechanical strength of these constructs, as cyclic stretch and flow can affect protein expression in vascular smooth muscle cells (Figure 3) (Seliktar et al., 2003). Silk fibroin can be integrated into collagen constructs, also increasing the mechanical strength of the resulting engineered vessels (Couet et al., 2007).

2.2.8 In vivo Vascular Tissue Engineering

One of the most novel techniques for engineering vascular grafts is in vivo vascular tissue engineering (Figure 3). This technique takes advantage of the body's capacity to act as a bioreactor, using a mandrel as the scaffold upon which tissue grows (Nakayama et al., 2004). This tissue is capable of growing in as little as two weeks and is comprised mainly of collagen matrix,

myofibroblasts, and mesothelial cells (Campbell et al., 1999). Once the tissue is formed, the mandrel and tissue can be removed from the body and the tissue removed from the mandrel and used as a vascular graft. These grafts have burst pressures up to 200mmHg and their formation can be controlled by using mandrels made of different materials or by placing the mandrels in different parts of the body, mainly the peritoneal cavity or subcutaneous pouch (Nakayama et al., 2004; Rothuizen et al., 2012). Although this method is good for producing autologous grafts, the grafts produced are not strong enough to handle the pressures coronary arteries experience, they have issues with thrombus formation as they lack a proper endothelium, and they lack elasticity.

2.3 The Extracellular Matrix in Blood Vessels

2.3.1 General Composition and Functions

The space surrounding the cells of multicellular organisms, called the extracellular matrix or ECM, is a dynamic and complex micro-environment. The ECM is composed of numerous proteins, including collagens, elastin, proteoglycans, glycosaminoglycans, and non-collagenous glycoproteins (Aumailley and Gayraud, 1998). The ECM has several important functions, including providing cells with an adhesive substrate, giving the tissues and organs of the body structural integrity and cushioning against external forces, allowing cell-cell communication via cell surface receptors, providing cells with information about their environment through mechanical forces, and storing a multitude of growth factors and providing them as needed (Rozario and DeSimone, 2010). The ECM is in a constant state of remodelling and turnover, where damaged or old matrix proteins are degraded by ECM enzymes such as matrix metalloproteinases, replaced by newly synthesized and secreted proteins, and assembled into final structures by cells or self-assembly (Lu et al., 2011). As with most processes, matrix remodelling is a tightly controlled process, and failure of any regulatory processes can have detrimental effects. Failure to regulate ECM production, deposition, assembly, or degradation can result in abnormal cell proliferation or invasion, resulting in a multitude of diseases including fibrosis and cancer (Ihn, 2002; Mead et al., 2018).

2.3.2 Basement Membrane

The basement membrane is a fibrous, sheet-like ECM no more than 60-120nm thick which underlies or envelops various tissues of the body, including the epidermis (skin, respiratory tract, and gastrointestinal tract), the endothelium of blood and lymph vessels, and the outer surfaces of internal organs. Architecturally, the basement membrane composed of two layers, the lamina lucida and lamina densa, so named due to their electron lucidity and density, respectively, when viewed by transmission electron microscopy. The basement membrane is composed of several proteins, including the large family of laminins, of which there are sixteen members, each a trimer composed of a combination from 5 alpha chains, 3 beta chains, and 3 gamma chains, type IV collagen, nidogen, and perlecan. Laminins form a 2-dimensional, fibrous network with themselves and with collagen IV, interact with cell-surface adhesion molecules such as dystroglycan and syndecan, and bind to α6β4 integrins present in hemidesmosomes on the basal surface of epithelial cells. Perlecan is a heparan sulfate proteoglycan which binds some cell-surface receptors and interacts with many ECM components, contributing to the meshwork structure of the basement membrane. Nidogens bind to laminins, collagen IV, and perlecan, providing further strength to the basement membrane (Noonan et al, 1991; Paulsson, 1992; Yousif et al, 2013).

Functionally, the basement membrane serves many important purposes. First and foremost, it serves as an anchor between the epithelium or endothelium and the underlying connective tissue, binding both cells and connective tissue components such as type VII collagen and fibrillin microfibrils. The basement membrane also acts as a physical barrier, being capable of preventing metastasis of cancer cells and also being used in the glomeruli of the kidney as a selective filter (Liotta et al., 1980; Paulsson, 1992). Furthermore, the basement membrane is essential in the process of angiogenesis, being capable of controlling endothelial cell proliferation and differentiation (Kubota et al., 1988). Malfunctions of the basement membrane can have severe effects, including bleeding from the kidneys and lungs caused by the autoimmune disease called Goodpasture Syndrome wherein collagen IV is targeted, hematuria and proteinuria found in the genetic disorder called Alport Syndrome, and painful blistering of the mucous mucosa and epidermis found in the group of genetic disorders called epidermolysis bullosa (Kluth et al., 1999; Savige, 2014; Sawamura et al., 2010).

2.3.3 Elastic Fibers

Elastic fibers are protein supra-structures deposited in the ECM of elastic tissues, such as the lungs, skin, major arteries and arterioles, ligaments, and epiglottal and auricular cartilage, during development and early postnatal life in a process called elastogenesis (Kielty, 2006; Zhang et al., 1994). The architecture of elastic fibers is quite simple, as they consist of a core of mature, cross-linked elastin, making roughly 90% of the fibers, surrounded by a sheath of microfibrils accounting for the remaining 10% (Figure 4) (Kirschner et al., 2011; Kozel et al., 2011). The major functions of elastic fibers in vertebrates are as follows: first, they confer the unique property of elasticity to elastic tissues, permitting such tissues to maintain their structure and function; second, they can facilitate cell attachment which can have effects on cell migration, differentiation, survival; third, they regulate the availability of growth factors from the TGF-β superfamily within elastic tissues (Gibson et al., 1995). On a molecular level, elastic fibers contain several proteins at the interface between the elastin core and microfibril sheath, including fibulin-2, -4, and -5 (FBLN-2, -4, and -5), latent TGF-β binding protein-2 and -4 (LTBP-2 and -4), and elastin microfibril interface-1 (EMILIN-1) (McLaughlin et al., 2006; Noda et al., 2013; Yanagisawa and Davis, 2010; Zanetti et al., 2004).

2.3.4 Elastogenesis

Elastogenesis, or the assembly of elastic fibers, is a complex and hierarchical molecular process which begins with the integrin-dependent assembly of fibronectin fibrils early in development (Singh et al., 2010). Next, FBN-1 microfibrils are assembled and deposited onto the fibronectin fibrils (Kinsey et al., 2008; Sabatier et al., 2009). Following the deposition of the microfibrils, tropoelastin, the monomeric and immature form of elastin, is deposited onto the FBN-1 microfibrils by accessory proteins including FBLN-4, FBLN-5, and LTBP-4 (Noda et al., 2013; Papke and Yanagisawa, 2014). Next, the enzymes LOX and LOXL-1 bind to FBLN-4 and FBLN-5, respectively, bringing them in close proximity to tropoelastin. Lastly, LOX and LOXL-1 cross-link the tropoelastin monomers, forming mature elastin (Figure 4) (Horiguchi et al., 2009; Liu et al., 2004). This complex process is incredibly important during development, and mutations in the proteins involved in elastogenesis can cause serious developmental disorders, such as Marfan syndrome and cutis laxa (Urbán and Boyd, 2000).

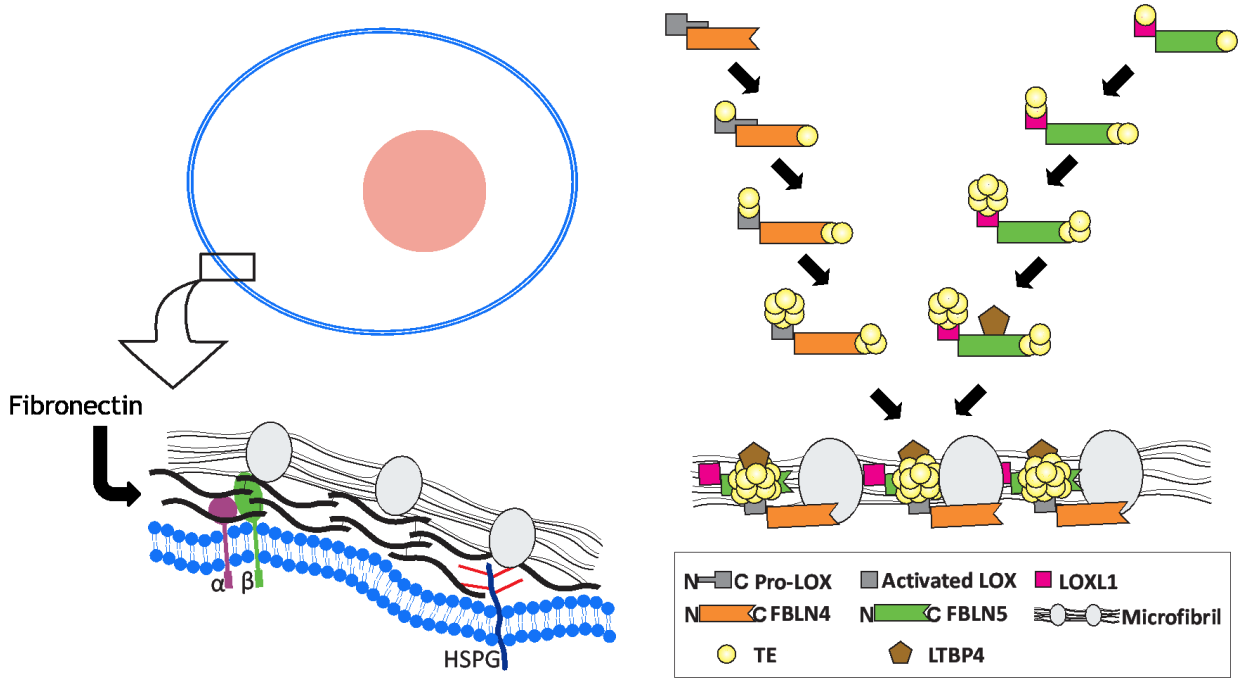

Figure 4. Elastic fibers and Elastogenesis.

Elastogenesis is a complex, hierarchical process involving the assembly of several proteins to form elastic fibers. Proteins involved in elastogenesis include fibronectin, FBN-1, FBLN-4, FBLN-5, LTBP-4, LOX, and LOXL-1. The above schematic illustrates the steps involved in elastogenesis. Figure adapted from Hana Hakami.

2.4 Proteins Associated with Elastogenesis

2.4.1 Fibronectin

Fibronectin is a dimeric glycoprotein composed of two ~250kDa subunits linked covalently by disulfide bonds at their C-termini. Structurally, it contains three types of repeating sequences termed FNI, FNII, and FNIII, of which it has 12 FNI repeats, two FNII domains, and 15-17 FNIII domains altogether accounting for nearly 90% of the total protein sequence. FNI domains, are roughly 40 amino acids in length with two disulfide bonds, FNII repeats are nearly 60 amino acids in length with two intrachain disulfide bonds, and FNIII repeats are approximately 90 amino acids long and contain no disulfide bonds. Fibronectin first appeared in early deuterostomes roughly 540

million years ago, and is highly conserved amongst mammals; for instance, porcine FN and human FN are approximately 94% identical and show similar effects on cells (Hsiao et al., 2017; Özbek et al., 2010; Pankov and Yamada, 2002; Patel et al., 1987).

Fibronectin is encoded by a single gene, though it exists in up to 20 different forms in humans as a consequence of alternative splicing of the pre-mRNA. There are two major sites of alternative splicing where exons are either included or excluded: between repeats $FNIII_{11}$ and $FNIII_{12}$ at a domain known as EDA and between repeats $FNIII_{7}$ and $FNIII_{8}$ at a domain known as EDB. A third region where alternative splicing takes place exists between $FNIII_{14}$ and $FNIII_{15}$. This domain is called the V domain (Figure 5), as it is of variable length, and structural differences in this domain are species dependent (Ffrench-Constant, 1995; Kosmehl et al., 1996).

Despite the capacity for fibronectin to have up to 20 isoforms in humans, it exists primarily in two major forms: plasma fibronectin and cellular fibronectin. Plasma fibronectin contains neither the EDA nor the EDB domain (Figure 5), though isoforms containing and lacking the V domain exist. It is produced predominantly by hepatocytes in the liver (Moretti et al., 2007; Tamkun and Hynes, 1983). Due to the alternative splicing of the protein, it exists in a closed conformation and is soluble, being found abundantly in the blood plasma at concentrations up to 600µg/mL (Zerlauth and Wolf, 1984). As it circulates throughout the body, plasma fibronectin can be taken up by various tissues and incorporated into the ECM along with locally produced cellular fibronectin, and it plays a role in thrombus regulation, considering that fibronectin contains two fibrin-binding regions and can be incorporated into a thrombus by activated platelets (Cho and Mosher, 2006; Moretti et al., 2007; To and Midwood, 2011). Cellular fibronectin, on the other hand, always contains either one or both the EDA and EDB domains and is secreted locally by mesenchymal cells within the ECM (Figure 5). Cellular fibronectin is much less soluble than plasma fibronectin, immediately binds cell surface receptors and is incorporated into the ECM by the cells which produce it, such as fibroblasts, myofibroblasts, and smooth muscle cells (Früh et al., 2015). Furthermore, EDA fibronectin is important during the process of wound healing, where it is secreted to repair the damaged ECM and used for cell adhesion and force sensing within wounds (Muro et al., 2003; To and Midwood, 2011). Fibronectin also plays important roles in guiding cell

adhesion and migration during embryonic development. Experiments using mice with the gene inactivated showed that it is essential in vertebrate development, as indicated by the early embryonic lethality of the mice (George et al., 1993). Fibronectin can be found ubiquitously throughout the tissues of the body, where it plays a crucial role in elastic fiber formation and is required for normal collagen fiber assembly, making it a master organizer or the ECM (Lee et al., 2017). Additionally, fibronectin is capable of binding to proteins including FBN-1, collagens I, III and VII, gelatin, syndecans, several integrins ($\alpha_5\beta_1$, $\alpha_v\beta_1$, $\alpha_4\beta_1$, $\alpha_4\beta_7$, $\alpha_9\beta_1$, and others), heparin, fibrin, the glycosaminoglycan chondroitin sulphate, and itself (Clark et al., 1982; Liao et al., 2002; Plow et al., 2000; Sabatier et al., 2009).

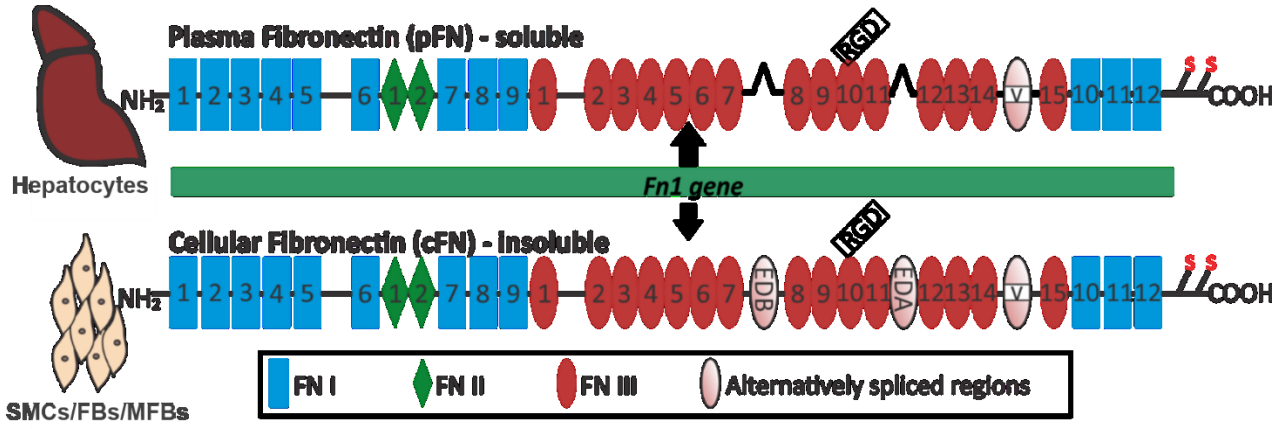

Figure 5. Structure and sequence of Plasma and Cellular Fibronectin.

Fibronectin is a large, dimeric glycoprotein found ubiquitously throughout the ECM of the various tissues of the body. Although fibronectin is encoded by a single gene, alternative splicing of the mRNA allows for the production of different isoforms, the two major isoforms being plasma fibronectin and cellular fibronectin. The structure and sequence of these proteins are shown in the diagram above (produced by Heena Kumra).

2.4.2 Fibrillins and Microfibrils

Fibrillins are large, disulfide-rich glycoproteins approximately 350kDa in size found throughout the ECM (Figure 6). Despite being encoded by different genes, the three isoforms of fibrillin,

fibrillin-1, -2, and -3, are well conserved in amino acid sequence between species and between themselves. Structurally, fibrillins are composed of repeating calcium-binding epidermal growth factor-like domains intermingled with hybrid domains and TGF-β-binding protein domains (Hubmacher et al., 2006). Fibrillins are produced by mesenchymal cells and secreted into the extracellular space, where furin-type convertases process them to form mature fibrillin (Milewicz et al., 1995). Mature fibrillins can then oligomerize into heptameric complexes via their C-terminal domains, which aggregate into bead-like globular structures. Carboxyl terminal multimerization induces the formation of high-affinity binding sites for the amino terminal tails, which then bind to the bead-like structure of other fibrillin multimers, resulting in the formation of microfibrils (Figure 6) (Hubmacher et al., 2008).

Microfibrils are fibers with a diameter roughly 10-12nm formed parallel to elastic fibers. Transmission electron tomography studies of microfibrils isolated from tissues and cell culture revealed a “beads on a string” structure with beads occurring every ~56nm (Figure 6) (Keene et al., 1991; Mithieux and Weiss, 2005). Although microfibrils are closely associated with elastic fibers within elastic tissues, they are also found in non-elastic tissues such as the kidney, ciliary zonules of the eye, and superficial regions of the skin (Kriz et al., 1990; Raviola, 1971). Microfibrils have three important roles: firstly, they act as a scaffold upon which tropoelastin is deposited and matured during elastic fiber assembly (Figure 4); secondly, they regulate the availability of TGF-β superfamily growth factors, such as bone morphogenic proteins and TGF-β1; and thirdly they aid in the maintenance of structural integrity near the basement membranes of tissues (Hubmacher and Reinhardt, 2011; Ramirez and Sakai, 2010).

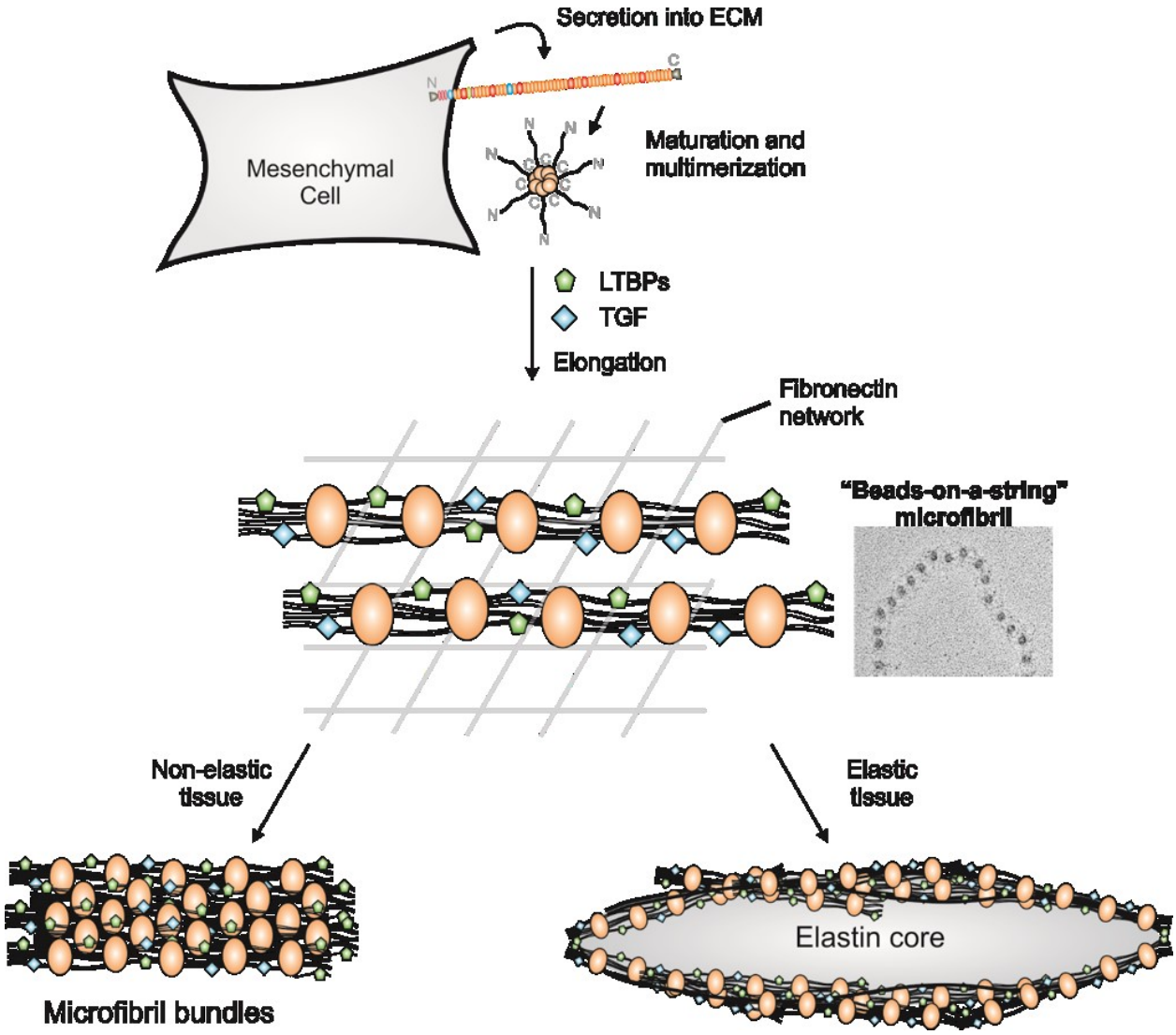

Figure 6. Fibrillin and Microfibrils.

Mesenchymal cells such as fibroblasts and smooth muscle cells produce and secrete fibrillins into the extracellular matrix, where they are matured. Mature fibrillins then assemble into octameric multimers, forming a bead-like globular domain from the interacting C-termini. These multimers then assemble into microfibrils via interaction of the N-termini of one multimer with the bead-like structure of another multimer, forming mature microfibrils with a “beads on a string” structure. Figure produced by Chae Syng Lee.

There are several connective tissues disorders caused by mutations in fibrillins, collectively known as fibrillinopathies. These disorders include the following: Marfan syndrome, stiff skin syndrome, and dominant type Weil-Marchesani syndrome, caused by mutations in fibrillin-1, and Beals-Hecht syndrome and congenital contractural arachnodactyly, caused by mutations in fibrillin-2 (Loeys et al., 2003). Furthermore, fibrillin-1 knockout mice die perinatally as a result of aortic aneurysm, diaphragmatic rupture, and/or diminished lung function caused by issues with elastogenesis in these tissues; however, fibrillin-2 knockout mice lack these issues. Mice deficient in both, fibrillin-1 and -2, die *in utero* due to impaired or retarded elastogenesis in the aorta, clearly indicating the importance of fibrillins to elastic fiber formation (Carta et al., 2006).

2.4.3 Fibulin-4 and Fibulin-5

Fibulins are a family of extracellular matrix glycoproteins found in the elastic tissues and organs of the body (Segade, 2010; Yanagisawa and Davis, 2010). The family of fibulins can be further subdivided into long fibulins, including fibulin-1, -2, and -6, and short fibulins, including fibulin-3, -4, -5, and -7. Fibulin-4 and fibulin-5, the most well-studied and understood members of the family, have critical roles in the formation of elastic fibers (Papke and Yanagisawa, 2014; Segade, 2010). Structurally, fibulin-4 and -5 are composed of six repeating calcium-binding epidermal growth factor-like domains followed by a carboxy terminal fibulin-type domain and have predicted molecular weight of 54kDa and 52kDa, respectively (Giltay et al., 1999; Jones et al., 2010; Nakamura et al., 1999). Both fibulin-4 and fibulin-5 have been shown to interact with various proteins involved in elastic fiber formation (Figure 4).

Fibulin-4 has been proven to interact with several elastogenesis-related proteins, including tropoelastin, lysyl oxidase, and fibrillin-1 (Choudhury et al., 2009; Kobayashi et al., 2007). Fibulin-4 has moderate binding affinity for tropoelastin, and its tropoelastin binding site is localised within the C-terminal fibulin domain (Choudhury et al., 2009). It also shows strong affinity for the crosslinking enzyme lysyl oxidase (Figure 4). Binding of lysyl oxidase to fibulin-4 has been shown to induce an increase in binding affinity between tropoelastin and fibulin-4, and further studies revealed that lysyl oxidase will not crosslink tropoelastin if fibulin-4 is not present,

suggesting that fibulin-4 may play a role in facilitating the crosslinking of tropoelastin by lysyl oxidase (Bultmann-Mellin et al., 2015; Horiguchi et al., 2009). Studies revealed that fibulin-4 contains binding sites for the amino terminal region of fibrillin-1, and thus likely interacts with fibrillin-1 microfibrils. Interestingly, the interaction between fibrillin-1 and fibulin-4 prevents fibulin-4 from binding to tropoelastin, suggesting that fibulin-4 brings tropoelastin and lysyl oxidase to fibrillin-1 microfibrils and unloads it nearby, allowing tropoelastin to bind microfibrils and be cross-linked by activated lysyl oxidase (Choudhury et al., 2009).

Fibulin-5 has been shown to bind tropoelastin more strongly than fibulin-4 and to have only very weak affinity for lysyl oxidase; however, it interacts with another crosslinking enzyme related to lysyl oxidase, called lysyl oxidase-like-1 (Figure 4), suggesting substrate specificity between the two fibulins (Choudhury et al., 2009; Liu et al., 2004; Wachi et al., 2008; Yanagisawa and Davis, 2010). Fibulin-5 also interacts with fibulin-4, indicating there may be some collaboration between the proteins during elastogenesis (Choudhury et al., 2009). It also interacts with latent TGF-β binding protein-2 and -4; fibulin-5 binding to latent TGF-β binding protein-2 causes a decrease in binding affinity between tropoelastin and fibulin-5, while fibulin-5 binding to latent TGF-β binding protein-4 is necessary for fibulin-5 to bind fibrillin-1 (Hirai et al., 2007; Sideek et al., 2014). Fibulin-5 interacts with the fibrillin-1 N-terminus similarly to fibulin-4 (Choudhury et al., 2009; Kobayashi et al., 2007).

Mutations in human fibulin-4 and fibulin-5 have been identified. These mutations cause a connective tissue disorder known as cutis laxa, which is associated with improper or reduced elastic fiber formation. Symptoms of cutis laxa are hence found within elastic tissues and organs, with symptoms including aortic aneurysms and tortuosity, skin that is wrinkled, hanging, loose, and lack elasticity, joint laxity, and lung and diaphragm abnormalities (Coucke et al., 2006; Hoyer et al., 2009). Mutations in human fibulin-4 cause more severe cases of cutis laxa, backed up by mouse knockout studies. Although mutations in human fibulin-5 still cause cutis laxa, patients do not present with aortic aneurysms despite having elastic fiber disruption within the aorta (Hu et al., 2006).

2.4.4 Lysyl Oxidase and Lysyl Oxidase-like protein-1

The lysyl oxidase family of proteins consists of five members: lysyl oxidase, or LOX, and lysyl oxidase-like proteins 1-4, or LOXL-1-4. The main structural components in these proteins are an N-terminal signal peptide, a centrally-located variable region, and a well-conserved amino acid sequence within the C-terminal domain of all members of the family. The lysyl oxidase family can be further subdivided into two groups, as LOX and LOXL-1 most closely resemble one another and the remaining lysyl oxidase-like proteins seemingly belong to a separate family of proteins (Lucero and Kagan, 2006). The main function of LOX and LOXL-1 is to catalyze crosslinking of tropoelastin and collagen, as this crosslinking is necessary for the processes of elastic fiber assembly and collagen fibrillogenesis. When they are secreted into the extracellular space, LOX and LOXL-1 lack enzymatic activity. They gain their enzymatic functions only after activation by processing from their pro forms by bone morphogenic protein family proteins such as bone morphogenic protein-1 (Borel et al., 2001; Lucero and Kagan, 2006). The enzymatic function of LOX and LOXL-1 is dependent on copper, which binds to histidine-rich regions within the mature enzymes. The enzymatic function of LOX and LOXL-1 is to bind lysine residues within tropoelastin and catalyze the formation of reactive aldehyde groups. These aldehydes then self-interact, resulting in the formation of desmosine and isodesmosine residues which confer elasticity to mature elastin (Partridge et al., 1964). LOX and LOXL-1 can be found within elastic tissues, where they often co-localize. However, some localisation differences arise as a result of sequence differences in the pro regions of the immature proteins, as the pro regions play a role in targeting the enzymes to their substrates (Hayashi et al., 2004; Thomassin et al., 2005).

Mouse knockout studies have revealed an important difference between the roles LOX and LOXL-1 play in elastic fiber formation. Mice lacking LOX die perinatally, and necropsies showed the cause of death to be aortic aneurysm and diaphragmatic collapse. Histology of the aorta revealed fragmented elastic lamellae within, the aortic wall, causing a reduction in vessel wall elasticity which led to vessel wall hypertrophy and aortic stenosis (Hornstra et al., 2003; Mäki et al., 2002). Furthermore, LOX knockout mice had irregular elastic fibers and collagen fibers within the skin and showed impaired airway development (Mäki et al., 2005). LOXL-1 knockout mice have a drastically different phenotype compared to LOX knockout mice, as mice lacking the LOXL-1

gene lacked the aortic and pulmonary defects found in the LOX knockouts and even had normal lifespans. However, knocking out LOXL-1 postnatally caused mice to develop vascular and pulmonary deformities, loose skin, and pelvic organ prolapse. The differences in phenotype between LOX and LOXL-1 knockout mice suggest that LOX plays a major role in elastic fiber formation during development while LOXL-1 plays a role in elastic fiber maintenance throughout the life of the organism (Liu et al., 2004).

2.4.5 Latent TGF-β Binding Protein 4

Latent TGF-β binding proteins 4 (LTBP-4) is one of a four-member family of ECM proteins called LTBPs (LTBP-1, -2, -3, -4). LTBPs are similar in structure to fibrillins, containing multiple EGF-like domains and multiple signature 8-Cys domains (Todorovic and Rifkin, 2012). LTBPs -1, -3, and -4 are capable of binding to the latent form of the growth factor TGF-β, composed of TGF-β non-covalently bound to its cleaved propeptide termed the latency associated peptide (LAP), via their third 8-Cys domain which forms disulfide bonds with LAP (Saharinen et al., 1996). LTBPs are secreted together with LAP and inactive TGF-β into the extracellular space where they bind to several ECM proteins, including fibrillins, fibronectin, and FBLN-5. As they bind latent TGF-β and are incorporated into the ECM, LTBPs have two major roles: sequestration of TGF-β into the ECM and involvement in the process of elastogenesis (Noda et al., 2013).

The LTBP most associated with elastogenesis is LTBP-4. *In vitro* studies have shown that LTBP-4 interacts with other elastogenic proteins, including FBN-1 and FBLN-5, and *in vivo* mouse studies have shown that mice with LTBP-4 mutations or null alleles have severely impaired elastic fiber formation in elastic tissues including blood vessels, lungs, and skin (Bultmann-Mellin et al., 2016; Urban et al., 2009). In LTBP-4 null mice, elastin is not incorporated onto microfibril bundles and instead forms large aggregates adjacent to the microfibrils (Dabovic et al., 2009). Although the exact mechanism by which LTBP-4 participates in elastogenesis remains to be elucidated, it has been suggested that LTBP-4 is responsible for targeting of FBLN-5 bound to tropoelastin and LOXL-1 to FBN-1 containing microfibrils (Dabovic et al., 2015; Noda et al., 2013).

2.4.6 Elastin

Tropoelastin, the monomer of elastin which first appeared roughly 419 million years ago in jawed fishes with the evolution of a closed, pressurized circulatory system, is a 60-70kDa protein composed mostly of hydrophobic amino acids, which form the many alternating hydrophobic domains contained within the protein (Sage et al., 1981; Kozel et al., 2011). It also contains several copies of two hydrophilic domains interspersed between the alternating hydrophobic domains, named the KA and KP domains, as they are rich in lysine + arginine and lysine + proline, respectively (Figure 7). As elastogenesis in vertebrates begins during mid-development and into the post-natal period, tropoelastin is highly expressed and produced *in utero* and during early life by mesenchymal cells, and its production declines precipitously during early life (Holzenberger et al., 1993). Despite the extreme decrease in tropoelastin production, gene expression is normal in adult tissues. Studies have shown that the extreme decrease in protein production is due to a post-transcriptional control mechanism which mediates the rapid destruction of tropoelastin mRNA transcripts, though low levels of protein may be produced following tissue injury thanks to TGF-β causing a slight decrease in mRNA degradation (Zhang et al., 1999). Elastin is a very durable protein due to its elasticity, and it has an extremely long lifespan of approximately 80 years, as revealed by ^{14}C turnover and aspartic acid racemisation measurements (Shapiro et al., 1991). Although elastin has the same properties in different organisms, orthologs of elastin show a high variability in nucleic acid and amino acid sequence amongst vertebrates, with pig elastin being 74.8% identical in nucleic acid sequence and 80.7% identical in amino acid sequence to human elastin (Piontkivska et al, 2004).

Tropoelastin is initially secreted as a soluble protein into the ECM, where it primarily interacts with other tropoelastin monomers via their hydrophobic domains in a process known as tropoelastin coacervation (Rapaka and Urry, 1978). This process is entropically driven, as it involves the disorganization of ordered water molecules trapped within unfolded hydrophobic regions of tropoelastin, permitting for proper folding of both hydrophobic and hydrophilic domains and resulting in a change in tropoelastin monomer alignment (Urry, 2004; Vrhovski et al., 1997). This alignment change permits for the proper cross-linking of tropoelastin monomers by the previously mentioned enzymes LOX and LOXL-1. As many as 36 of the ~40 lysine residues within

tropoelastin become cross-linked by the activity of these enzymes, wherein reactive allysine residues are formed and interact with each other and form desmosine and isodesmosine residues (Partridge et al., 1964; Vrhovski et al., 1997). Tropoelastin cross-linking into mature elastin grants it its important properties of elasticity, stability, and extreme insolubility. Furthermore, the formation of desmosine and isodesmosine residues grants mature elastin the interesting property of autofluorescence, as both residues contain aromatic ring structures which contain unconjugated pi electrons capable of absorbing shorter wavelength visible light and emitting the excess energy as 495-570nm wavelength photons (WANG et al., 2010; Yeo et al., 2011).

Elastin knockout mice die perinatally as a result of vascular obstruction caused by smooth muscle cell overproliferation. Moreover, histological analysis of the affected vessels revealed thicker vessel walls and disorganization and misalignment of the smooth muscle cells within the walls (Li et al., 1998a). In contrast, mice heterozygous for the elastin gene have normal lifespans, though they have significant hypertension, smaller blood vessel lumen, and thinner blood vessel walls (Li et al., 1998b). Human mutations in the elastin gene have been reported to result in elastic fiber-related diseases as well as cardiovascular complications, including autosomal dominant cutis laxa, characterized by the presence of blue-tinged sclera of the eyes, loose skin, and joint hypermobility, Willam-Beuren syndrome, characterized by developmental disability, unusual facial features, heart defects, and hernias, and supravalvular aortic stenosis, revealed as a narrowing of the aorta directly above the aortic valve(Curran et al., 1993; Ewart et al., 1993; Tassabehji et al., 1998).

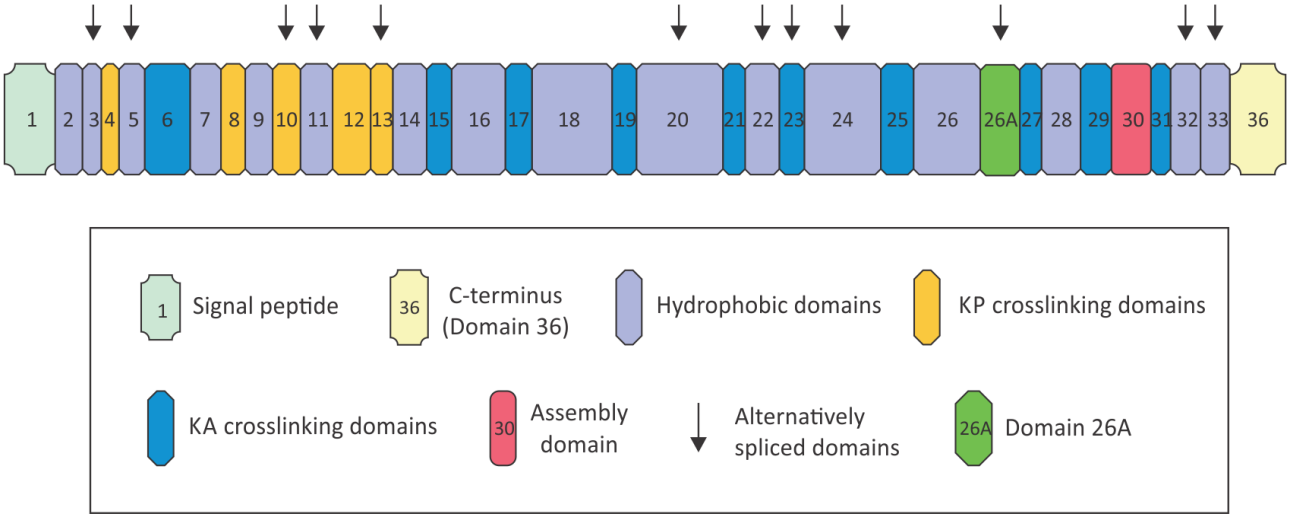

Figure 7. Structure of Elastin and its domains.

Human tropoelastin consists of a total of 34 individual domains, as it lacks exons 34 and 35 which are found in other mammalian variants, 32 of which are alternating hydrophobic (purple) and lysine-rich hydrophilic (orange and blue) domains. The hydrophobic domains within tropoelastin are responsible for coacervation of multiple tropoelastin monomers, while the lysine-rich hydrophilic domains allow for cross-linking of tropoelastin monomers by LOX and LOXL-1 to form mature elastin, an important step in the formation of elastic fibers. Figure produced by Chae Syng Lee.

3 OBJECTIVES: CHAPTER 1

Previous studies have shown that fibronectin is required for elastic fiber formation, as it is required for assembly of fibrillin-1 microfibrils upon which elastin monomers are deposited and cross-linked to form mature elastic fibers. Limited elastic fiber formation is the underlying cause behind the lack of elasticity in collagen gel-based engineered vascular constructs, and current methods to increase elastic fiber formation cause insufficient elastogenesis or take too long to reach appreciable levels of elastin within the constructs. This study seeks to develop a method for increasing elastogenesis in collagen gel-based engineered blood vessels.

The specific objectives of this study are:

1. To determine whether the addition of human plasma fibronectin to 3D single layer collagen gel-based engineered blood vessels increases protein production and deposition.

2. To analyze if human plasma fibronectin causes changes in mRNA expression in porcine aortic smooth muscle cells.

3. To investigate whether the addition of human plasma fibronectin to porcine aortic smooth muscle cells in 2D cell culture increases the assembly of elastic fibers.

4. To examine whether elastin produced by porcine aortic smooth muscle cells in collagen gel-based engineered blood vessels is mature.

5. To study the effect of co-culturing vascular cells in collagen gel-based engineered blood vessels on elastic fiber-related protein production and elastogenesis.

6. To determine whether short fibronectin fragments have a similar effect on elastic fiber-related protein production by human smooth muscle cells seeded in planar collagen gel-based constructs.

4 MATERIALS AND METHODS

4.1 Antibodies

Antibodies were used for indirect immunofluorescence and immunohistochemistry assays. The primary polyclonal antibodies used included anti-human FN (Sigma, CAT#F3648), anti-human TE (Elastin Products Company, CAT#PR398), anti-human lysyl oxidase (Novus Biologicals, CAT#NB100-2527), anti-SM22α (Abcam, CAT#ab14106) anti-human latent TGF-β binding protein 4 (produced in the lab), anti-human fibulin-4 and fibulin-5 (El-Hallous et al., 2007), anti-human FBN-1 and FBN-2 (Tiedemann et al., 2001) antibodies. The primary monoclonal antibodies used included anti-human cellular FN (Abcam, CAT#ab6328) and anti-αSMA (Dako, CAT#M0851). The secondary antibodies used to detect polyclonal antisera were goat anti-rabbit conjugated to Cy3 (ThermoFisher Scientific, CAT#A10520) or Alexa 488 (ThermoFisher Scientific, CAT#A11034) and Labelled Polymer-HRP Anti-Rabbit (Dako, REF#4008). The secondary antibodies used to detect monoclonal antisera were goat anti-mouse IgG (H+L) conjugated to Cy3 (ThermoFisher Scientific, CAT#A10521) and Labelled Polymer-HRP Anti-Mouse (Dako, REF#K4004).

4.2 Cell Culture

4.2.1 Porcine Aortic Smooth Muscle Cells

PAoSMCs were obtained from adult pig aorta in the Mantovani Lab using the following procedure: First, a portion of the aorta was obtained and rinsed using cold Krebs-Henseleit solution to remove any trace of blood. Next, any excess or undesirable tissue was removed using scissors, the aorta was cut into annular sections ~1 cm thick, and the sections were placed in medium 199 supplemented with 1% PS. Following this, the tunica adventitia and external third of the tunica media were carefully removed using a scalpel and forceps, followed by removal of the intima and inner third of the tunica media. Next, the rings of tunica media were cut into small sections roughly 1 × 5mm in size and placed in a sterile petri dish containing medium 199 (Gibco, Life Technologies) supplemented with 10% fetal bovine serum (Gibco) and 1% penicillin/streptomycin (Gibco). Once enough PAoSMCs migrated out of the tissues, the explants were removed and the medium was replaced with complete smooth muscle cell growth medium and allowed to expand

to near-confluence (never permitted to become over confluent). Some PAoSMCs were frozen in FBS containing 10% dimethylsulfoxide and shipped on dry ice to our lab for experimentation.

PAoSMCs sent to our lab were thawed and placed in sterile 175cm2 plastic cell culture flasks (SARSTEDT, REF#83.3912.003) containing 25 mL of Dulbecco's Modification Eagle's Medium (Wisent Inc., CAT#319-005-CL) supplemented with 10% FBS and 1% penicillin/streptomycin/L-glutamine (Wisent Inc., CAT#450-202-EL), hereafter referred to as complete medium. The cells were expanded in an incubator with a humidified atmosphere of 5% CO2, were kept subconfluent, and used in immunofluorescence, reverse transcription polymerase chain reaction, and quantitative polymerase chain reaction experiments as described below.

4.2.2 Mouse Skin Fibroblasts

Mouse skin fibroblasts were obtained from P3-P8 mouse pups expressing Cre recombinase-ERT2 under the α-smooth muscle actin promoter with the FN gene flanked by LoxP sites (FN(fl/fl); αSMA-CreERt2/+). First, the mouse pups were euthanized and skin was removed from the backs of the animals and placed in cold PBS. Next, the tissues were cut into pieces roughly 4mm2 using alcohol-sterilized forceps and a scalpel. The resulting pieces of skin were then placed dermis side down in 25cm2 plastic cell culture flasks containing 3mL of complete medium and left upright (to allow the skin to stick to the flask) overnight in an incubator with a humidified atmosphere of 5% CO2 at 37°C. The flasks were carefully laid horizontally the following morning to allow the medium to contact the tissues. Once enough MSFs migrated out of the skin explants, the tissues were removed from the flasks and the cells permitted to expand to near-confluence and subsequently moved to 175cm2 plastic cell culture flasks. MSFs were used in immunofluorescence and polymerase chain reaction experiments as described below.

4.3 Engineered Tissue Fabrication

4.3.1 Preparation of Cellularized Collagen Gels

Cellularized collagen gels were prepared according to Pezzoli et al. 2018: Type I collagen was extracted from rat tail tendons, solubilized in 0.02 N acetic acid at a concentration of 4mg/mL and sterilized by multiple cycles of dialysis in 1% chloroform and 0.02 N acetic acid as previously described (Rajan et al., 2006). Cellularised collagen gels were prepared as previously described (Bono et al., 2016). Briefly, 2 parts of sterile collagen solution were mixed with 1 part of buffer solution (3.5-fold concentrated DMEM supplemented with 60mM NaOH and 10mM HEPES) and 1 part of cell suspension (2×10^6 cells/mL in DMEM +10% FBS and 1% PS) to obtain a final cell density of 5×10^5 cells/mL, a collagen concentration of 2g/L and a pH of 7.2. For conditions with supplemental FN, an aqueous solution containing human plasma FN (Advanced Biomatrix) was added to gels to obtain FN-loaded gels at a final concentration of 0.05mg/mL (Pezzoli et al., 2018).

4.3.2 Monolayer Tissue Engineered Blood Vessels

Monolayer tissue engineered blood vessels were prepared according to Pezzoli et al. 2018: For the preparation of tubular samples, 2mL of collagen-cell suspension was poured in ad hoc made sterile tubular moulds composed of a central cylindrical polypropylene mandrel with a diameter of 3.8mm, of a tubular polypropylene mould with an internal diameter of 9mm, and two gaskets. Samples were incubated for 1h at room temperature., then the external mould was removed and the mandrel, surrounded by the collagen tube, was placed in a sterile tube containing DMEM +10% FBS and 1% PS, and the constructs were incubated in a humidified atmosphere of 5% CO2 at 37°C for 1, 3 or 7 days. The medium was changed every second day (Pezzoli et al., 2018).

4.3.3 Planar Engineered Tissues

Planar engineered tissues were prepared according to Pezzoli et al. 2018: For the preparation of disk-shaped samples, the collagen-cell suspension was immediately poured into 24-well plates (0.5mL/well) and incubated for 1h at room temperature to allow sample gelation. Each gel was gently detached from the wall and the bottom of the well with a microspatula, 0.5mL of fresh

DMEM + 10% FBS and 1% PS were added (Pezzoli et al., 2018). The constructs were then cultured as described above with the difference of using either full length human EDA FN, short human EDA FN fragment FNIII8-EDA, or FNIII8-EDA containing a mutation of the RGD sequence to RGA (Figure 22). The fragments were produced by Rongmo Zhang, a Ph.D. candidate in the lab.

4.3.4 Multilayered Tissue Engineered Blood Vessels

The tri-culture collagen-based models were assembled according to Loy et al. 2018: a media-like layer was prepared by adding 2.5mL of collagen-SMCs suspension in the tubular mould of the Tubular Multilayered-Tissue Culture System (TMCS, made in the Mantovani Lab) and allowed to jellify at 37°C for 1h. Then, accelerated densification of the gel was performed according to the method previously described by (Loy et al., 2018). Briefly, the external mould was removed and the reservoir was mounted on the TMCS. The closed system was subsequently mounted on a home-made rotating bioreactor operating at five revolutions/min to homogenously remove the water and obtain a construct of homogenous thickness. The rotation process was performed for 1h at room temperature. Then, a larger diameter, sterile tubular mould was installed. An adventitia-like layer was prepared by adding 4mL of collagen-FBs suspension in the tubular mould and allowed to jellify at 37°C for 1h. The external mould was next removed and the circuit was closed. The resulting constructs were carefully transferred into the TMCS reservoir containing 40mL of cDMEM (composed of DMEM supplemented with 5% FBS, 1% PS, 2ng/mL fibroblast growth factor-basic, 3ng/mL epidermal growth factor, 2µg/mL ascorbic acid, 5µg/mL insulin, 1µg/mL hydrocortisone, and 50µg/mL heparin) and incubated at 37°C overnight. To endothelialize the lumen of the construct (intima-like layer), the mandrel was carefully removed from the construct under sterile conditions and a suspension of ECs was poured into the tubular collagen gel at a concentration corresponding to a cell seeding density of 8 × 104 cells/cm2. After closing all the external tubular inlets/outlets, the system was mounted on the rotating bioreactor operated at 5rpm and placed inside a cell culture incubator. After 24h of incubation under rotation, the medium within the tubular construct was replaced with fresh cDMEM and this time point was defined as t0. Both internal and external media were changed every 2 days. The mono- and bi-culture constructs were prepared for comparison as described above. Constructs were all matured in static

conditions for 1 or 2 weeks for the proof of concept of the developed TMCS as static bioreactor (Loy et al., 2018).

4.4 Histological Analysis

4.4.1 Immunohistochemistry

Dako EnVisionTM + System-HRP (AEC) kits (Dako North America, Inc.) against mouse primary antibodies (REF#K4004) and rabbit primary antibodies (REF#4008) were used for staining immunohistochemical analysis. The analysis was conducted on 4μm thick, paraffin embedded sections of monolayer and multilayer tubular engineered blood vessel constructs and planar constructs. The sections, affixed on glass microscopy slides, were first deparaffinised by 2 ×3min incubations in CitriSolv Hybrid solution (Deacon Laboratories, Inc, CAT#1601H). Following deparaffinisation, the sections were rehydrated in graded solutions of ethanol and water, with each incubation being 3min in duration. Next, antigen retrieval was conducted by incubating the sections in a solution of 10mM citric acid + 0.05% Tween 20 (pH=6) at 98°C for 20min, followed by a 20min cooling period in the solution and 3 × 5min washes in distilled H_2O. Next, endogenous peroxidase activity was blocked with a 5min incubation in peroxidase blocking solution supplied in the Dako EnVisionTM + System-HRP (AEC) kit, followed by 3 × 5min washes in solutions of TBS + 0.05% Tween 20. Next, a final round of antigen retrieval was conducted with a 5min incubation in a solution of Proteinase XXIV (Sigma-Aldrich, Co., CAT#P8083-50MG) diluted 10x in 50mM tris solution (pH=7.6), followed by 4 × 5min washes in solutions of TBS + 0.05% Tween 20. Next, the sections were incubated overnight in a humidity chamber at 4°C with primary antibodies against pFN (1:250), EDA FN (1:200), TE (1:250), FBN-1 (1:250), FBN-2 (1:250), FBLN-4 (1:250), FBLN-5 (1:250), LOX (1:100), and LTBP-4 (1:250), diluted in a solution of 1% BSA in TBS. Following the primary antibody incubation, the sections were washed 3 ×5min in a solution of TBS + Tween 20 and subsequently incubated for 30min in either Labelled Polymer-HRP Anti-Mouse or Labelled Polymer-HRP Anti-Rabbit solution (from the Dako EnVision TM + System HRP (AEC) kit), followed by 3 × 5min washes in solutions of TBS + Tween 20. Next, the sections were incubated for 17min in AEC + Substrate Chromogen (Dako EnVisionTM + System HRP (AEC) kit), followed by 3 × 10min washes in distilled H_2O. Lastly, the slides were covered using glass coverslips and Dako Faramount Aqueous Mounting Medium (Dako North

America, Inc., REF#S3025) and images were acquired using an epifluorescence microscope (AxioImager M2; Zeiss) with an AxioCam ICc5 color camera and Zen Pro software (Zeiss).

4.4.2 Autofluorescence Assay

Paraffin-embedded, 4µm thick sections of monolayer TEBVs were deparaffinised and rehydrated as described above. After rehydration was completed, the slides were covered using glass coverslips and Dako Faramount Aqueous Mounting Medium. Autofluorescence analysis was conducted using 495nm wavelength light and an epifluorescence microscope (AxioImager M2; Zeiss) with an Orca Flash 4.0 CMOS gray scale camera. Gray-scale images were false-colored using Zen Pro software (Zeiss).

4.5 Indirect Immunofluorescence Assay

4.5.1 Elastogenesis Experiments in Porcine Aortic Smooth Muscle Cells

For immunofluorescence analysis of elastogenesis, adult PAoSMCs were seeded in glass 8-well chamber slides (20,000 per well) with complete medium. Half of the wells were supplemented with 0.05 mg/mL human plasma FN (Millipore). After 3 or 7 days post-seeding, the cells were washed with 100µL PBS for 3min and subsequently fixed with 500µL of cold 70:30 methanol:acetone solution. Next, the cells were washed 3 × 3min with 100µL of PBS. After the washes, the cells were incubated for 30min at room temperature with 150µL of 10:1 PBS:normal goat serum (Jackson Immuno Research Laboratories, CAT#005-000121) to block non-specific antibody binding. After blocking, the cells were washed with 100µL of PBS for 3min and stained for 90min in a humid box at room temperature using 150µL of blocking solution-diluted antibodies against: pFN (1:500), EDA FN (1:200), TE (1:400), FBN-1 (1:500), FBN-2 (1:1000), FBLN-4 (1:1000), FBLN-5 (1:500), LOX (1:100), and LTBP-4 (1:1000). Next, the cells were washed 3 × 5min with 100µL PBS, followed by secondary antibody staining. Secondary antibody staining was done for 60min in a dark humid box at room temperature using Cy3-goat anti-mouse IgG (H+L) and Cy3-goat anti-rabbit IgG (H+L) diluted in blocking solution to a concentration of 1:200. Next, the cells were washed 3 × 3min with 100µL PBS and counterstained for 3min with DAPI (Life Technologies, CAT#D1306) diluted to 1:2000 in PBS. After counterstaining, the cells were washed 3 × 3min with 100µL of PBS, excess solution was removed, the plastic wells were

separated from the slides, and the cells were covered using glass coverslips and Vectashield Mounting Medium (Vector Laboratories, Inc., CAT#H-1000). Fluorescence images were acquired using the same microscope and camera described in the autofluorescence analysis above.

4.5.2 Verification of Fibronectin Deletion in Mouse Skin Fibroblasts

Mouse skin fibroblasts were isolated from P3-P8 FN(fl/fl); αSMA-CreERt2/+ mouse pups. To induce expression of αSMA, the MSFs were transdifferentiated to myofibroblasts by incubation with 5ng/mL of sterility-filtered TGF-β1 for 3 days. To induce deletion of the FN gene, half of the cells were incubated with 5ng/mL tamoxifen for 3 days and half were incubated with an equal volume of ethanol, resulting in two conditions: TGF-β1 + ethanol, and TGF-β1 + Tamoxifen. Following these treatments, the cells were trypsinized and seeded in glass 8-well chamber slides (75,000 per well) with DMEM containing FN-depleted FBS, 100µg/ml penicillin/streptomycin, and 2mM glutamine. After 2 days of incubation, the cells were treated for indirect immunofluorescence as described above, but were stained using primary antibodies against αSMA (1:100), SM22α (1:100), pFN (1:500), and EDA FN (1:200). Secondary antibody staining was accomplished using Cy3-goat anti-mouse IgG (H+L) and AlexaFluor488-goat anti-rabbit IgG (H+L) at the same concentration as above. Mounting and image acquisition were accomplished using the same materials and instruments as described above.

4.6 RNA Isolation

4.6.1 Engineered Tissues

The Qiagen RNeasy Mini Kit (Qiagen, CAT#74104) was used to isolate RNA from cellularized collagen gels. The gels were first thawed on ice and subsequently weighed to determine the volume of Buffer RLT + β-mercaptoethanol solution (1:100 ratio β-ME:Buffer RLT) needed for homogenization, 350µL for tissues <20mg and 600µL for tissues ≤30mg. Next, the tissues were homogenized completely using a Branson Sonifier 150 ultrasonic homogenizer (Branson Ultrasonics Corp) for 3 × 10s intervals with 30s cooling on ice between homogenization intervals. Following homogenization, the tissue lysate was centrifuged for 3min at maximum speed, the

supernatant was carefully removed by pipetting, and one volume of 70% ethanol was added to the pellet and mixed by pipetting. Next, up to 700µL of the mixture was added to an RNeasy Mini spin column (supplied in the kit) placed in a 2mL collection tube. The mixture was subsequently centrifuged for 15s at 8000g and the flow-through was discarded. Next, 700µL of Buffer RW1 (supplied in the kit) was added to the RNeasy Mini spin column, followed by centrifugation for 15sat 8000g and removal of the flow-through. Following this, 500µL of Buffer RPE was added to the RNeasy Mini spin column, which was subsequently centrifuged for 15s at 8000g and removal of the flow-through. Next, another 500µL of Buffer RPE was added to the RNeasy Mini spin column, followed by centrifugation for 2min at 8000g, placement of the RNeasy Mini spin column into a new 2mL collection tube, and another centrifugation for 1min at full speed. Following this step, the RNeasy Mini spin column was placed into a 1.5mL collection tube and 50µL of RNAse free H2O (Fisher Scientific, CAT#BP561-1) was added to the column, followed by a final centrifugation for 1min at 8000g to elute the RNA. Lastly, the concentration of RNA was determined using an Ultrospec 2100 Pro UV/Visible spectrophotometer (Biocrom Ltd).

4.6.2 RNA Preparation

The Qiagen RNeasy Mini Kit was also used to obtain RNA from cells. First, subconfluent cells were washed twice with 20mL of sterile PBS and were subsequently incubated for 1min in 3mL of 37°C solution of 0.05% trypsin and 0.53mM EDTA with sodium bicarbonate (Wisent Inc., CAT#325-542-EL). To stop the trypsinization reaction, 7mL of complete medium was added to the cells, which were subsequently transferred to a sterile 15mL tube and centrifuged for 5min at 1200g. Following centrifugation, the supernatant was removed, the pelleted cells were re-suspended in 5mL of complete medium, and the cells were counted using a hemocytometer and inverted light microscope (Zeiss). Next, the cells were mixed with an appropriate amount of Buffer RLT + β-ME (350µL if $<5 \times 106$ cells, 600µL if $\leq 1 \times 107$ cells) and lysed by pipetting up and down. The cell lysate was then treated as the tissue lysate was as described above. Isolated RNA was either used immediately or stored at -80°C for future use in RT-PCR experiments.

4.7 Reverse Transcription Polymerase Chain Reaction

RT-PCR was accomplished using the ProtoScript II First Strand cDNA Synthesis Kit (New England Biolabs, CAT#E6560S). First, RNA was isolated from tissues or cells according to the above methods. Next, up to 1µg of RNA, 2µL of random primer mix, and nuclease-free H2O to a total volume of 8µL were added to a 0.5mL microcentrifuge tube. The mixture was then incubated for 5min at 65°C in a PTC-200 Peltier thermal cycler (MJ Research), spun briefly, and put promptly on ice. Next, 10µL of ProtoScript II Reaction Mix and 2µL of ProtoScript II Enzyme Mix were added to the RNA mixture (total reaction volume 20µL) and mixed by pipetting up and down. Next, the cDNA synthesis reaction was incubated for 5min at 25°C, then incubated for 1h at 42°C, and finally incubated for 5min at 80°C using the Peltier thermal cycler. cDNA obtained from RT-PCR was either immediately used or kept in -20°C for future use in qPCR experiments.

4.8 Real-time Quantitative Polymerase Chain Reaction

Gene expression levels for FN1, FBN1, FBN2, ELN, EFEMP2, FBLN5, LTBP4, LOX, and ACTB were investigated using qPCR. First, cDNA obtained from RT-PCR of RNA obtained from both cells and engineered tissues was diluted 10x by adding 180µL of RNase-free H2O. Next, a qPCR reaction mixture was made using 5µL of SYBR Green Select Master Mix (Life Technologies, CAT# 4472908), 0.5µL forward primer, 0.5µL reverse primer (see table below for primers, primers designed using PrimerBLAST), and 4µL of diluted cDNA, making a total volume of 10µL per reaction (all targets were investigated in triplicate in order to account for technical error within the experiments). The reaction mixtures were made in a MicroAmp® EnduraPlate Optical 384-Well Clear Reaction Plate (Life Technologies, REF#4483285) and mixed by pipetting. Lastly, the plate was covered using a MicroAmp™ Optical Adhesive Film (Applied Biosystems, REF#4311971) and placed in a QuantStudio® 5 Real-Time PCR Instrument (Applied Biosystems, REF#A21835). The PCR reaction was activated with 2min incubation at 50°C followed by 2min incubation at 95°C. Following activation, the reaction was thermally cycled 40 times with a 15s denaturing step at 95°C, then a 15s annealing step at 58°C, and lastly a 1min extension step at 72°C. Data obtained from qPCR experiments were analyzed using the ΔΔCt method. Statistical significance was calculated in Microsoft Excel using the two-tailed t-test, and results were graphed using OriginPro software.

Table 1. Primers used for qPCR.

Target	Sequence (5'→3')	Length (bp)	T_m (°C)	GC%	Product Length (bp)
FN1	Fwd: TGAACTCGGTCCCGAAGGCT	20	64	60	106
	Rev: CATGAAGCACTCAATTGGGCAG	22	66	50	
FBN1	Fwd: CCAGTGGCTGGAACCTATTCA	21	64	52.38	105
	Rev: ACCACTGAGGTAGTCTTTGTCA	22	64	45.45	
FBN2	Fwd: TCTCCCAAGGGAATGATGACG	21	64	52.38	107
	Rev: TTCCAGTGTGTATGTGCCAGG	21	64	52.38	
FBLN4	Fwd: GGCAAATCAACAACGTCAGCG	21	64	52.38	108
	Rev: AGCTCATGAGGGAGTTCATGG	21	64	52.38	
FBLN5	Fwd: ACCCTGGTGATGACACGTCC	20	64	60	100
	Rev: CGGAGCTGCCTCTGAAGTTG	20	64	60	
LOX	Fwd: CTAAAGGTCAGTGTGAACCCC	21	64	52.38	95
	Rev: GCATGATGTCCTGTGTAGCGA	21	64	52.38	
LTBP4	Fwd: GACAGCCGAGTACCAGTCAC	20	64	60	91
	Rev: ACACTCGTCCACGTTTCTCC	20	62	55	
ELN	Fwd: GAATTGGTGGCAAACCTCCC	20	62	55	108
	Rev: AAGCTCACTTTCTCTTCCGGC	21	62	52.38	
ACTB	Fwd: CTCCAGAGCGCAAGTACTCC	20	64	60	90
	Rev: ACTCCTGCTTGCTGATCCAC	20	62	55	

*All primers above were designed against porcine genes

4.9 Genomic DNA Isolation

Genomic DNA was isolated from 3T3 cells and $FN^{(fl/fl)}$; αSMA-Cre^{ERt2}/+ MSFs to determine if the FN1 gene had been deleted in cells treated with Tamoxifen using the GenElute™ Mammalian Genomic DNA miniprep Kit (Sigma Aldrich, CAT#G1N70). First, 5×10^6 cells were harvested by treatment with trypsin to release them from the plastic cell culture flask and placed in a 1.5mL microcentrifuge tube, followed by centrifugation for 5min at 300*g*. Next, the supernatant was carefully removed and discarded, the pelleted cells were resuspended in 200µL of Resuspension Solution, 20µL of RNase A Solution was added to the tube, and the mixture was incubated for 2min at room temperature. Next, 20µL of Proteinase K Solution and 200µL of Lysis Solution C were added to the tube, the contents were thoroughly vortexed, and the tube was incubated at 70°C 10min in a heated block. During the incubation step, a pre-assembled GenElute Miniprep Binding Column was prepared by adding 500µL of Column Preparation Solution to the column and centrifuging it at 12,000*g* for 1min. After the incubation step, 200µL of 95% ethanol was added to the cell lysate and mixed by vortexing until homogenous. Next, the entire contents of the tube were added to the binding column, the column was centrifuged at 6,500*g* for 1min, and the collection tube containing the flow through liquid was discarded and replaced with a new collection tube. Next, the column was washed twice; the first wash was accomplished by adding 500µL of Wash solution to the binding column and centrifuging it at 6,500*g* for 1min and discarding the flow through, and the second wash by adding 500µL of Wash solution and centrifuging at 12,000*g* for 3min and then discarding the flowthough. Lastly, the binding column was placed in a fresh 2mL collection tube, 100µL of Elution Solution was added to the column, and the column was centrifuged at 6,500*g* to elute the DNA. The DNA obtained was then either stored at -20°C or used in deletion PCR experiments.

4.10 Deletion Polymerase Chain Reaction

To determine whether the FN gene had been deleted in $FN^{(fl/fl)}$; αSMA-Cre^{ERt2}/+ MSFs treated with and without Tamoxifen, genomic DNA was isolated as described above and mixed with reagents from the ZmTech Taq Polymerase Kit (ZmTech Scientifique, CAT#T207025). First, 2µL of DNA was mixed with 2.5µL of 10X PCR Buffer (provided in the kit), 0.5µL of 10mM dNTP mix, 1µL of each primer (forward and reverse), 0.2µL of Taq DNA Polymerase (provided in the

kit), and RNAse-free H_2O up to a volume of 25µL. The mixture was mixed thoroughly by pipetting up and down gently to avoid shearing the DNA and was subsequently incubated for 5min at 94°C in a Peltier thermal cycler to begin the PCR reaction. Next, the mixture was incubated for 40 cycles in the following order: 94°C for 1min, 56°C for 30s, and 72°C for 1min 40s.

During the PCR cycling, a 1.7% agarose gel was made by mixing 40mL of Tris-acetate-EDTA with 0.68g of agarose (Fisher Scientific, CAT#BP1356-500), heating the mixture until the agarose was completely dissolved, adding 2.4µL of 1% ethidium bromide (Fisher Scientific, CAT#BP1302-10) to the heated mixture, and pouring it into a gel mould. After the gel solidified, it was removed from the mould and placed in a gel electrophoresis chamber containing sufficient Tris-acetate-EDTA + ethidium bromide solution to cover the gel.

Upon completion of the thermal cycling, the mixture was cooled to 4°C and 5µL of purple 6X Gel Loading Dye (New England BioLabs, Inc., CAT#B7024S) was added and mixed by pipetting. Next, the 12µL of the PCR mixture was placed in the wells of the gel and 12µL of 100bp DNA ladder (2µL ladder + 2µL loading dye + 8µL RNAse-free H_2O) was placed in a separate well for DNA fragment length determination. Once the gel was loaded, electrophoresis at 100 volts was conducted until the leading edge of the mixture migrated ½ to ¾ the length of the gel. Lastly, the gel was removed from the electrophoresis chamber and imaged using a Gel Logic 200 UV imaging system.

Table 2. Primers used for Deletion PCR.

Target	Sequence (5'→3')	Expected Product Length
Mouse FN1	Fwd: GTACTGTCCCATATAAGCCTCTG Rev: GCCAATAACCCCAGCTCTGTAG	Intact FN1 gene: 1200bp Deleted FN1 gene: 380bp

4.11 Quantification

4.11.1 Stain Quantification in Monolayer Engineered Blood Vessels

To quantify the change in protein production shown in immunohistochemistry images, entire monolayer engineered blood vessel sections were imaged at 200x using an AxioImager M2 microscope set to brightfield mode (Zeiss). ImageJ was used to measure the pixel intensity of the tissue sections only by outlining the tissues and using the "measure" tool within the software (Schneider et al., 2012). Next, using Microsoft Excel software, the average pixel intensity values from ImageJ (Schneider et al., 2012) were subtracted from 255, the maximum possible pixel intensity value, the resulting numbers were averaged for each condition, the standard deviation of each data set was calculated, and the significance determined using the two tailed t-test. All results were graphed using OriginPro 2017 software.

4.11.2 Fiber Quantification in Immunofluorescence

ECM fibers were quantified using the following method developed in the lab. Single-channel images were opened in ImageJ software and converted to 8-bit format and a threshold was applied to isolate the fibers in each image (thresholds were the same in images stained for the same proteins but varied from protein to protein). Next, noise was reduced by using the "despeckle" function three times for each image and the scale was set for each image (images are 2048x2048 pixels, equivalent to 332.8μm × 332.8μm). Next, the images were "skeletonized" using the skeleton plugin and the skeletons were analyzed using the "analyze skeleton" function (Schneider et al., 2012). Data from this measurement were then saved and opened in Microsoft Excel where they were averaged and graphed.

5 RESULTS: CHAPTER 1

5.1 Human plasma FN increases the production of some elastogenic proteins by PAoSMCs in tubular collagen gels.

To determine whether exogenously added human plasma FN may alter the production and deposition of elastic fiber related proteins by PAoSMCs seeded in tubular collagen gel constructs, which were either untreated or treated with 0.05mg/mL of exogenous human plasma FN for 3 or 7 days, immunohistochemistry was performed on paraffin-embedded sections. The construct sections were stained with antibodies against total FN (plasma and cellular FN), cellular FN (EDA FN), TE, FBN-1, FBN-2, FBLN-4, FBLN-5, LOX, and LTBP-4. As expected, at day 3, constructs matured with supplemental plasma FN showed a significant 2-fold increase in total FN demonstrating that the added plasma FN is retained within the constructs. Endogenously produced cellular FN was also significantly increased by almost 3-fold, albeit at a low base level. FBN-1 and LOX deposition increased modestly at day 3 by about 39 and 30%, respectively, whereas all other tested proteins changed very little (FBN-2, FBLN-4), or not at all (TE, FBLN-5, LTBP-4) (Figure 9a). At day 7, plasma FN-matured constructs still retained the added FN, whereas the endogenous cellular FN production was unchanged compared to the controls. Importantly, the deposition of TE was significantly enhanced (53%) after 7 days of culture. Some other critical proteins required for elastic fiber formation were also significantly increased at this time point, including FBN-1 (79%), LOX (44%), and LTBP-4 (63%); whereas the other tested proteins remained unchanged (Figure 9b).

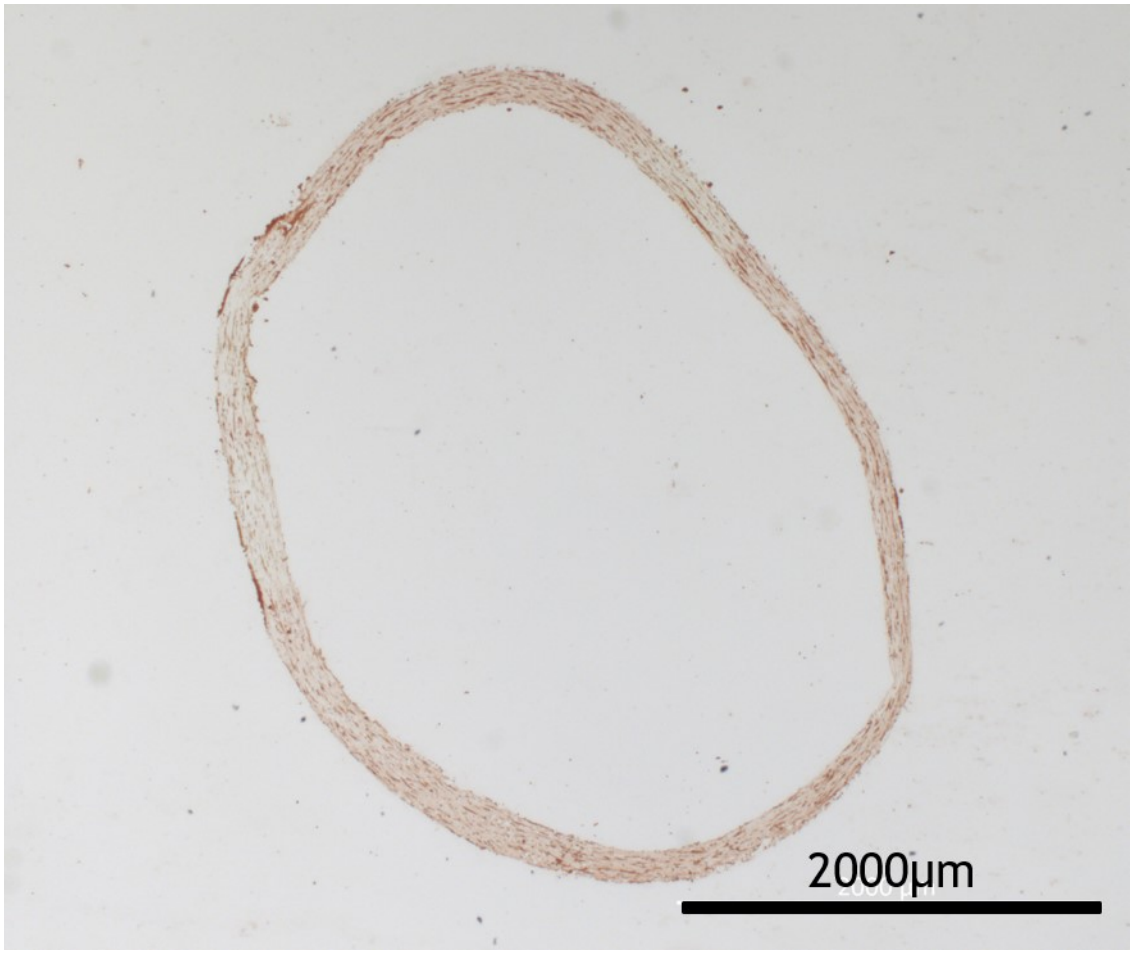

Figure 8. Overview of cellularized monolayer tubular collagen constructs. The monolayer constructs have a large lumen about 2.5-3.0mm in diameter with a thin "vessel wall" composed of Type I collagen and PAoSMCs.

Figure 9a.

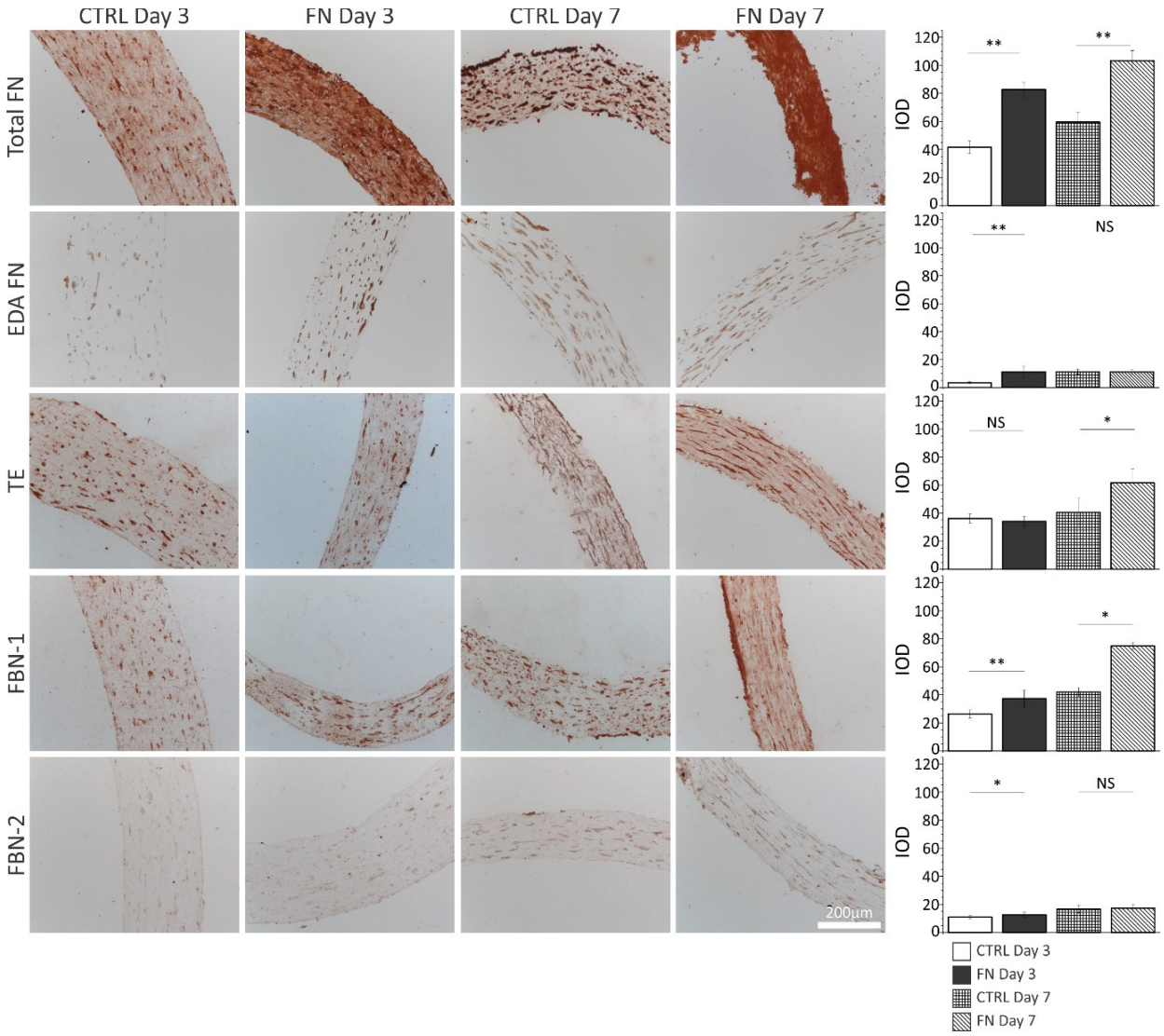
CTRL Day 3
FN Day 3
CTRL Day 7
FN Day 7
Total FN
EDA FN
TE
FBN-1
FBN-2
200μm
IOD
**
**
**
NS
NS
*
**
*
*
NS
CTRL Day 3
FN Day 3
CTRL Day 7
FN Day 7

Figure 9b.

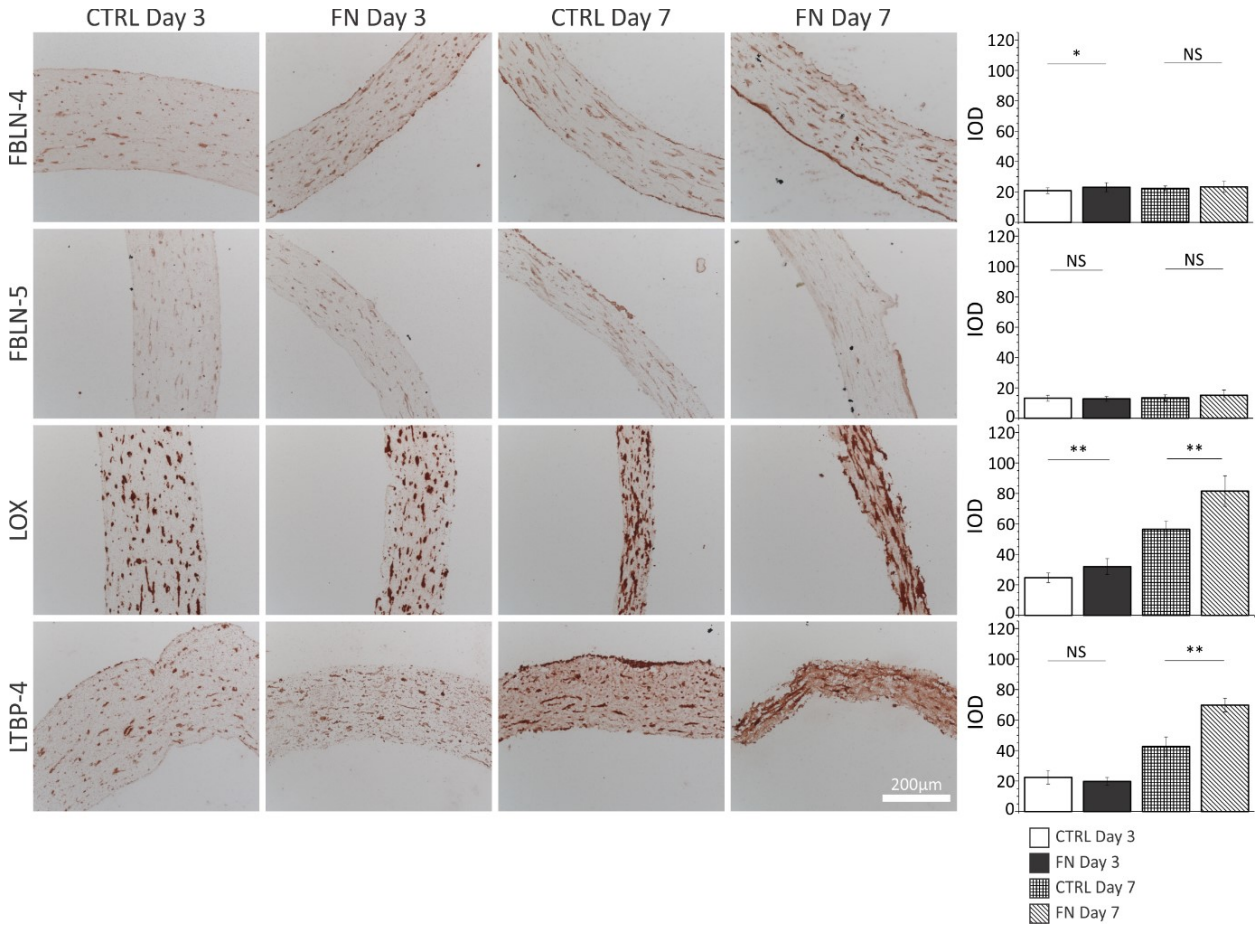

Figure 9. Human plasma FN increases production of TE, FBN-1 (Fig. 9a), LOX, and LTBP-4 (Fig. 9b) by SMCs in tubular collagen gel constructs. Tubular collagen constructs cellularized with PAoSMCs were grown for 3 or 7 days in the absence (CTRL) or presence of exogenously added 0.05 mg/mL plasma FN (FN). The constructs were fixed and stained for critical extracellular matrix proteins associated with elastic fiber formation, including in (fig. 9a) total fibronectin (total FN), EDA fibronectin (EDA FN), tropoelastin (TE), fibrillin-1 (FBN-1), fibrillin-2 (FBN-2), and in (fig. 9b) fibulin-4 (FBLN-4), fibulin-5 (FBLN-5), lysyl oxidase (LOX), and latent TGF-β binding protein-4 (LTBP-4). Nuclear counterstain was omitted to allow quantification of the specific signals shown on the right side (*p-value<0.01, **p-value<0.001, NS= non-significant). The scale bar represents 200 µm for all images.

5.2 Human plasma FN causes alterations in the RNA levels of elastogenic proteins in PAoSMCs.

To investigate whether supplementation with human plasma FN induced any change in ECM protein expression in PAoSMCs, quantitative PCR was conducted. RNA was isolated from control and plasma FN supplemented 3 day old and 7 day old cellularized, disk-shaped collagen gels. RT-PCR was performed to generate cDNA from the RNA transcripts, and qPCR was performed using the cDNA and specific primers generated against fibronectin (FN), fibrillin-1 (FBN1), fibrillin-2 (FBN2), fibulin-4 (FBLN4), fibulin-5 (FBLN5), lysyl oxidase (LOX), latent TGF-β binding protein 4 (LTBP4), and elastin (ELN). Results showed that supplementation with human plasma FN causes changes in the expression patterns of the ECM proteins shown, particularly elastin and fibrillin-1 (Figure 10).

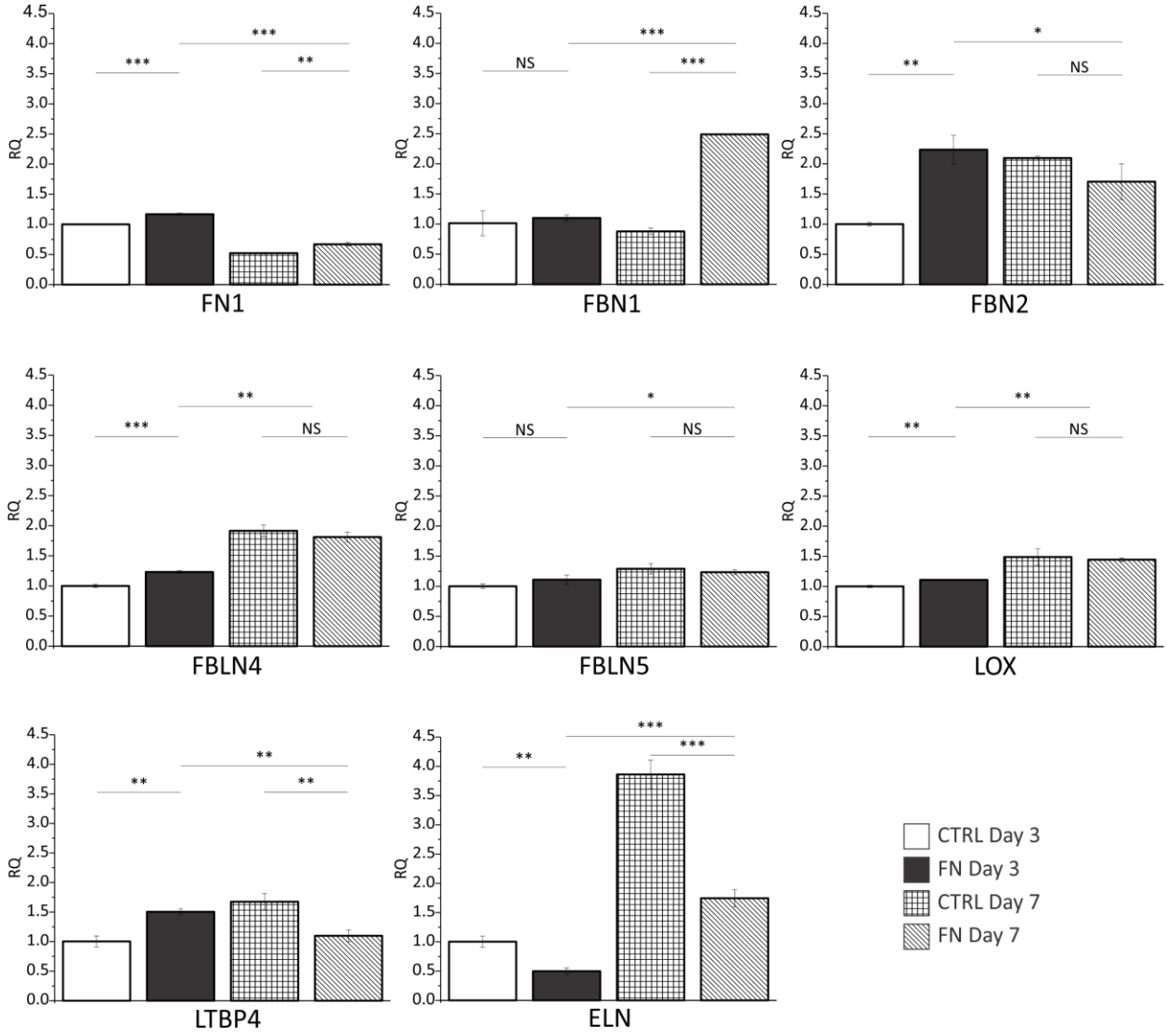

Figure 10. Human plasma FN causes alterations in the RNA levels of elastogenic proteins in PAoSMCs embedded in disk-shaped collagen gels. Relative expression of elastic fiber related protein expression including fibronectin (FN1), fibrillin-1 (FBN1), fibrillin-2 (FBN2), fibulin-4 (FBLN4), fibulin-5 (FBLN5), lysyl oxidase (LOX), latent TGF-β binding protein 4 (LTBP4), and elastin (ELN). *p-value < 0.05, **p-value < 0.01, ***p-value < 0.001, NS = non significant.

5.3 Human plasma FN increases the assembly of elastic fibers by PAoSMCs in 2D cell culture.

To further test whether exogenously added-plasma FN drives only the enhancement of the deposition of elastic fiber-related proteins or also the assembly of elastic fibers and related proteins, PAoSMCs were seeded directly on 2D glass slides (in the absence of a 3D collagen scaffold) and analysed through immunofluorescence staining. This method allows a more detailed view of assembly of matrix fibers as compared to the immunohistochemistry used previously. The PAoSMCs were cultured for 3 or 7 days in the presence or in the absence of exogenous plasma FN (0.05mg/mL), and stained for total FN (plasma and cellular FN), cellular FN (EDA FN), TE, FBN-1, FBN-2, FBLN-4, FBLN-5, LOX, and LTBP-4. After 3 days of maturation with supplemental plasma FN, both total FN and FBLN-4 showed prominent increases in the number and maturity of fibers, whereas extracellular deposition of the other proteins tested remained unchanged (Figure 11). After 7 days of PAoSMCs maturation in the presence of supplemental plasma FN, marked increases in the number and maturity of the ECM fibers were observed for total FN, TE, FBN-1, FBN-2, FBLN-4, FBLN-5, and LOX, while LTBP-4 showed a modest increase and EDA FN showed no change (Figure 11). Quantification was accomplished using a protocol made in the lab (see materials and methods). The total number of fiber branches (Figure 12a) and average fiber branch (Figure 12b) length correlated well with the images.

Figure 11a.

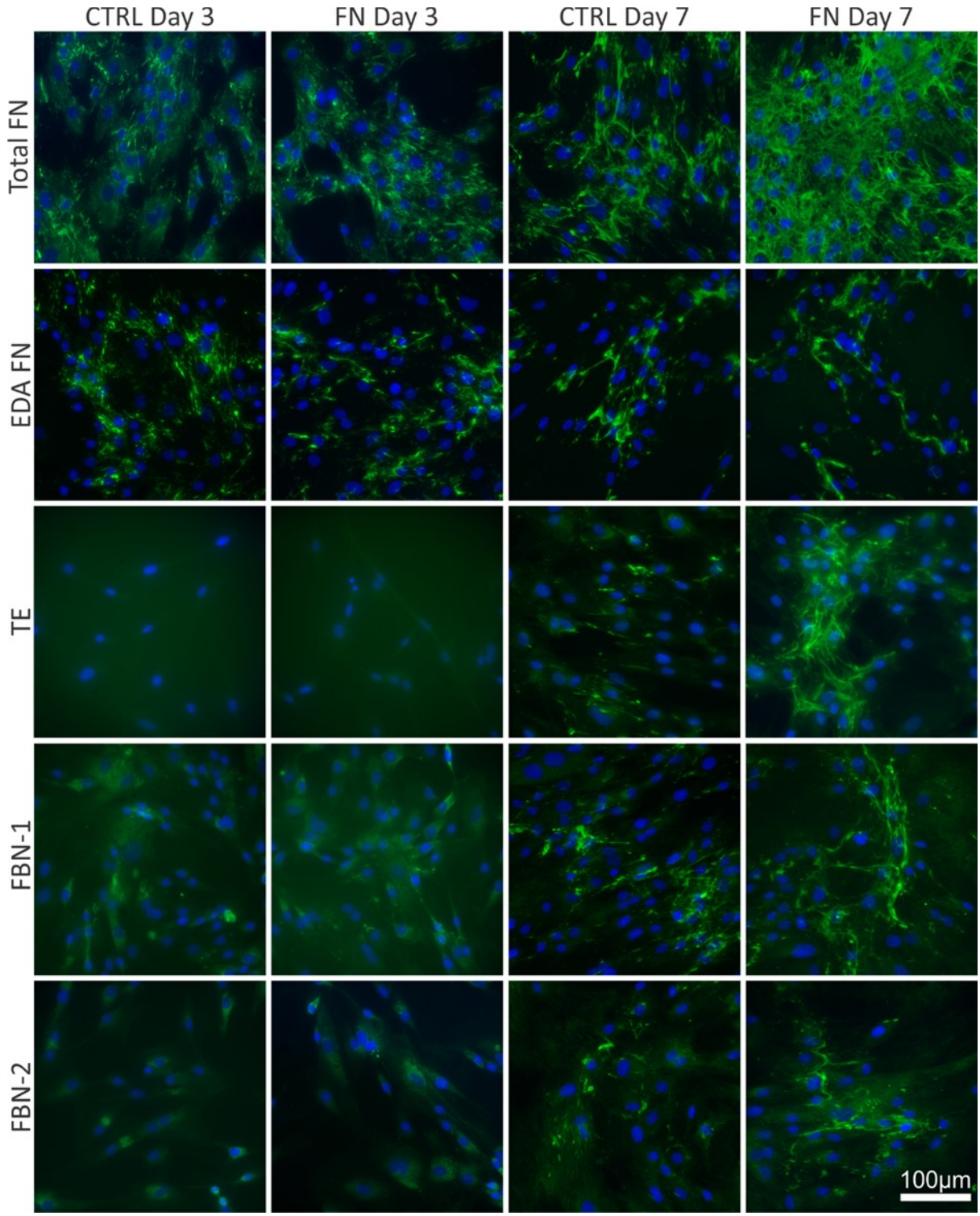
CTRL Day 3
FN Day 3
CTRL Day 7
FN Day 7
Total FN
EDA FN
TE
FBN-1
FBN-2
100µm

Figure 11b.

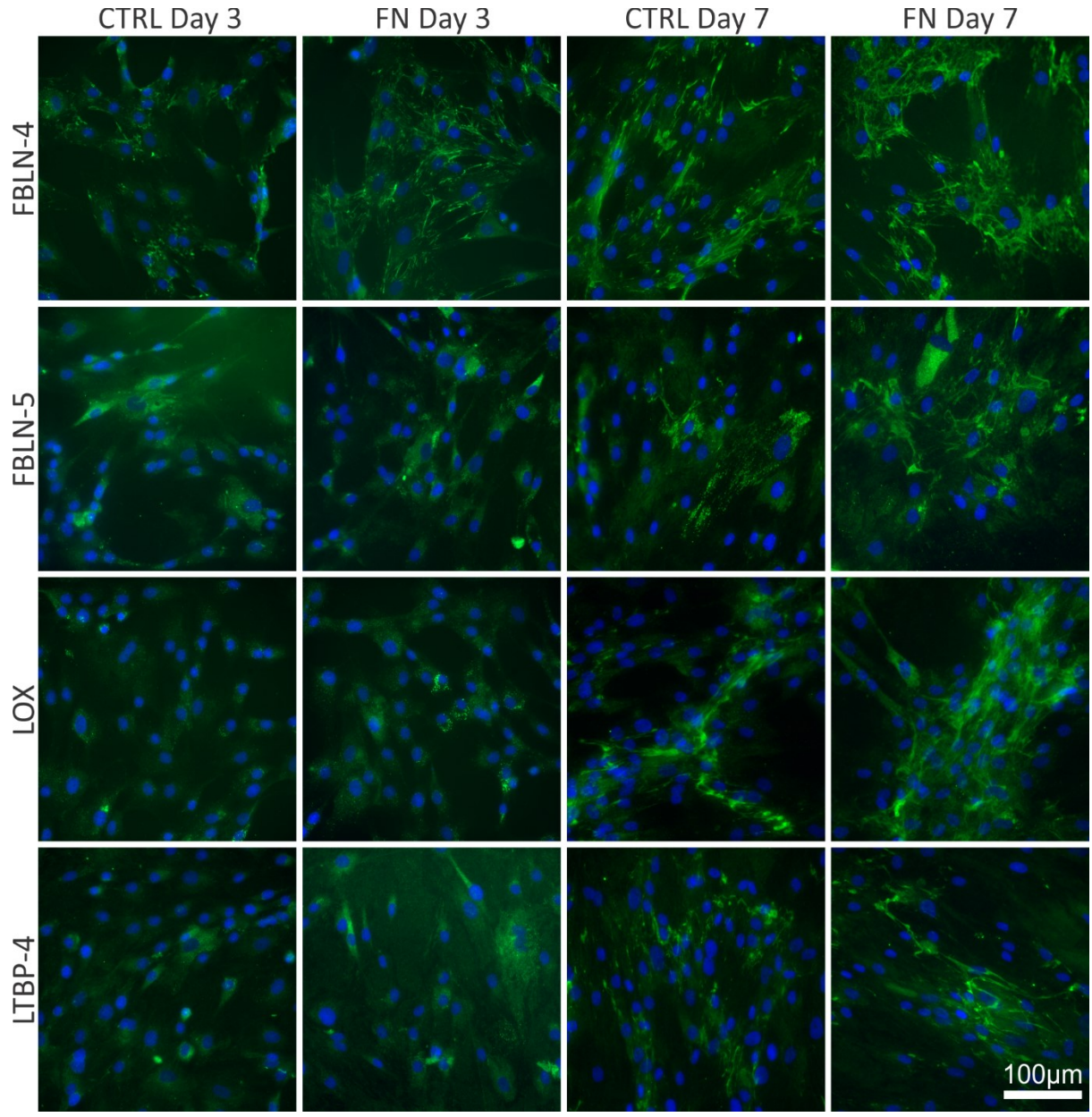
CTRL Day 3
FN Day 3
CTRL Day 7
FN Day 7
FBLN-4
FBLN-5
LOX
LTBP-4
100µm

Figure 11. 2D Immunofluorescence analysis of adult PAoSMCs. Adult PAoSMCs (20,000 per well) were seeded and cultured in 8-well immunofluorescence slides for 3 or 7 days in the absence (CTRL) or presence (FN) of 0.05 mg/mL exogenous plasma FN. After culturing, the cells were fixed and stained for proteins (green) associated with elastic fiber formation, including in (fig. 11a) total fibronectin (Total FN), cellular fibronectin (EDA FN), tropoelastin (TE), fibrillin-1 (FBN-1), fibrillin-2 (FBN-2), and in (fig. 11b) fibulin-4 (FBLN-4), fibulin-5 (FBLN-5), lysyl oxidase (LOX), and latent TGF-β binding protein-4 (LTBP-4). Cell nuclei are counterstained with DAPI (blue). The scale bar represents 100μm for all images.

Figure 12a.

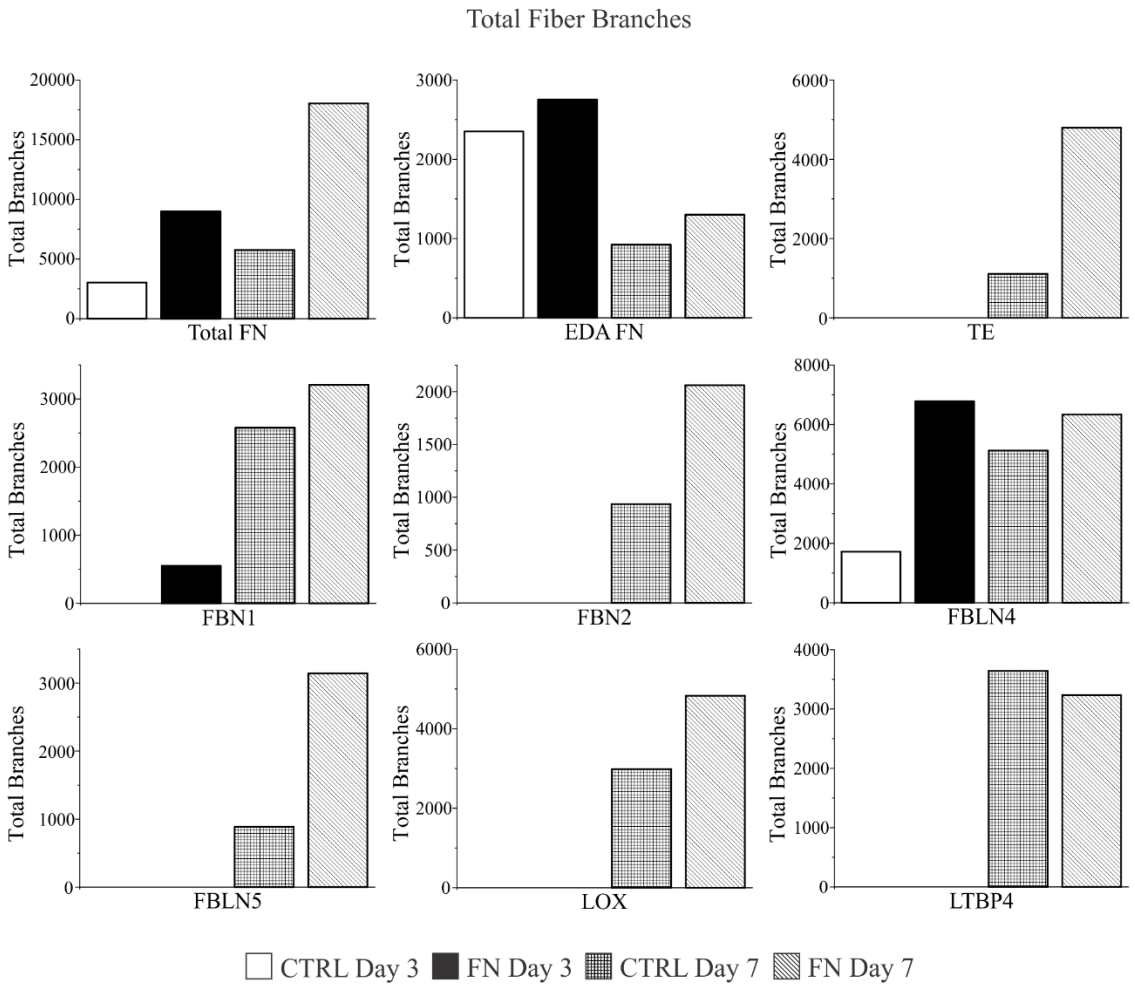

Figure 12b.

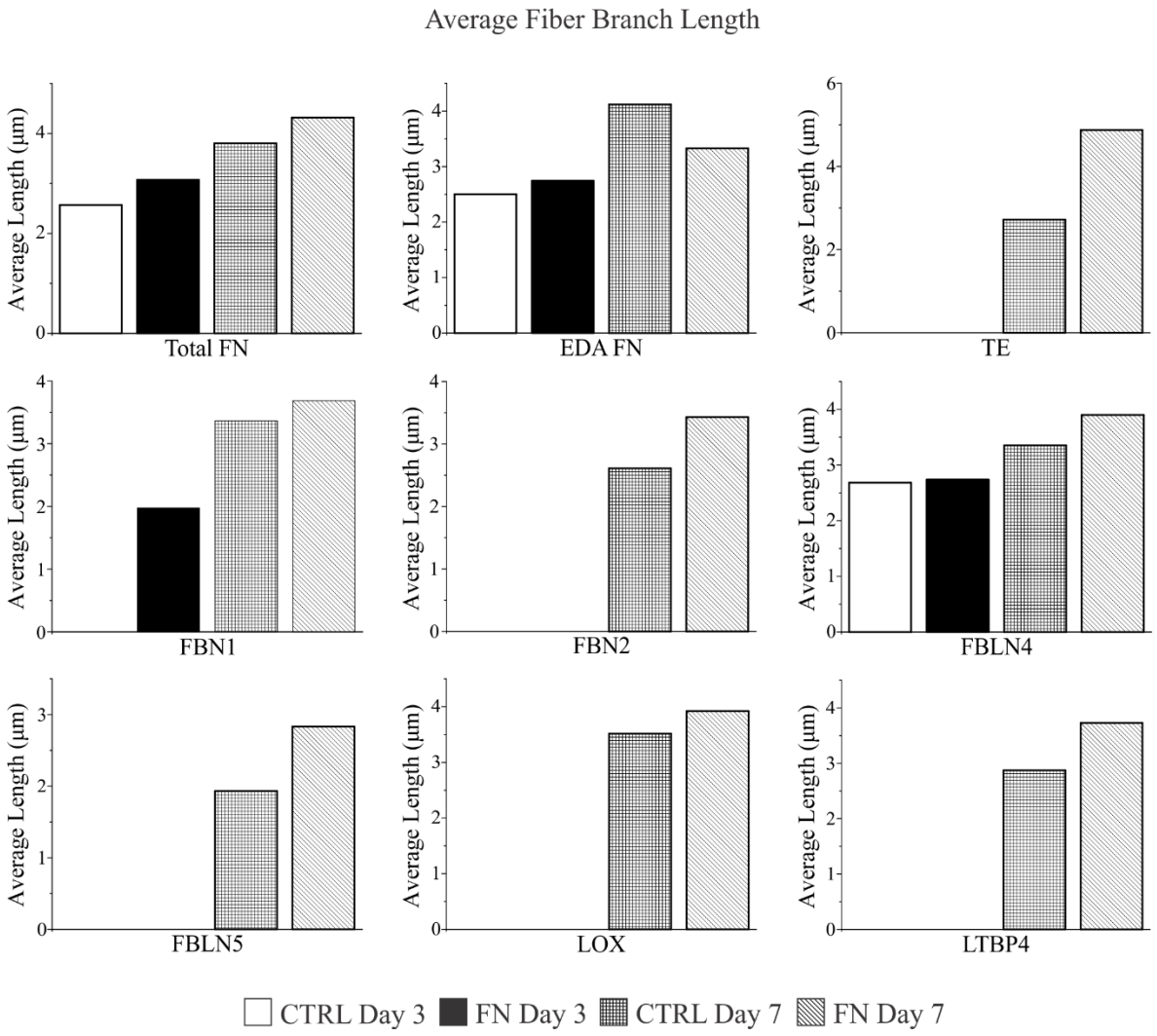

Figure 12. Quantifications of the Total Fiber Branches and Average Fiber Branch Length of immunofluorescence images. Quantifications closely match the observed results in Figure 11, with human plasma FN supplemented conditions showing increases in both the total number of fiber branches and the average length of the fiber branches. Abbreviations are as follows: total fibronectin (Total FN), cellular fibronectin (EDA FN), tropoelastin (TE), fibrillin-1 (FBN1), fibrillin-2 (FBN-), fibulin-4 (FBLN4), fibulin-5 (FBLN5), lysyl oxidase (LOX), and latent TGF-β binding protein-4 (LTBP4).

5.4 Some elastin produced by PAoSMCs seeded in collagen gel vascular constructs is mature, crosslinked elastin.

To investigate whether the elastin produced by PAoSMCs seeded in collagen gel vascular constructs was mature and crosslinked, autofluorescence experiments were conducted. Autofluorescence of mature elastin is caused by the presence of multiple desmosine and isodesmosine residues in mature elastin, which are formed by the crosslinking of tropoelastin monomers. These residues contain aromatic ring structures with unconjugated pi electrons capable of absorbing light between 495-570nm and releasing the absorbed energy as a lower energy photon of roughly 520nm. Paraffin-embedded sections of tubular collagen gel constructs seeded with adult PAoSMCs were deparaffinised, rehydrated, and mounted for analysis using 495nm light. Only the day 7 time point was analysed because previous immunohistochemical staining for tropoelastin showed no significant change in tropoelastin production when for constructs supplemented with human pFN. Results showed an increase in the autofluorescence signal in sections supplemented with human pFN, revealed by the increased brightness of structures within the constructs and the overall increase in contrast, as lower exposure times had to be used to visualize the constructs supplemented with human pFN compared to the control constructs. The increase in autofluorescence signal indicates the presence of mature, biologically functional elastin. Interestingly, some short fibers appeared to exist within the collagen gel constructs, matching the immunohistochemistry results for tropoelastin-stained sections shown previously (Figure 13).

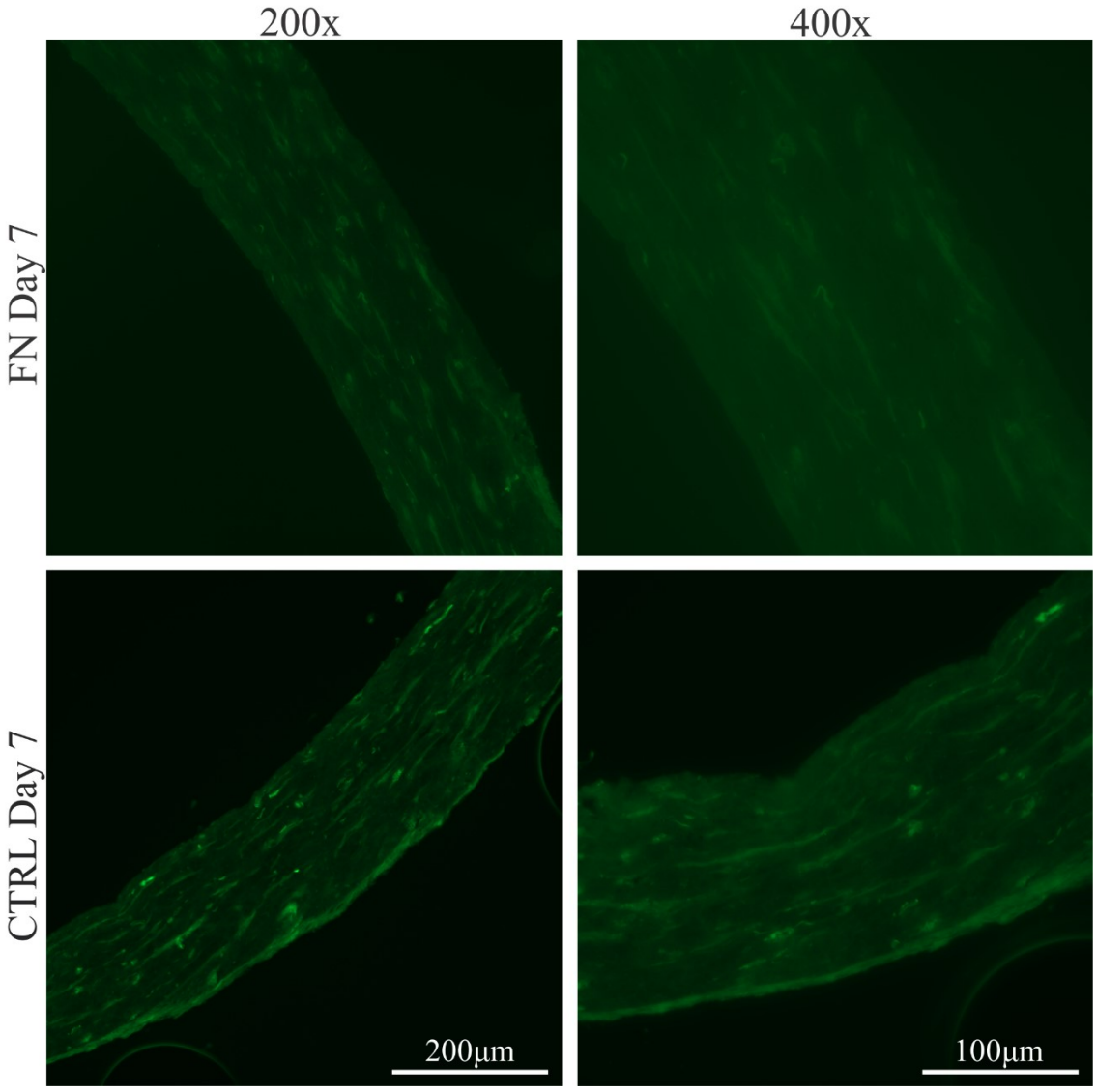

Figure 13. Autofluorescence analysis of tubular collagen gel constructs cellularised with adult PAoSMCs. Tubular collagen constructs cellularized with PAoSMCs were grown for 7 days in the absence (CTRL) or presence of exogenously added 0.05 mg/mL plasma FN (FN). Constructs were prepared for autofluorescence analysis by deparaffinization and rehydration according to the methods section. The prepared sections were analyzed using 495nm light and imaged at 200x and 400x as shown in the images. The scale bar in 200x images is 200µm and the scale bar in 400x images is 100µm.

5.5 Co-culturing SMCs with other cell types normally found in blood vessels can induce changes in production of some elastic fiber related proteins by SMCs.

To investigate the role of fibroblasts and endothelial cells in the production of elastic fiber related proteins by SMCs seeded in multilayer, tubular collagen gel-based constructs, immunohistochemistry was performed on paraffin-embedded sections. The constructs were matured statically for 7 or 14 days in the following conditions: Mono, comprising only collagen seeded with SMCs; BiEC, comprising collagen seeded with SMCs and lumenally lined with a monolayer of endothelial cells; BiFB, comprising an outer layer of collagen seeded with fibroblasts and an inner layer of collagen seeded with SMCs; and Tri, comprising an outer layer of fibroblasts, and inner layer of SMCs, and a luminal monolayer of endothelial cells (all cells are human). The construct sections were stained with antibodies against total FN (plasma and cellular FN), cellular FN (EDA FN), TE, FBN-1, FBLN-4, FBLN-5, LOX, and LTBP-4. Only the SMC layers are comparable, as SMCs are the only cell type found in all the constructs. Results are preliminary as the experiment was only performed once.

In the day 7 BiEC constructs, there was a slight increase in FBLN-5 while there were no changes in production of any other proteins (LOX omitted due to improper staining). In the day 7 BiFB constructs, there was an increase in FBN-1, were slight increases in production of several proteins, including total FN, FBLN-4, FBLN-5, and LTBP-4, and no changes in the remaining proteins. In the day 7 Tri constructs, there were major increases in production of both FBN-1 and TE, increases in LOX (as compared to BiEC and BiFB conditions) and LTBP-4, slight increases in total FN and FBLN-5, and no changes in the remaining proteins (Figure 15).

In the day 14 BiEC constructs, there was a decrease in LOX production, slight decreases in TE and LTBP-4, and no changes in the remaining proteins. In the day 14 BiFB constructs, there was a slight increase in TE but no changes in all other proteins. In the day 14 Tri constructs, there was a slight increase in TE production, a slight decrease in total FN production, and no changes in the production of all other proteins (Figure 16).

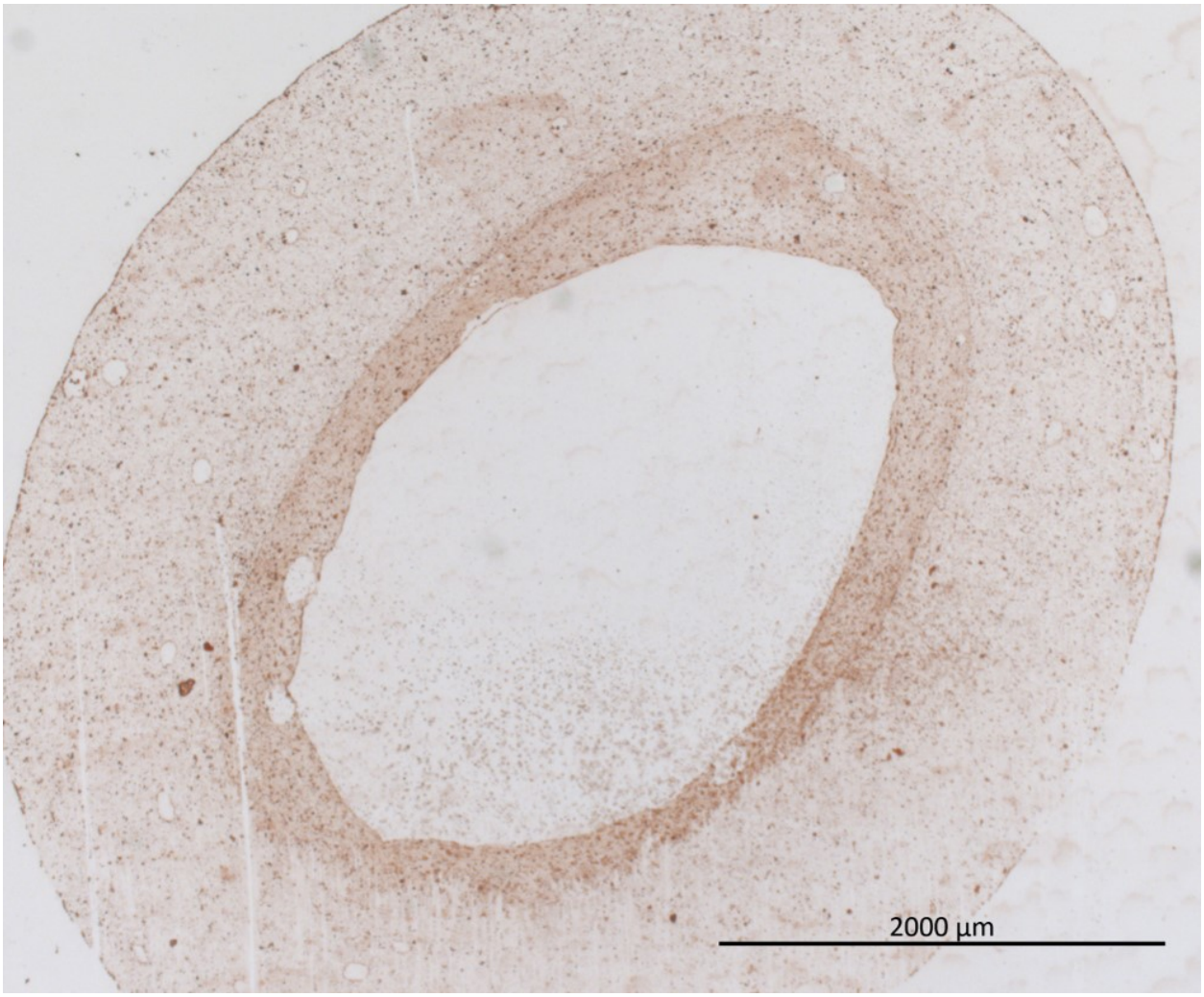

Figure 14. Overview of cellularized multilayered collagen gel constructs. The multilayered constructs have a human endothelial cell-lined lumen about 2.0-2.5mm in diameter with a thick "vessel wall" composed of Type I collagen seeded with human fibroblasts (outer layer) and human SMCs (inner layer). The multilayered constructs more closely resemble native small-diameter muscular arteries such as the coronary arteries.

Figure 15a.

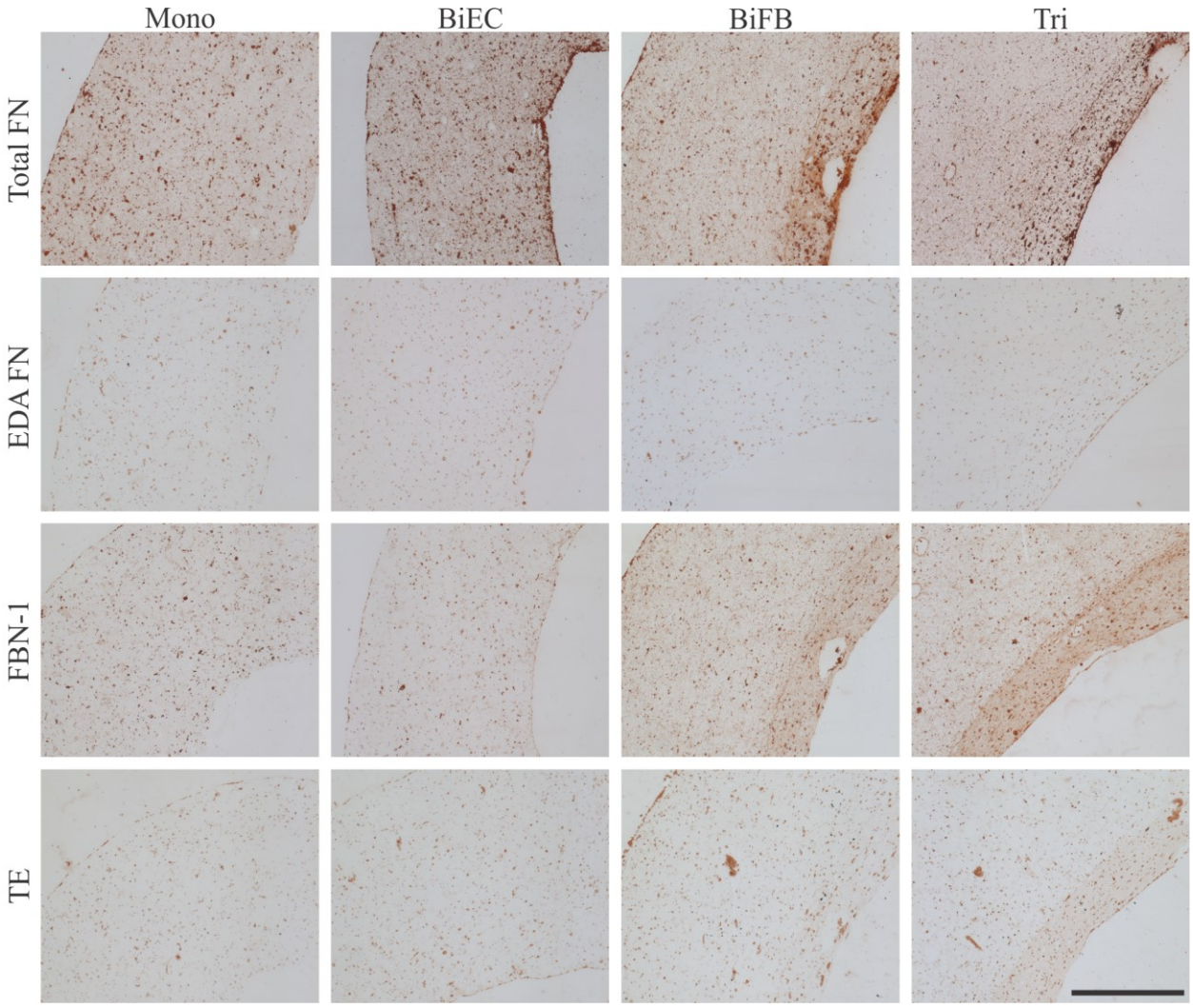

Figure 15b.

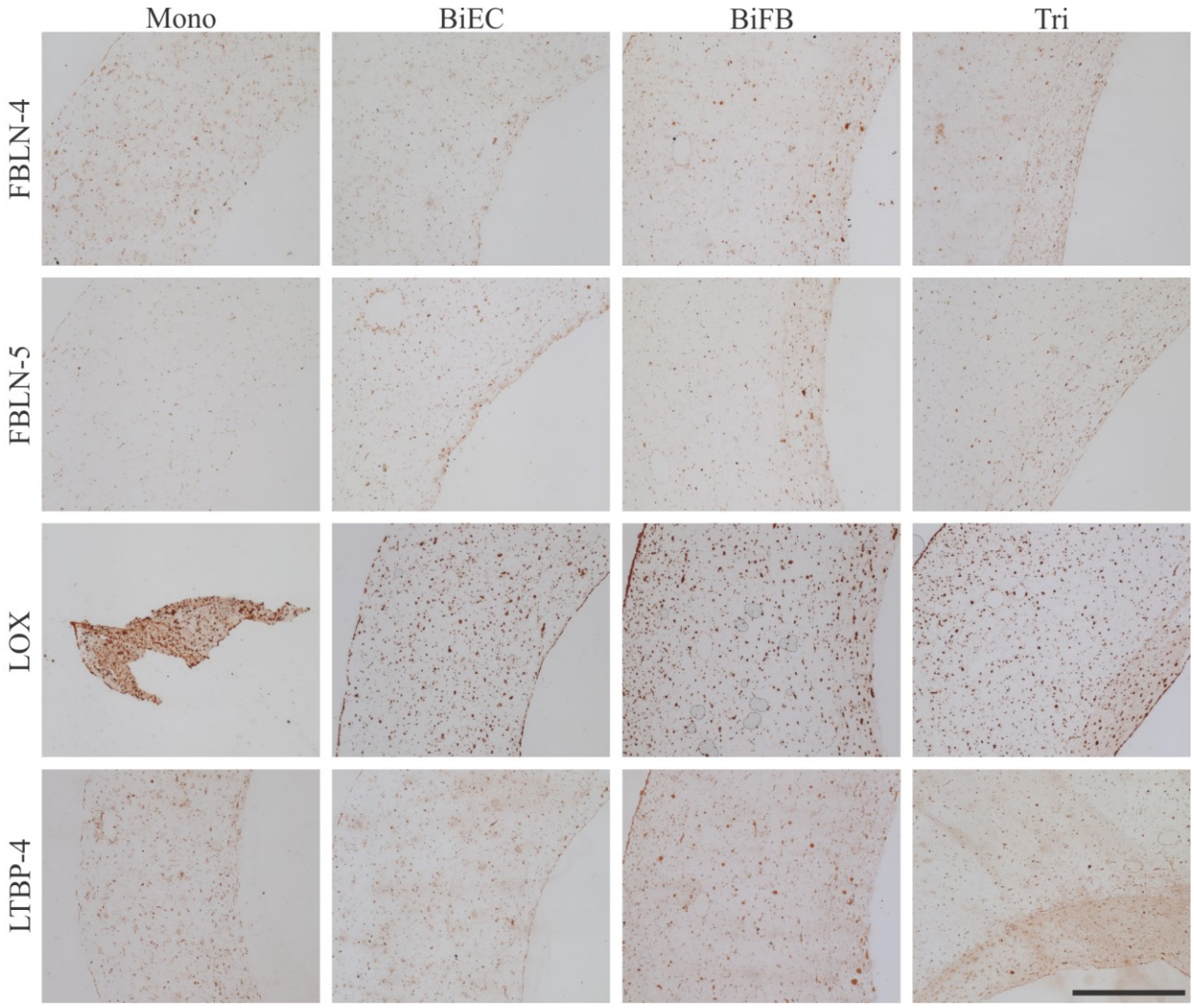

Figure 15. Immunohistochemical analysis of cellularized multilayered tubular collagen constructs matured for 7 days. Tubular collagen constructs cellularized with human SMCs, FBs, and ECs were grown for 7 days in various co-culture conditions: Mono, only SMCS; BiEC, SMCs + ECs; BiFB, FBs + SMCs; Tri, FBs + SMCs + ECs. The constructs were fixed and stained for critical extracellular matrix proteins associated with elastic fiber formation, including in (fig. 15a) total fibronectin (total FN), EDA fibronectin (EDA FN), tropoelastin (TE), fibrillin-1 (FBN-1), and in (fig. 15b) fibulin-4 (FBLN-4), fibulin-5 (FBLN-5), lysyl oxidase (LOX), and latent TGF-β binding protein-4 (LTBP-4). Scale bars represents 500μm.

Figure 16a.

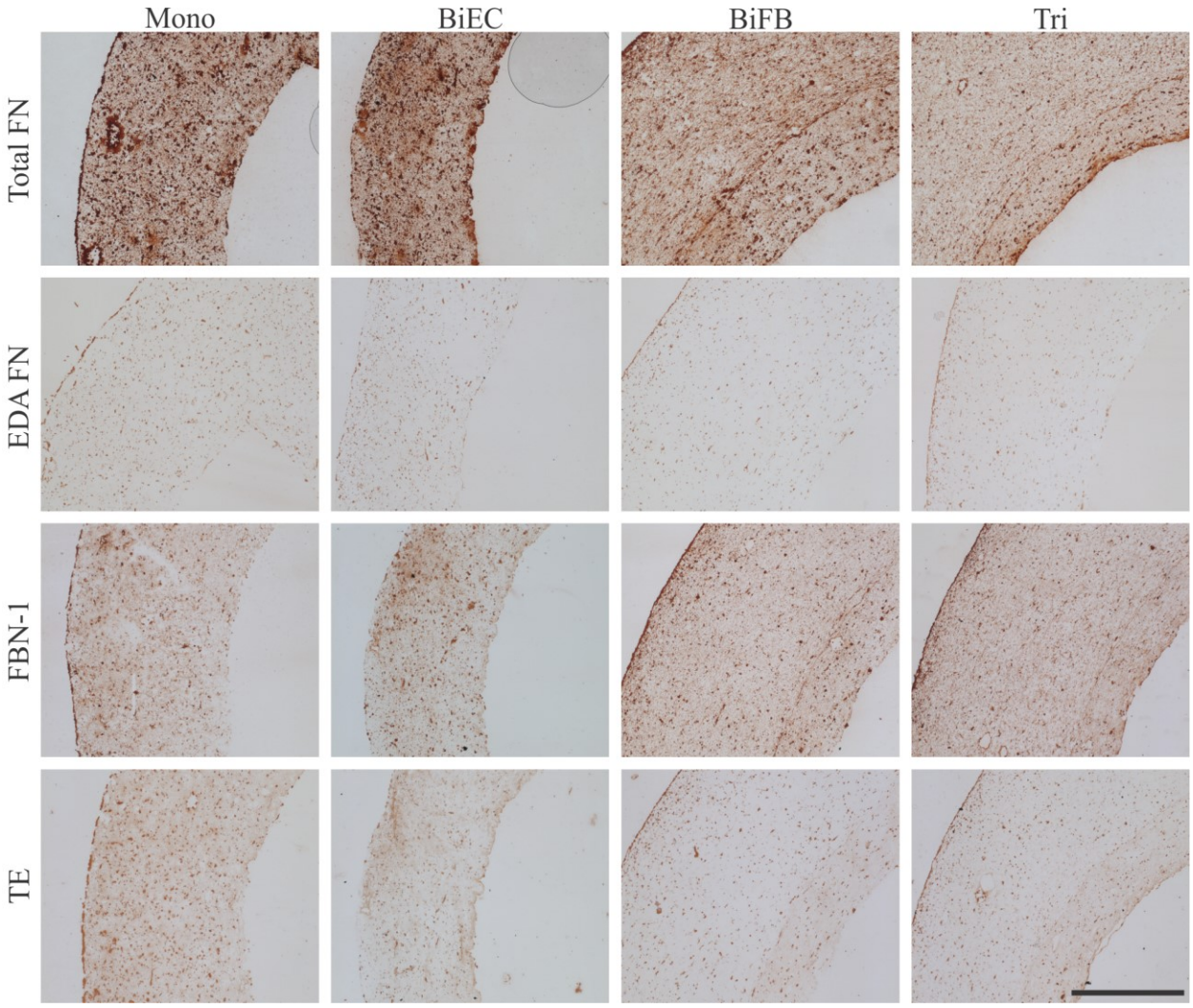

Figure 16b.

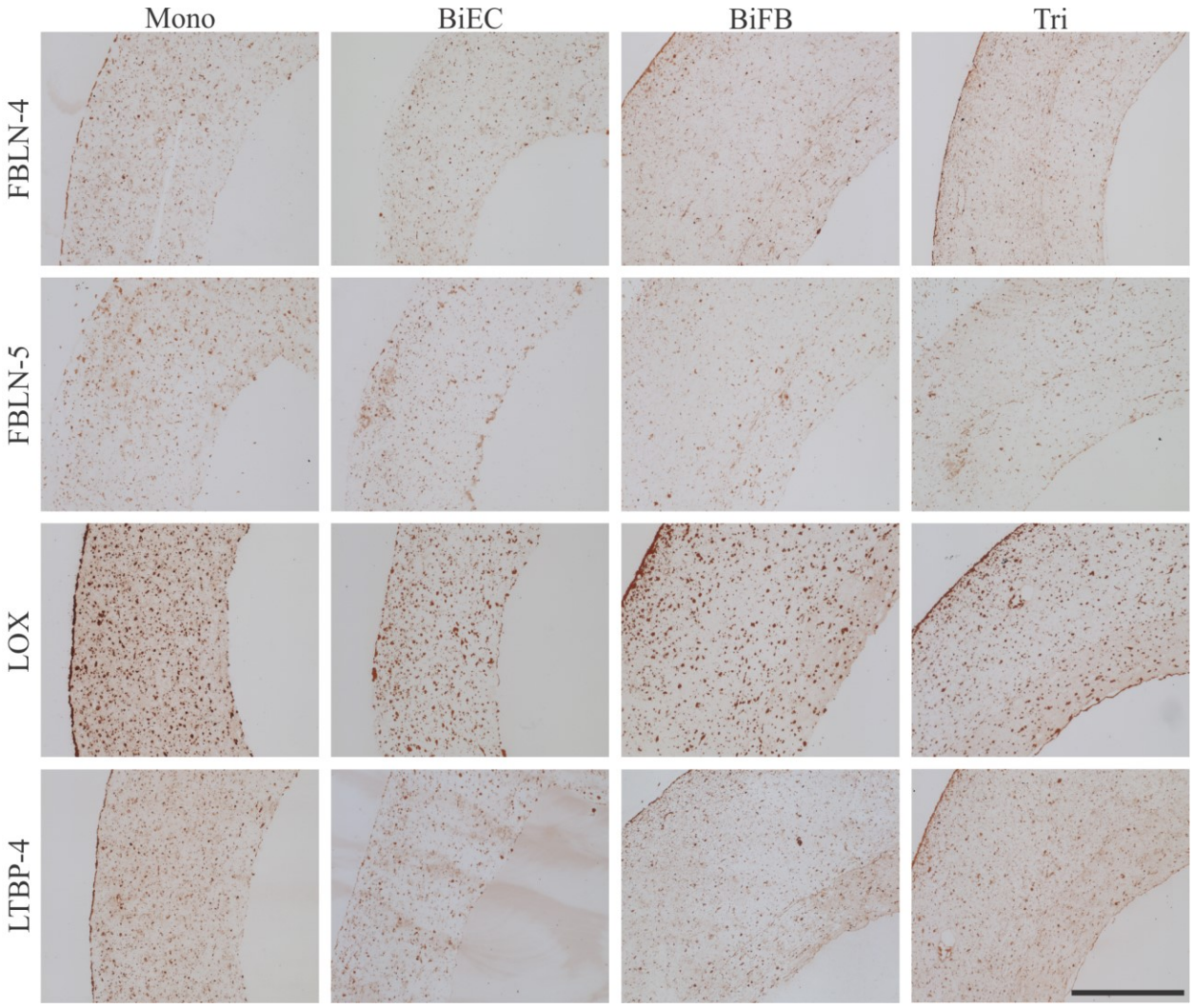

Figure 16. Immunohistochemical analysis of cellularized multilayered tubular collagen constructs matured for 14 days. Tubular collagen constructs cellularized with human SMCs, FBs, and ECs were grown for 14 days in various co-culture conditions: Mono, only SMCS; BiEC, SMCs + ECs; BiFB, FBs + SMCs; Tri, FBs + SMCs + ECs. The constructs were fixed and stained for critical extracellular matrix proteins associated with elastic fiber formation, including in (fig. 16a) total fibronectin (total FN), EDA fibronectin (EDA FN), tropoelastin (TE), fibrillin-1 (FBN-1), and in (fig. 16b) fibulin-4 (FBLN-4), fibulin-5 (FBLN-5), lysyl oxidase (LOX), and latent TGF-β binding protein-4 (LTBP-4). Scale bars represents 500μm.

5.6 FN fragments increases the production of some elastogenic proteins by PAoSMCs in disk-shaped collagen gels.

To investigate the role of the integrin-binding RGD sequence of FN in the production of elastic fiber related proteins by SMCs seeded in disk-shaped, planar collagen gel-based constructs, immunohistochemistry was performed on paraffin-embedded sections. The constructs were matured statically for 3 or 7 days with either 0.05mg/mL supplemental full-length human EDA FN (FN WT condition), 0.05mg/mL of a short fragment of human EDA FN ($FNIII_8$-EDA_RGD) containing the intact RGD sequence (FN RGD condition), or 0.05mg/mL of the identical short fragment except with a non cell-binding RGA mutation ($FNIII_8$-EDA_RGA; FN RGA condition) (Figure 17). The construct sections were stained with antibodies against FBN-1, TE, FBLN-4, FBLN-5, LOX, and LTBP-4.

In the 3 day matured constructs, there were increases for all added fragments tested in FBN-1, TE, and LOX production by SMCs as compared to the control while there were no differences between the fragments themselves in terms of protein deposition. There were no changes in deposition of any other proteins investigated, despite construct supplementation with full length EDA FN or short EDA FN fragments (Figure 18a). In the 7 day matured constructs, there was a substantial increase in the production of FBN-1, slight increases in production of TE, FBLN-4, and LOX, and no change in the production of any remaining proteins investigated. Again, there were no differences between the FN WT, FN RGD, and FN RGA conditions despite any changes in production compared to the control (Figure 18b).

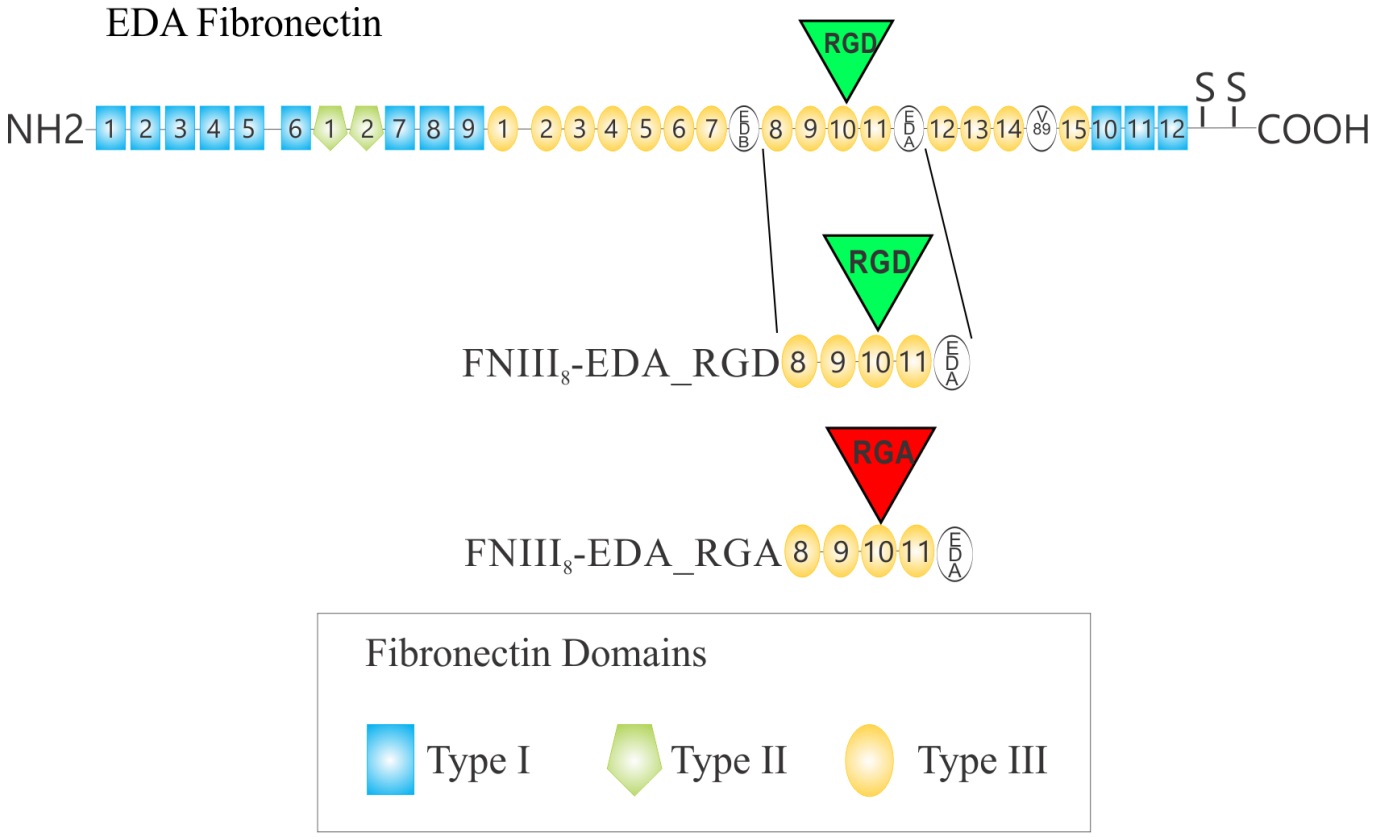

Figure 17. Structure of EDA Fibronectin and EDA Fibronectin Fragments. The three structures above represent the EDA FN protein used for the experiments in section 5.6. EDA FN was used in the FN WT condition, FNIII$_8$-EDA_RGD was used in the FN RGD condition, and FNIII$_8$-EDA_RGA was used in the FN RGA condition. FNIII$_8$-EDA_RGA contains a D → A mutation (aspartic acid → alanine), resulting in loss of function of the integrin-binding RGD site. Figure modified from Rongmo Zhang.

Figure 18a.

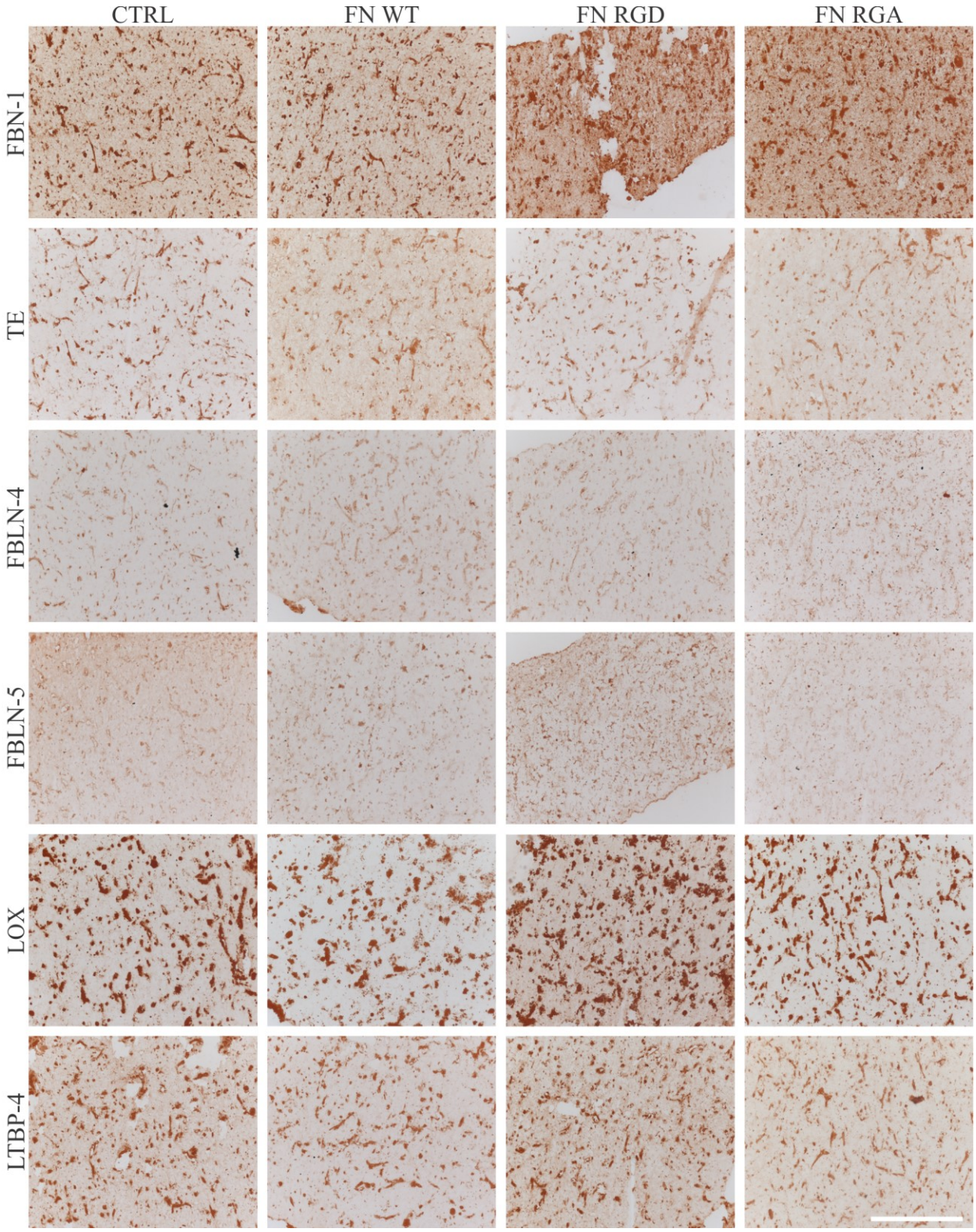

Figure 18b.

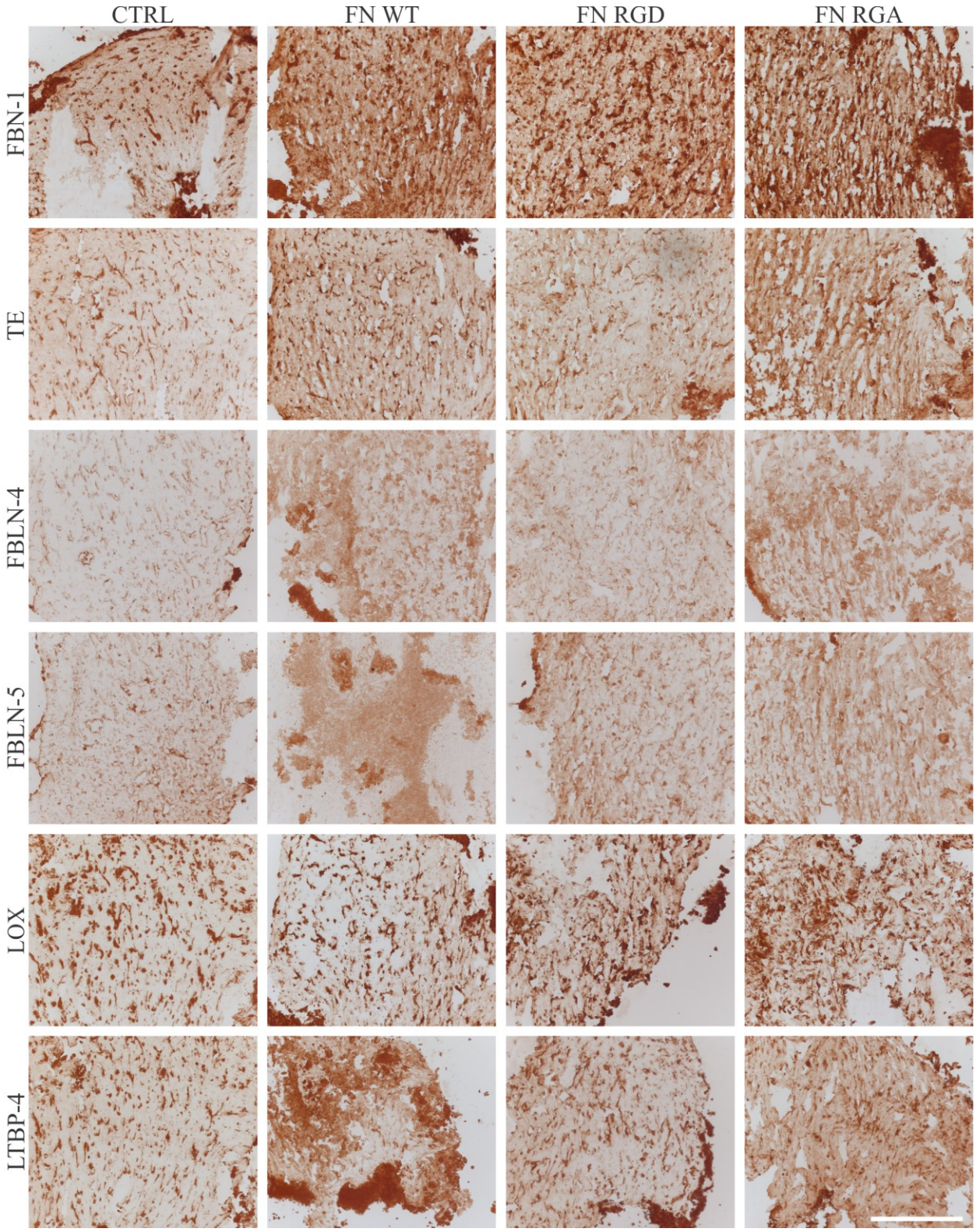

Figure 18. Immunohistochemical analysis of cellularized disk-shaped collagen constructs matured for 3 or 7 days. Planar collagen gel constructs cellularized with human SMCs were grown for 3 or 7 days in various culture conditions: CTRL, no protein supplementation of the collagen gels; FN WT, collagen gels supplemented with 0.05mg/mL of full length human EDA FN; FN RGD, collagen gels supplemented with 0.05mg/mL of short human EDA FN fragment $FNIII_8$-EDA_RGD; FN RGA, collagen gels supplemented with 0.05mg/mL of short human EDA FN fragment with a D → A mutation named $FNIII_8$-EDA_RGA. The constructs were fixed and stained for critical extracellular matrix proteins associated with elastic fiber formation, including fibrillin-1 (FBN-1), tropoelastin (TE), fibulin-4 (FBLN-4), fibulin-5 (FBLN-5), lysyl oxidase (LOX), and latent TGF-β binding protein-4 (LTBP-4). Scale bars represents 200μm.

6 RATIONALE, DISCUSSION, AND CONCLUSIONS: CHAPTER 1

6.1 Rationale

As previously described in the introduction, there is currently a massive need for vascular grafts for cardiovascular bypass surgeries owing to the substantial increase in cardiovascular disease. Autologous grafts have been the gold standard in CABG surgery for decades, they have several limitations and are accompanied by some undesirable and possibly dangerous side effects. Considering this, engineered vascular grafts have been proposed as alternatives to autologous vessels. Research over the last few decades has revealed the potential of collagen gel-based engineered vascular constructs as a source of vascular grafts, as collagen in non-immunogenic and readily available and cells may be obtained from the host. Furthermore, these engineered vessels may be used as *in vitro* vascular wall models to study vascular pathology and physiology, and for development of pharmacological compounds.

Although collagen gel-based engineered blood vessels are attractive for the aforementioned reasons, they suffer from one major drawback: a lack of elasticity and mechanical strength owing to the absence of elastic fiber formation by cells seeded within the constructs. Elastic fiber formation, or elastogenesis, is a complex, hierarchical process involving the spatiotemporal control of protein production, secretion, and assembly by cells in the ECM. Although there are several proteins required for proper elastogenesis, the first and arguably the most important step is the production of fibronectin and formation of a fibronectin matrix. Considering the importance of fibronectin and cells to elastogenesis and the lack of elastic fiber formation plaguing cell-seeded collagen gel-based engineered vascular constructs, our lab sought to test the effect of two methods on elastic fiber-related protein production and elastogenesis: 1) supplementing smooth muscle cell seeded collagen gel-based engineered vessels with exogenous plasma fibronectin; and 2) co-culturing vascular cell types (endothelial cells, smooth muscle cells, and fibroblasts) within the collagen constructs.

6.2 Discussion

6.2.1 Effect of pFN supplementation of elastic fiber-related protein production and elastogenesis

Immunohistochemical analysis showed that human pFN supplementation of collagen gel-based vascular constructs (fabricated by our collaborators) seeded with porcine aortic smooth muscle cells caused a consistent increase in total FN protein levels within the constructs, supporting studies showing pFN can be incorporated into the matrix independent of the species of origin (Hayman and Ruoslahti, 1979; Peters et al., 1990). At the day 3 time point, increases in EDA FN, FBN-1, and LOX were observed. At the day 7 time point, increases in TE, FBN-1, LOX, and LTBP-4 were observed. The increase in TE, FBN-1, and LOX are very promising, as the formation of FBN-1 containing microfibrils is necessary for TE deposition, LOX is necessary for TE crosslinking into mature elastin, and all three proteins are required for proper elastogenesis. Additionally, results obtained by our collaborators revealed that supplementation of the constructs with pFN caused increases in mechanical properties and collagen gel contraction (Pezzoli et al., 2018).

Further experiments were conducted to determine whether pFN causes changes in protein expression at the mRNA level. To verify whether pFN impacted gene expression of elastic fiber-related proteins, qPCR experiments were conducted, however the results were difficult to interpret. This is likely due to the nature of expression of elastic fiber-related proteins; some proteins, such as FN and FBN-1, are expressed earlier during elastogenesis, while other proteins, such as TE and LOX, are expressed later during elastogenesis. As such, analyzing mRNA levels at only day 3 and day 7 may not be adequate for determining the effect of pFN on expression levels and a continuous temporal evaluation may be more optimal. Furthermore, qPCR may not be optimal for detecting differences in the levels of certain mRNAs; for instance, TE gene expression remains constant throughout life, but protein production sharply decreases shortly after birth. This control is actually on the level of mRNA translation and not gene transcription, as shown by a 1999 study (Zhang et al., 1999). Despite these challenges, results did show consistent changes in mRNA levels, indicating pFN may in fact have an effect on gene expression of some proteins.

As our previous IHC experiments had shown strong increases of production and deposition of elastic fiber components by adult PAoSMCs, we sought to determine whether the cells were assembling the proteins into elastic fibers. Immunofluorescence results strongly correlated with the immunohistochemistry results, as human pFN was also shown to be incorporated into the matrix and increases were observed in similar proteins at similar time points. Importantly, the results of these experiments revealed that the cells were not merely producing and depositing protein into the ECM, but that they were also capable of assembling the components into elastic fibers. This result is particularly important, as it shows that adult cells, which normally produce no TE, are still capable of ramping up protein production in certain conditions, further supporting previous studies (Zhang et al., 1995).

As our results had shown that PAoSMCs were capable of assembling elastic fibers and that their supplementation with human pFN caused increases in both elastic fiber-related protein production and elastic fiber assembly, we sought to determine the maturity of elastin within the blood vessel constructs. To do so, we took advantage of an interesting property of mature, cross-linked elastin: its ability to autofluoresce due to the presence of aromatic ring structures formed as a consequence of crosslinking by LOX. Our analysis revealed that both the control and pFN supplemented constructs contained mature, crosslinked elastin. In concordance with our previous IHC and IF results, those constructs supplemented with human pFN showed increases in autofluorescence signal, especially at day 7, indicating that the PAoSMCs within the collagen gel were capable of producing proper elastic fibers. These results also support our collaborators' (Dr. Daniele Pezzoli and Dr. Diego Mantovani, Laval University) findings of increased mechanical properties, as elastin is one of the primary proteins responsible for the mechanical properties of elastic tissues.

6.2.2 Cell-cell crosstalk in collagen gel-based engineered blood vessels

To investigate the effect of co-culturing vascular cells on elastic fiber-related protein production in collagen gel-based engineered blood vessels, our collaborators produced layered tubular constructs mimicking the anatomy of *in vivo* muscular arteries. Immunohistochemical analysis revealed promising preliminary results. Increases were seen in important elastogenic proteins

including FBN-1 and TE in constructs seeded with either SMCs and FBs, or ECs, SMCs, and FBs, supporting a recent study using planar layered vascular wall models (Loy et al., 2017). Interestingly, any changes in protein production and deposition seemed to be localised only to the middle layer of the constructs where the SMCs were initially seeded (mimicking the tunica media of muscular arteries). Taken together, these results point to a possible cell-cell crosstalk causing changes in SMC gene expression and thus elastogenic protein production. Despite these promising preliminary results, much work remains to be done to determine what exactly is occurring within these constructs. For instance, it is unknown whether the cells maintain their localisation within the constructs, thus staining using specific markers is necessary to properly delineate the borders of the cell layers and determine if the crosstalk is possibly mediated via direct cell-cell interaction or via diffusible cytokines. Furthermore, the phenotype of the cells is unknown. Thus, it is possible that these cells are reverting to a somewhat developmental or stem cell-like phenotype where they are more "crosstalkative" (Rohban et al., 2017).

6.2.3 Cellular fibronectin fragments and elastogenic protein production

Our lab previously generated small cellular fibronectin fragments containing either an intact RGD site or mutated RGD → RGA site ($FNIII_8$-EDA_RGD and $FNIII_8$-EDA_RGA, respectively). Considering our previous results with supplementation of collagen gel-based engineered vascular constructs seeded with SMCs, we attempted similar experiments using these fragments in SMC seeded planar collagen gels. Results revealed similar results at the day 3 time point, with slight increases in FBN1, TE, and LOX. At day 7, results showed a significant increase in FBN-1 and slight increases in TE, LOX, and LTBP-4, in partial concordance with the pFN experiments. These results indicate two important characteristics of fibronectin: firstly that the small FN fragments can induce similar effects compared to full-length FN, and secondly that the integrin-binding RGD site is not required for fibronectin to have its effect on production of elastic fiber-related proteins.

6.2.4 Study limitations

Despite the many interesting and exciting results revealed by this study, there are several limitations. First and foremost, it must be noted that further work is desperately required to further

increase the mechanical properties of the engineered vessels produced by our collaborators, as they are still far weaker than native vessels despite the observed increases in mechanical properties. Another issue afflicting these constructs is their relative instability during antigen retrieval for IHC analysis. Engineered vessels treated with pFN and aged for longer periods tended to be more fragile than their younger and untreated counterparts, resulting in damage ranging from partial deterioration to absolute destruction during the relatively intense process of heating in 98°C citric acid. Issues also existed with the PAoSMCs used for IF experiments to determine whether they could assemble elastic fibers. The PAoSMCs often did not express TE at all, most likely owing to the number of times they were passaged (up to P8) and that they originated from adult tissues.

Further issues existed not with the experiments but rather with result quantification. Considering that IHC is a non-stoichiometric method of analysis, quantification of the relative darkness, or amount of staining, between conditions and proteins can differ between individual experiments, rendering absolute quantification impossible and thus making quantifications between different experiments quite challenging. Further issues were encountered with quantification of IF experiments. Considering the nature of the ECM and elastic fibers, quantification by measuring fluorescence signal only yields results which do not match the images. Considering this, our lab developed a fiber quantification protocol using the ImageJ software. Despite being better than simply measuring fluorescence intensity, this method still has several issues which need to be solved, including how to properly set a threshold for all images being compared and how to account for false positives when identifying fibers.

6.3 Conclusions

The investigation of the effect of human plasma fibronectin on elastic fiber formation in collagen gel-based engineered blood vessels seeded with vascular smooth muscle cells revealed the capacity of fibronectin to cause increases in elastic fiber-related protein production and elastic fiber assembly both within the 3D constructs and in 2D cell culture. Furthermore, elastic fibers in engineered blood vessels were found to be more mature, indicating an increase in engineered blood vessel maturation in as little as 7 days as compared to controls. Although the increases in protein

production and fiber assembly were quite clear, mRNA analysis was mostly inconclusive, thus the mechanism behind the increases requires further investigation.

The analysis of the effect of co-culturing vascular smooth muscle cells, fibroblasts, and endothelial cells in collagen gel-based engineered blood vessels showed exciting preliminary results, where proteins including fibrillin-1 and tropoelastin were found to increase in constructs where either fibroblasts and smooth muscle cells or all three cell types were co-cultured. Results also showed some localisation to the protein increases, particularly in the medial layers where smooth muscle cells were originally seeded, indicating that cell-cell crosstalk may be occurring within the constructs. Further work should be conducted to investigate whether there is any cell migration taking place and to investigate what may be mediating the communication between these cells, if there is any. Future work with these constructs should attempt to further increase elastic fiber-related protein production using different maturation techniques or supplementing the construct with elastogenic proteins such as fibronectin.

The investigation of the effect of fibronectin fragment supplementation of planar collagen gel-based constructs seeded with smooth muscle cells yielded important results, mainly that small fibronectin fragments can cause similar or slightly lesser increases in elastic fiber-related protein production compared to full length fibronectin. Furthermore, the lack of difference between fragments with intact RGD sites and those with mutated RGD sites indicates that the integrin-binding RGD site may not be required for fibronectin to have its effect. Future work should be conducted to determine the exact mechanisms underlying these results.

7 REFERENCES

1. Abbott, W.M., Callow, A., Moore, W., Rutherford, R., Veith, F., and Weinberg, S. (1993). Evaluation and performance standards for arterial prostheses. Journal of Vascular Surgery *17*, 746-756.
2. Asahara, T., Murohara, T., Sullivan, A., Silver, M., van der Zee, R., Li, T., Witzenbichler, B., Schatteman, G., and Isner, J.M. (1997). Isolation of putative progenitor endothelial cells for angiogenesis. Science *275*, 964-966.
3. Aumailley, M., and Gayraud, B. (1998). Structure and biological activity of the extracellular matrix. Journal of Molecular Medicine *76*, 253-265.
4. Baguneid, M., de Mel, A., Yildirimer, L., Fuller, B.J., Hamilton, G., and Seifalian, A.M. (2011). In vivo study of a model tissue-engineered small-diameter vascular bypass graft. Biotechnology and Applied Biochemistry *58*, 14-24.
5. Bajpai, V.K., and Andreadis, S.T. (2012). Stem cell sources for vascular tissue engineering and regeneration. Tissue Engineering Part B: Reviews *18*, 405-425.
6. Barner, H.B. (2008). Operative treatment of coronary atherosclerosis. Annals of Thoracic Surgery *85*, 1473-1482.
7. Birchall, M., and Hamilton, G. (2012). Tissue-engineered vascular replacements for children. Lancet *380*, 197-198.
8. Bittl, J.A. (1996). Advances in coronary angioplasty. New England Journal of Medicine *335*, 1290-1302.
9. Boccafoschi, F., Habermehl, J., Vesentini, S., and Mantovani, D. (2005). Biological performances of collagen-based scaffolds for vascular tissue engineering. Biomaterials *26*, 7410-7417.
10. Bono, N., Pezzoli, D., Levesque, L., Loy, C., Candiani, G., Fiore, G.B., and Mantovani, D. (2016). Unraveling the role of mechanical stimulation on smooth muscle cells: A comparative study between 2D and 3D models. Biotechnology and Bioengineering *113*, 2254-2263.
11. Borel, A., Eichenberger, D., Farjanel, J., Kessler, E., Gleyzal, C., Hulmes, D.J., Sommer, P., and Font, B. (2001). Lysyl oxidase-like protein from bovine aorta isolation and maturation to an active form by bone morphogenetic protein-1. Journal of Biological Chemistry *276*, 48944-48949.

12. Bultmann-Mellin, I., Conradi, A., Maul, A.C., Dinger, K., Wempe, F., Wohl, A.P., Imhof, T., Wunderlich, F.T., Bunck, A.C., and Nakamura, T. (2015). Modeling autosomal recessive cutis laxa type 1C in mice reveals distinct functions for Ltbp-4 isoforms. Disease Models & Mechanisms *8*, 403-415.
13. Bultmann-Mellin, I., Essers, J., van Heijingen, P.M., von Melchner, H., Sengle, G., and Sterner-Kock, A. (2016). Function of Ltbp-4L and fibulin-4 in survival and elastogenesis. Disease Models & Mechanisms *9*, 1367-1374.
14. Campbell, J.H., Efendy, J.L., and Campbell, G.R. (1999). Novel vascular graft grown within recipient's own peritoneal cavity. Circulation Research *85*, 1173-1178.
15. Carta, L., Pereira, L., Arteaga-Solis, E., Lee-Arteaga, S.Y., Lenart, B., Starcher, B., Merkel, C.A., Sukoyan, M., Kerkis, A., and Hazeki, N. (2006). Fibrillins 1 and 2 perform partially overlapping functions during aortic development. Journal of Biological Chemistry *281*, 8016-8023.
16. Coronary Artery Bypass Surgery (referral). (n.d.). Retrieved March 27, 2018, from http://www.ottawacvcentre.com/services-bypass-grafting.html
17. Cho, J., and Mosher, D.F. (2006). Role of fibronectin assembly in platelet thrombus formation. Journal of Thrombosis and Haemostasis *4*, 1461-1469.
18. Cho, S.-W., Lim, S.H., Kim, I.-K., Hong, Y.S., Kim, S.-S., Yoo, K.J., Park, H.-Y., Jang, Y., Chang, B.C., and Choi, C.Y. (2005). Small-diameter blood vessels engineered with bone marrow–derived cells. Annals of Surgery *241*, 506-515.
19. Choudhury, R., McGovern, A., Ridley, C., Cain, S.A., Baldwin, A., Wang, M.-C., Guo, C., Mironov, A., Drymoussi, Z., and Trump, D. (2009). Differential regulation of elastic fiber formation by fibulin-4 and-5. Journal of Biological Chemistry *284*, 24553-24567.
20. Clark, R.A., An, J.-Q., Greiling, D., Khan, A., and Schwarzbauer, J.E. (2003). Fibroblast migration on fibronectin requires three distinct functional domains. Journal of Investigative Dermatology *121*, 695-705.
21. Clark, R.A., Lanigan, J.M., DellaPelle, P., Manseau, E., Dvorak, H.F., and Colvin, R.B. (1982). Fibronectin and fibrin provide a provisional matrix for epidermal cell migration during wound reepithelialization. Journal of Investigative Dermatology *79*, 264-269.
22. Coucke, P.J., Willaert, A., Wessels, M.W., Callewaert, B., Zoppi, N., De Backer, J., Fox, J.E., Mancini, G.M., Kambouris, M., and Gardella, R. (2006). Mutations in the facilitative

glucose transporter GLUT10 alter angiogenesis and cause arterial tortuosity syndrome. Nature Genetics *38*, 452-457.

23. Couet, F., Rajan, N., Vesentini, S., and Mantovani, D. (2007). Design of a collagen/silk mechano-compatible composite scaffold for the vascular tissue engineering: focus on compliance. Key Engineering Materials. *334-335*, 1169-1172.
24. Curran, M.E., Atkinson, D.L., Ewart, A.K., Morris, C.A., Leppert, M.F., and Keating, M.T. (1993). The elastin gene is disrupted by a translocation associated with supravalvular aortic stenosis. Cell *73*, 159-168.
25. Dabovic, B., Chen, Y., Choi, J., Vassallo, M., Dietz, H.C., Ramirez, F., Von Melchner, H., Davis, E.C., and Rifkin, D.B. (2009). Dual functions for LTBP in lung development: LTBP-4 independently modulates elastogenesis and TGF-β activity. Journal of Cellular Physiology *219*, 14-22.
26. Dabovic, B., Robertson, I.B., Zilberberg, L., Vassallo, M., Davis, E.C., and Rifkin, D.B. (2015). Function of latent TGFβ binding protein 4 and fibulin 5 in elastogenesis and lung development. Journal of Cellular Physiology *230*, 226-236.
27. Desmet, W., Vanhaecke, J., Vrolix, M., Van de Werf, F., Piessens, J., Willems, J., and De Geest, H. (1992). Isolated single coronary artery: a review of 50 000 consecutive coronary angiographies. European Heart Journal *13*, 1637-1640.
28. Desmouliere, A., Redard, M., Darby, I., and Gabbiani, G. (1995). Apoptosis mediates the decrease in cellularity during the transition between granulation tissue and scar. American Journal of Pathology *146*, 56.
29. Dinarello, C.A. (2000). Proinflammatory cytokines. Chest *118*, 503-508.
30. El-Hallous, E., Sasaki, T., Hubmacher, D., Getie, M., Tiedemann, K., Brinckmann, J., Bätge, B., Davis, E.C., and Reinhardt, D.P. (2007). Fibrillin-1 interactions with fibulins depend on the first hybrid domain and provide an adaptor function to tropoelastin. Journal of Biological Chemistry *282*, 8935-8946.
31. Ewart, A.K., Morris, C.A., Atkinson, D., Jin, W., Sternes, K., Spallone, P., Stock, A.D., Leppert, M., and Keating, M.T. (1993). Hemizygosity at the elastin locus in a developmental disorder, Williams syndrome. Nature Genetics *5*, 11-16.

32. Feil, R., Wagner, J., Metzger, D., and Chambon, P. (1997). Regulation of Cre recombinase activity by mutated estrogen receptor ligand-binding domains. Biochemical and Biophysical Research Communications *237*, 752-757.
33. Feil, S., Valtcheva, N., and Feil, R. (2009). Inducible cre mice. In Gene knockout protocols (Springer), pp. 343-363.
34. Fernandez-Sauze, S., Grall, D., Cseh, B., and Van Obberghen-Schilling, E. (2009). Regulation of fibronectin matrix assembly and capillary morphogenesis in endothelial cells by Rho family GTPases. Experimental Cell Research *315*, 2092-2104.
35. Ffrench-Constant, C. (1995). Alternative Splicing of Fibronectin–Many Different Proteins but Few Different Functions. Experimental Cell Research. *221*, 261-271.
36. Früh, S.M., Schoen, I., Ries, J., and Vogel, V. (2015). Molecular architecture of native fibronectin fibrils. Nature Communications *6*, 7275.
37. George, E.L., Georges-Labouesse, E.N., Patel-King, R.S., Rayburn, H., and Hynes, R.O. (1993). Defects in mesoderm, neural tube and vascular development in mouse embryos lacking fibronectin. Development *119*, 1079-1091.
38. Gibson, M.A., Hatzinikolas, G., Davis, E.C., Baker, E., Sutherland, G.R., and Mecham, R.P. (1995). Bovine latent transforming growth factor beta 1-binding protein 2: molecular cloning, identification of tissue isoforms, and immunolocalization to elastin-associated microfibrils. Molecular and Cellular Biology *15*, 6932-6942.
39. Giltay, R., Timpl, R., and Kostka, G. (1999). Sequence, recombinant expression and tissue localization of two novel extracellular matrix proteins, fibulin-3 and fibulin-4. Matrix Biology *18*, 469-480.
40. Gosain, A., and DiPietro, L.A. (2004). Aging and wound healing. World Journal of Surgery *28*, 321-326.
41. Guo, S.a., and DiPietro, L.A. (2010). Factors affecting wound healing. Journal of Dental Research *89*, 219-229.
42. Haisch, A., Loch, A., David, J., Pruss, A., Hansen, R., and Sittinger, M. (2000). Preparation of a pure autologous biodegradable fibrin matrix for tissue engineering. Medical and Biological Engineering and Computing *38*, 686-689.
43. Hashi, C.K., Zhu, Y., Yang, G.-Y., Young, W.L., Hsiao, B.S., Wang, K., Chu, B., and Li, S. (2007). Antithrombogenic property of bone marrow mesenchymal stem cells in

nanofibrous vascular grafts. Proceedings of the National Academy of Sciences *104*, 11915-11920.

44. Hayashi, K., Fong, K.S., Mercier, F., Boyd, C.D., Csiszar, K., and Hayashi, M. (2004). Comparative immunocytochemical localization of lysyl oxidase (LOX) and the lysyl oxidase-like (LOXL) proteins: changes in the expression of LOXL during development and growth of mouse tissues. Journal of Molecular Histology *35*, 845-855.
45. Hayman, E.G., and Ruoslahti, E. (1979). Distribution of fetal bovine serum fibronectin and endogenous rat cell fibronectin in extracellular matrix. Journal of Cell Biology *83*, 255-259.
46. Hayward, P.A., Hare, D.L., Gordon, I., Matalanis, G., and Buxton, B.F. (2007). Which arterial conduit? Radial artery versus free right internal thoracic artery: six-year clinical results of a randomized controlled trial. Annals of Thoracic Surgery *84*, 493-497.
47. Higgins, S.P., Solan, A.K., and Niklason, L.E. (2003). Effects of polyglycolic acid on porcine smooth muscle cell growth and differentiation. Journal of Biomedical Materials Research Part A *67*, 295-302.
48. Hinz, B. (2009). Tissue stiffness, latent TGF-β1 activation, and mechanical signal transduction: implications for the pathogenesis and treatment of fibrosis. Current Rheumatology Reports *11*, 120-126.
49. Hinz, B., and Gabbiani, G. (2003). Mechanisms of force generation and transmission by myofibroblasts. Current Opinion in Biotechnology *14*, 538-546.
50. Hirai, M., Horiguchi, M., Ohbayashi, T., Kita, T., Chien, K.R., and Nakamura, T. (2007). Latent TGF-β-binding protein 2 binds to DANCE/fibulin-5 and regulates elastic fiber assembly. EMBO Journal *26*, 3283-3295.
51. Holzenberger, M., Ayer-Le Lievre, C., and Robert, L. (1993). Tropoelastin gene expression in the developing vascular system of the chicken: an in situ hybridization study. Anatomy and Embryology *188*, 481-492.
52. Horiguchi, M., Inoue, T., Ohbayashi, T., Hirai, M., Noda, K., Marmorstein, L.Y., Yabe, D., Takagi, K., Akama, T.O., and Kita, T. (2009). Fibulin-4 conducts proper elastogenesis via interaction with cross-linking enzyme lysyl oxidase. Proceedings of the National Academy of Sciences *106*, 19029-19034.

53. Hornstra, I.K., Birge, S., Starcher, B., Bailey, A.J., Mecham, R.P., and Shapiro, S.D. (2003). Lysyl oxidase is required for vascular and diaphragmatic development in mice. Journal of Biological Chemistry *278*, 14387-14393.
54. Hoyer, J., Kraus, C., Hammersen, G., Geppert, J.P., and Rauch, A. (2009). Lethal cutis laxa with contractural arachnodactyly, overgrowth and soft tissue bleeding due to a novel homozygous fibulin-4 gene mutation. Clinical Genetics *76*, 276-281.
55. Hsiao, C. T., Cheng, H. W., Huang, C. M., Li, H. R., Ou, M. H., Huang, J. R., ... & Chiou, A. (2017). Fibronectin in cell adhesion and migration via N-glycosylation. Oncotarget *8*, 70653.
56. Hu, Q., Loeys, B.L., Coucke, P.J., De Paepe, A., Mecham, R.P., Choi, J., Davis, E.C., and Urban, Z. (2006). Fibulin-5 mutations: mechanisms of impaired elastic fiber formation in recessive cutis laxa. Human Molecular Genetics *15*, 3379-3386.
57. Hubmacher, D., El-Hallous, E.I., Nelea, V., Kaartinen, M.T., Lee, E.R., and Reinhardt, D.P. (2008). Biogenesis of extracellular microfibrils: Multimerization of the fibrillin-1 C terminus into bead-like structures enables self-assembly. Proceedings of the National Academy of Sciences *105*, 6548-6553.
58. Hubmacher, D., and Reinhardt, D.P. (2011). Microfibrils and fibrillin. In The Extracellular Matrix: an Overview (Springer), pp. 233-265.
59. Hubmacher, D., Tiedemann, K., and Reinhardt, D.P. (2006). Fibrillins: from biogenesis of microfibrils to signaling functions. Current Topics in Developmental Biology *75*, 93-123.
60. Ihn, H. (2002). Pathogenesis of fibrosis: role of TGF-β and CTGF. Current Opinion in Rheumatology *14*, 681-685.
61. Jones, R.P., Ridley, C., Jowitt, T.A., Wang, M.-C., Howard, M., Bobola, N., Wang, T., Bishop, P.N., Kielty, C.M., and Baldock, C. (2010). Structural effects of fibulin 5 missense mutations associated with age-related macular degeneration and cutis laxa. Investigative Ophthalmology & Visual Science *51*, 2356-2362.
62. K., P. (2011). Cre/lox Breeding for Dummies. Retrieved March 29, 2018, from https://www.jax.org/news-and-insights/jax-blog/2011/september/cre-lox-breeding-for-dummies.
63. Kassem, M., Abdallah, B.M., Yu, Z., Ditzel, N., and Burns, J.S. (2004). The use of hTERT-immortalized cells in tissue engineering. Cytotechnology *45*, 39-46.

64. Keane, T.J., Londono, R., Turner, N.J., and Badylak, S.F. (2012). Consequences of ineffective decellularization of biologic scaffolds on the host response. Biomaterials *33*, 1771-1781.
65. Keene, D., Maddox, B., Kuo, H.-J., Sakai, L., and Glanville, R. (1991). Extraction of extendable beaded structures and their identification as fibrillin-containing extracellular matrix microfibrils. Journal of Histochemistry & Cytochemistry *39*, 441-449.
66. Kielty, C.M. (2006). Elastic fibres in health and disease. Expert Reviews in Molecular Medicine *8*, 1-23.
67. Kim, B.-S., and Mooney, D.J. (1998). Development of biocompatible synthetic extracellular matrices for tissue engineering. Trends in Biotechnology *16*, 224-230.
68. Kinsey, R., Williamson, M.R., Chaudhry, S., Mellody, K.T., McGovern, A., Takahashi, S., Shuttleworth, C.A., and Kielty, C.M. (2008). Fibrillin-1 microfibril deposition is dependent on fibronectin assembly. Journal of Cell Science *121*, 2696-2704.
69. Kirschner, R., Hubmacher, D., Iyengar, G., Kaur, J., Fagotto-Kaufmann, C., Brömme, D., Bartels, R., and Reinhardt, D.P. (2011). Classical and neonatal Marfan syndrome mutations in fibrillin-1 cause differential protease susceptibilities and protein function. Journal of Biological Chemistry *286*, 32810-32823.
70. Kluth, D. C., & Rees, A. J. (1999). Anti-glomerular basement membrane disease. Journal of the American Society of Nephrology *10*, 2446-2453.
71. Kobayashi, N., Kostka, G., Garbe, J.H., Keene, D.R., Bächinger, H.P., Hanisch, F.-G., Markova, D., Tsuda, T., Timpl, R., and Chu, M.-L. (2007). A comparative analysis of the fibulin protein family biochemical characterization, binding interactions, and tissue localization. Journal of Biological Chemistry *282*, 11805-11816.
72. Kosmehl, H., Berndt, A., and Katenkamp, D. (1996). Molecular variants of fibronectin and laminin: structure, physiological occurrence and histopathological aspects. Virchows Archiv *429*, 311-322.
73. Kozel, B.A., Mecham, R.P., and Rosenbloom, J. (2011). Elastin. In The Extracellular Matrix: an Overview (Springer), pp. 267-301.
74. Kristianto, J., Johnson, M.G., Zastrow, R.K., Radcliff, A.B., and Blank, R.D. (2017). Spontaneous recombinase activity of Cre–ERT2 in vivo. Transgenic Research *26*, 411-417.

75. Kriz, W., Elger, M., Lemley, K., and Sakai, T. (1990). Structure of the glomerular mesangium: a biomechanical interpretation. Kidney International Supplement. *30*, S2–S9.
76. Kubota, Y., Kleinman, H. K., Martin, G. R., & Lawley, T. J. (1988). Role of laminin and basement membrane in the morphological differentiation of human endothelial cells into capillary-like structures. The Journal of Cell Biology *107*, 1589-1598.
77. Kurpinski, K., Lam, H., Chu, J., Wang, A., Kim, A., Tsay, E., Agrawal, S., Schaffer, D.V., and Li, S. (2010). Transforming Growth Factor-β and Notch Signaling Mediate Stem Cell Differentiation into Smooth Muscle Cells. Stem Cells *28*, 734-742.
78. L'Heureux, N., Dusserre, N., Konig, G., Victor, B., Keire, P., Wight, T.N., Chronos, N.A., Kyles, A.E., Gregory, C.R., and Hoyt, G. (2006). Human tissue-engineered blood vessels for adult arterial revascularization. Nature Medicine *12*, 361-365.
79. L'heureux, N., Dusserre, N., Marini, A., Garrido, S., De La Fuente, L., and McAllister, T. (2007). Technology insight: the evolution of tissue-engineered vascular grafts—from research to clinical practice. Nature Reviews Cardiology *4*, 389-395.
80. L'heureux, N., Pâquet, S., Labbé, R., Germain, L., and Auger, F.A. (1998). A completely biological tissue-engineered human blood vessel. FASEB Journal *12*, 47-56.
81. Lee, C.S., Fu, H., Baratang, N., Rousseau, J., Kumra, H., Sutton, V.R., Niceta, M., Ciolfi, A., Yamamoto, G., and Bertola, D. (2017). Mutations in Fibronectin Cause a Subtype of Spondylometaphyseal Dysplasia with "Corner Fractures". American Journal of Human Genetics *101*, 815-823.
82. Leyh, R., Wilhelmi, M., Walles, T., Kallenbach, K., Rebe, P., Oberbeck, A., Herden, T., Haverich, A., and Mertsching, H. (2003). Acellularized porcine heart valve scaffolds for heart valve tissue engineering and the risk of cross-species transmission of porcine endogenous retrovirus. Journal of Thoracic and Cardiovascular Surgery *126*, 1000-1004.
83. Li, D.Y., Brooke, B., Davis, E.C., Mecham, R.P., Sorensen, L.K., Boak, B.B., Eichwald, E., and Keating, M.T. (1998a). Elastin is an essential determinant of arterial morphogenesis. Nature *393*, 276-280.
84. Li, D.Y., Faury, G., Taylor, D.G., Davis, E.C., Boyle, W.A., Mecham, R.P., Stenzel, P., Boak, B., and Keating, M.T. (1998b). Novel arterial pathology in mice and humans hemizygous for elastin. Journal of Clinical Investigation *102*, 1783-1787.

85. Li, S., and Henry, J.J. (2011). Nonthrombogenic approaches to cardiovascular bioengineering. Annual Review of Biomedical Engineering *13*, 451-475.
86. Li, S., Sengupta, D., and Chien, S. (2014). Vascular tissue engineering: from in vitro to in situ. Wiley Interdisciplinary Reviews: Systems Biology and Medicine *6*, 61-76.
87. Liao, Y.-F., Gotwals, P.J., Koteliansky, V.E., Sheppard, D., and Van De Water, L. (2002). The EIIIA Segment of Fibronectin Is a Ligand for Integrins α9β1 and α4β1Providing a Novel Mechanism for Regulating Cell Adhesion by Alternative Splicing. Journal of Biological Chemistry *277*, 14467-14474.
88. Liotta, L. A., Tryggvason, K., Garbisa, S., Hart, I., Foltz, C. M., & Shafie, S. (1980). Metastatic potential correlates with enzymatic degradation of basement membrane collagen. Nature *284*, 67-68.
89. Liu, X., Zhao, Y., Gao, J., Pawlyk, B., Starcher, B., Spencer, J.A., Yanagisawa, H., Zuo, J., and Li, T. (2004). Elastic fiber homeostasis requires lysyl oxidase–like 1 protein. Nature Genetics *36*, 178-182.
90. Loeys, B., Matthys, D., and De Paepe, A. (2003). Genetic fibrillinopathies: new insights in molecular diagnosis and clinical management. Acta Clinica Belgica. *58(1)*, 3-11.
91. Loy, C., Meghezi, S., Lévesque, L., Pezzoli, D., Kumra, H., Reinhardt, D., Kizhakkedathu, J.N., and Mantovani, D. (2017). A planar model of the vessel wall from cellularized-collagen scaffolds: focus on cell–matrix interactions in mono-, bi-and tri-culture models. Biomaterials Science *5*, 153-162.
92. Loy, C., Pezzoli, D., Candiani, G., and Mantovani, D. (2018). A Cost-Effective Culture System for the In Vitro Assembly, Maturation, and Stimulation of Advanced Multilayered Multiculture Tubular Tissue Models. Biotechnology Journal *13*, 1700359.
93. Lu, P., Takai, K., Weaver, V.M., and Werb, Z. (2011). Extracellular matrix degradation and remodeling in development and disease. Cold Spring Harbor Perspectives in Biology *3*, a005058.
94. Lucero, H., and Kagan, H. (2006). Lysyl oxidase: an oxidative enzyme and effector of cell function. Cellular and Molecular Life Sciences CMLS *63*, 2304-2316.
95. Mäki, J.M., Räsänen, J., Tikkanen, H., Sormunen, R., Mäkikallio, K., Kivirikko, K.I., and Soininen, R. (2002). Inactivation of the lysyl oxidase gene Lox leads to aortic aneurysms, cardiovascular dysfunction, and perinatal death in mice. Circulation *106*, 2503-2509.

96. Mäki, J.M., Sormunen, R., Lippo, S., Kaarteenaho-Wiik, R., Soininen, R., and Myllyharju, J. (2005). Lysyl oxidase is essential for normal development and function of the respiratory system and for the integrity of elastic and collagen fibers in various tissues. American Journal of Pathology *167*, 927-936.
97. Mathieu, D., Linke, J.-C., and Wattel, F. (2006). Non-healing wounds. In Handbook on Hyperbaric Medicine (Springer), pp. 401-428.
98. Matsumura, G., Miyagawa-Tomita, S., Shin'oka, T., Ikada, Y., and Kurosawa, H. (2003). First evidence that bone marrow cells contribute to the construction of tissue-engineered vascular autografts in vivo. Circulation *108*, 1729-1734.
99. Maynard, J. (2015, December 18). How Wounds Heal: The 4 Main Phases of Wound Healing. Retrieved May 04, 2018, from http://www.shieldhealthcare.com/community/wound/2015/12/18/how-wounds-heal-the-4-main-phases-of-wound-healing/
100. McKee, J.A., Banik, S.S., Boyer, M.J., Hamad, N.M., Lawson, J.H., Niklason, L.E., and Counter, C.M. (2003). Human arteries engineered in vitro. EMBO Reports *4*, 633-638.
101. McLaughlin, P.J., Chen, Q., Horiguchi, M., Starcher, B.C., Stanton, J.B., Broekelmann, T.J., Marmorstein, A.D., McKay, B., Mecham, R., and Nakamura, T. (2006). Targeted disruption of fibulin-4 abolishes elastogenesis and causes perinatal lethality in mice. Molecular and Cellular Biology *26*, 1700-1709.
102. Mead, T.J., Du, Y., Nelson, C.M., Gueye, N.-A., Drazba, J., Dancevic, C.M., Vankemmelbeke, M., Buttle, D.J., and Apte, S.S. (2018). ADAMTS9-Regulated Pericellular Matrix Dynamics Governs Focal Adhesion-Dependent Smooth Muscle Differentiation. Cell Reports *23*, 485-498.
103. Milewicz, D.M., Grossfield, J., Cao, S., Kielty, C., Covitz, W., and Jewett, T. (1995). A mutation in FBN1 disrupts profibrillin processing and results in isolated skeletal features of the Marfan syndrome. Journal of Clinical Investigation *95*, 2373-2378.
104. Mithieux, S.M., and Weiss, A.S. (2005). Elastin. In Advances in protein chemistry (Elsevier), pp. 437-461.
105. Moretti, F.A., Chauhan, A.K., Iaconcig, A., Porro, F., Baralle, F.E., and Muro, A.F. (2007). A major fraction of fibronectin present in the extracellular matrix of tissues is plasma-derived. Journal of Biological Chemistry *282*, 28057-28062.

106. Mosser, D.M., and Edwards, J.P. (2008). Exploring the full spectrum of macrophage activation. Nature Reviews Immunology *8*, 958-969.
107. Muro, A.F., Chauhan, A.K., Gajovic, S., Iaconcig, A., Porro, F., Stanta, G., and Baralle, F.E. (2003). Regulated splicing of the fibronectin EDA exon is essential for proper skin wound healing and normal lifespan. Journal of Cell Biology *162*, 149-160.
108. Nakamura, T., Ruiz-Lozano, P., Lindner, V., Yabe, D., Taniwaki, M., Furukawa, Y., Kobuke, K., Tashiro, K., Lu, Z., and Andon, N.L. (1999). DANCE, a novel secreted RGD protein expressed in developing, atherosclerotic, and balloon-injured arteries. Journal of Biological Chemistry *274*, 22476-22483.
109. Nakayama, Y., Ishibashi-Ueda, H., and Takamizawa, K. (2004). In vivo tissue-engineered small-caliber arterial graft prosthesis consisting of autologous tissue (biotube). Cell Transplantation *13*, 439-449.
110. Nerem, R.M., and Seliktar, D. (2001). Vascular tissue engineering. Annual Review of Biomedical Engineering *3*, 225-243.
111. Coronary Heart Disease. (2014, September 29). Retrieved March 27, 2018, from https://www.nhlbi.nih.gov/health-topics/coronary-heart-disease
112. Niklason, L., Gao, J., Abbott, W., Hirschi, K., Houser, S., Marini, R., and Langer, R. (1999). Functional arteries grown in vitro. Science *284*, 489-493.
113. Noda, K., Dabovic, B., Takagi, K., Inoue, T., Horiguchi, M., Hirai, M., Fujikawa, Y., Akama, T.O., Kusumoto, K., Zilberberg, L., Sakai, L., Koli, K., Naitoh, M., von Melchner, H., Suzuki, S., Rifkin, D., and Nakamura, T. (2013). Latent TGF-β binding protein 4 promotes elastic fiber assembly by interacting with fibulin-5. Proceedings of the National Academy of Sciences *110*, 2852-2857.
114. Noonan, D. M., Fulle, A., Valente, P., Cai, S., Horigan, E., Sasaki, M., ... & Hassell, J. R. (1991). The complete sequence of perlecan, a basement membrane heparan sulfate proteoglycan, reveals extensive similarity with laminin A chain, low density lipoprotein-receptor, and the neural cell adhesion molecule. Journal of Biological Chemistry *266*, 22939-22947.
115. Olausson, M., Patil, P.B., Kuna, V.K., Chougule, P., Hernandez, N., Methe, K., Kullberg-Lindh, C., Borg, H., Ejnell, H., and Sumitran-Holgersson, S. (2012). Transplantation of an

allogeneic vein bioengineered with autologous stem cells: a proof-of-concept study. Lancet *380*, 230-237.

116. Orban, P.C., Chui, D., and Marth, J.D. (1992). Tissue-and site-specific DNA recombination in transgenic mice. Proceedings of the National Academy of Sciences *89*, 6861-6865.
117. Özbek, S., Balasubramanian, P. G., Chiquet-Ehrismann, R., Tucker, R. P., & Adams, J. C. (2010). The evolution of extracellular matrix. Molecular Biology of the Cell *21*, 4300-4305.
118. Pankov, R., and Yamada, K.M. (2002). Fibronectin at a glance. Journal of Cell Science *115*, 3861-3863.
119. Papke, C.L., and Yanagisawa, H. (2014). Fibulin-4 and fibulin-5 in elastogenesis and beyond: Insights from mouse and human studies. Matrix Biology *37*, 142-149.
120. Partridge, S., Elsden, D., Thomas, J., Dorfman, A., Telser, A., and Ho, P.-L. (1964). Biosynthesis of the desmosine and isodesmosine cross-bridges in elastin. Biochemical Journal *93*, 30C-33C.
121. Patel, R.S., Odermatt, E., Schwarzbauer, J., and Hynes, R. (1987). Organization of the fibronectin gene provides evidence for exon shuffling during evolution. EMBO Journal *6*, 2565-2572.
122. Paulsson, M. (1992). Basement membrane proteins: structure, assembly, and cellular interactions. Critical Reviews in Biochemistry and Molecular Biology *27*, 93-127.
123. Peck, M., Gebhart, D., Dusserre, N., McAllister, T.N., and L'Heureux, N. (2012). The evolution of vascular tissue engineering and current state of the art. Cells Tissues Organs *195*, 144-158.
124. Peck, M.K., Dusserre, N., Zagalski, K., Garrido, S.A., Wystrychowski, W., Glickman, M.H., Chronos, N.A., Cierpka, L., L'heureux, N., and McAllister, T.N. (2011). New biological solutions for hemodialysis access. Journal of Vascular Access *12*, 185-192.
125. Peters, D., Portz, L.M., Fullenwider, J., and Mosher, D.F. (1990). Co-assembly of plasma and cellular fibronectins into fibrils in human fibroblast cultures. Journal of cell biology *111*, 249-256.
126. Pezzoli, D., Di Paolo, J., Kumra, H., Fois, G., Candiani, G., Reinhardt, D.P., and Mantovani, D. (2018). Fibronectin promotes elastin deposition, elasticity and mechanical strength in cellularised collagen-based scaffolds. Biomaterials. *180*, 130-142.

127. Piontkivska, H., Zhang, Y., Green, E. D., & Elnitski, L. (2004). Multi-species sequence comparison reveals dynamic evolution of the elastin gene that has involved purifying selection and lineage-specific insertions/deletions. BMC Genomics *5*, 31.
128. Platt, J., and Nagayasu, T. (1999). Current status of xenotransplantation. Clinical and Experimental Pharmacology and Physiology *26*, 1026-1032.
129. Plow, E.F., Haas, T.A., Zhang, L., Loftus, J., and Smith, J.W. (2000). Ligand binding to integrins. Journal of Biological Chemistry *275*, 21785-21788.
130. Poh, M., Boyer, M., Solan, A., Dahl, S.L., Pedrotty, D., Banik, S.S., McKee, J.A., Klinger, R.Y., Counter, C.M., and Niklason, L.E. (2005). Blood vessels engineered from human cells. Lancet *365*, 2122-2124.
131. Prater, D.N., Case, J., Ingram, D.A., and Yoder, M.C. (2007). Working hypothesis to redefine endothelial progenitor cells. Leukemia *21*, 1141-1149.
132. Quint, C., Arief, M., Muto, A., Dardik, A., and Niklason, L.E. (2012). Allogeneic human tissue-engineered blood vessel. Journal of Vascular Surgery *55*, 790-798.
133. Quint, C., Kondo, Y., Manson, R.J., Lawson, J.H., Dardik, A., and Niklason, L.E. (2011). Decellularized tissue-engineered blood vessel as an arterial conduit. Proceedings of the National Academy of Sciences *108*, 9214-9219.
134. Rabkin, E., and Schoen, F.J. (2002). Cardiovascular tissue engineering. Cardiovascular Pathology *11*, 305-317.
135. Rajan, N., Habermehl, J., Coté, M.-F., Doillon, C.J., and Mantovani, D. (2006). Preparation of ready-to-use, storable and reconstituted type I collagen from rat tail tendon for tissue engineering applications. Nature Protocols *1*, 2753-2758.
136. Ramirez, F., and Sakai, L.Y. (2010). Biogenesis and function of fibrillin assemblies. Cell and Tissue Research *339*, 71-82.
137. Rapaka, R., and Urry, D. (1978). Coacervation of sequential polypeptide models of tropoelastin. Chemical Biology & Drug Design *11*, 97-108.
138. Raviola, G. (1971). The fine structure of the ciliary zonule and ciliary epithelium: with special regard to the organization and insertion of the zonular fibrils. Investigative Ophthalmology & Visual Science *10*, 851-869.

139. Repesh, L.A., Fitzgerald, T.J., and Furcht, L. (1982). Fibronectin involvement in granulation tissue and wound healing in rabbits. Journal of Histochemistry & Cytochemistry *30*, 351-358.
140. Rohban, R., Prietl, B., and Pieber, T.R. (2017). Crosstalk between stem and progenitor cellular mediators with special emphasis on vasculogenesis. Transfusion Medicine and Hemotherapy *44*, 174-182.
141. Rothuizen, T. C., Damanik, F., Cox, M. A. J., Moroni, L., Rabelink, T. J., & Rotmans, J. (2012). In vivo tissue engineered blood vessels for hemodialysis vascular access. -.
142. Rozario, T., and DeSimone, D.W. (2010). The extracellular matrix in development and morphogenesis: a dynamic view. Developmental Biology *341*, 126-140.
143. Sabatier, L., Chen, D., Fagotto-Kaufmann, C., Hubmacher, D., McKee, M.D., Annis, D.S., Mosher, D.F., and Reinhardt, D.P. (2009). Fibrillin assembly requires fibronectin. Molecular Biology of the Cell *20*, 846-858.
144. Sage, H., & Gray, W. R. (1981). Studies on the evolution of elastin—III. The ancestral protein. Comparative Biochemistry and Physiology Part B: Comparative Biochemistry *68*, 473-480.
145. Saharinen, J., Taipale, J., and Keski-Oja, J. (1996). Association of the small latent transforming growth factor-beta with an eight cysteine repeat of its binding protein LTBP-1. EMBO Journal *15*, 245-253.
146. Sakai, T., Johnson, K.J., Murozono, M., Sakai, K., Magnuson, M.A., Wieloch, T., Cronberg, T., Isshiki, A., Erickson, H.P., and Fässler, R. (2001). Plasma fibronectin supports neuronal survival and reduces brain injury following transient focal cerebral ischemia but is not essential for skin-wound healing and hemostasis. Nature Medicine *7*, 324-330.
147. Sauer, B., and Henderson, N. (1988). Site-specific DNA recombination in mammalian cells by the Cre recombinase of bacteriophage P1. Proceedings of the National Academy of Sciences *85*, 5166-5170.
148. Savige, J. (2014). Alport syndrome: its effects on the glomerular filtration barrier and implications for future treatment. The Journal of Physiology *592*, 4013-4023.
149. Sawamura, D., Nakano, H., & Matsuzaki, Y. (2010). Overview of epidermolysis bullosa. The Journal of Dermatology *37*, 214-219.

150. Schneider, C.A., Rasband, W.S., and Eliceiri, K.W. (2012). NIH Image to ImageJ: 25 years of image analysis. Nature Methods *9*, 671-675.
151. Segade, F. (2010). Molecular evolution of the fibulins: implications on the functionality of the elastic fibulins. Gene *464*, 17-31.
152. Seifu, D.G., Purnama, A., Mequanint, K., and Mantovani, D. (2013). Small-diameter vascular tissue engineering. Nature Reviews Cardiology *10*, 410-421.
153. Seliktar, D., Nerem, R.M., and Galis, Z.S. (2003). Mechanical strain-stimulated remodeling of tissue-engineered blood vessel constructs. Tissue Engineering *9*, 657-666.
154. Serini, G., Bochaton-Piallat, M.-L., Ropraz, P., Geinoz, A., Borsi, L., Zardi, L., and Gabbiani, G. (1998). The fibronectin domain ED-A is crucial for myofibroblastic phenotype induction by transforming growth factor-β1. Journal of Cell Biology *142*, 873-881.
155. Shapiro, S., Endicott, S., Province, M., Pierce, J., and Campbell, E. (1991). Marked longevity of human lung parenchymal elastic fibers deduced from prevalence of D-aspartate and nuclear weapons-related radiocarbon. Journal of Clinical Investigation *87*, 1828-1834.
156. Shin'oka, T., Imai, Y., and Ikada, Y. (2001). Transplantation of a tissue-engineered pulmonary artery. New England Journal of Medicine *344*, 532-533.
157. Sideek, M.A., Menz, C., Parsi, M.K., and Gibson, M.A. (2014). LTBP-2 competes with tropoelastin for binding to fibulin-5 and heparin, and is a negative modulator of elastinogenesis. Matrix Biology *34*, 114-123.
158. Singh, P., Carraher, C., and Schwarzbauer, J.E. (2010). Assembly of fibronectin extracellular matrix. Annual Review of Cell and Developmental Biology *26*, 397-419.
159. Sottile, J., and Mosher, D.F. (1997). N-terminal type I modules required for fibronectin binding to fibroblasts and to fibronectin's III1 module. Biochemical Journal *323*, 51-60.
160. Stegemann, J.P., Kaszuba, S.N., and Rowe, S.L. (2007). Advances in vascular tissue engineering using protein-based biomaterials. Tissue Engineering *13*, 2601-2613.
161. Tamkun, J., and Hynes, R. (1983). Plasma fibronectin is synthesized and secreted by hepatocytes. Journal of Biological Chemistry *258*, 4641-4647.

162. Tan, M.H., Sun, Z., Opitz, S.L., Schmidt, T.E., Peters, J.H., and George, E.L. (2004). Deletion of the alternatively spliced fibronectin EIIIA domain in mice reduces atherosclerosis. Blood *104*, 11-18.

163. Tassabehji, M., Metcalfe, K., Hurst, J., Ashcroft, G.S., Kielty, C., Wilmot, C., Donnai, D., Read, A.P., and Jones, C.J. (1998). An elastin gene mutation producing abnormal tropoelastin and abnormal elastic fibres in a patient with autosomal dominant cutis laxa. Human Molecular Genetics *7*, 1021-1028.

164. Tate, C.C., García, A.J., and LaPlaca, M.C. (2007). Plasma fibronectin is neuroprotective following traumatic brain injury. Experimental Neurology *207*, 13-22.

165. Thomassin, L., Werneck, C.C., Broekelmann, T.J., Gleyzal, C., Hornstra, I.K., Mecham, R.P., and Sommer, P. (2005). The Pro-regions of lysyl oxidase and lysyl oxidase-like 1 are required for deposition onto elastic fibers. Journal of Biological Chemistry *280*, 42848-42855.

166. Tiedemann, K., Bätge, B., Müller, P.K., and Reinhardt, D.P. (2001). Interactions of fibrillin-1 with heparin/heparan sulfate, implications for microfibrillar assembly. Journal of Biological Chemistry *276*, 36035-36042.

167. Tiwari, A., Salacinski, H., Seifalian, A.M., and Hamilton, G. (2002). New prostheses for use in bypass grafts with special emphasis on polyurethanes. Cardiovascular Surgery *10*, 191-197.

168. To, W.S., and Midwood, K.S. (2011). Plasma and cellular fibronectin: distinct and independent functions during tissue repair. Fibrogenesis & Tissue Repair *4*, 21.

169. Todorovic, V., and Rifkin, D.B. (2012). LTBPs, more than just an escort service. Journal of Cellular Biochemistry *113*, 410-418.

170. Tomasek, J.J., Gabbiani, G., Hinz, B., Chaponnier, C., and Brown, R.A. (2002). Myofibroblasts and mechano-regulation of connective tissue remodelling. Nature Reviews Molecular Cell Biology *3*, 349-363.

171. Torpy, J.M., Burke, A.E., and Glass, R.M. (2009). Coronary heart disease risk factors. Jama *302*, 2388-2388.

172. Urbán, Z., and Boyd, C.D. (2000). Elastic-fiber pathologies: primary defects in assembly—and secondary disorders in transport and delivery. American Journal of Human Genetics *67*, 4-7.

173. Urban, Z., Hucthagowder, V., Schürmann, N., Todorovic, V., Zilberberg, L., Choi, J., Sens, C., Brown, C.W., Clark, R.D., and Holland, K.E. (2009). Mutations in LTBP4 cause a syndrome of impaired pulmonary, gastrointestinal, genitourinary, musculoskeletal, and dermal development. American Journal of Human Genetics *85*, 593-605.
174. Urry, D.W. (2004). The change in Gibbs free energy for hydrophobic association: Derivation and evaluation by means of inverse temperature transitions. Chemical Physics Letters *399*, 177-183.
175. van Putten, S., Shafieyan, Y., and Hinz, B. (2016). Mechanical control of cardiac myofibroblasts. Journal of Molecular and Cellular Cardiology *93*, 133-142.
176. Vos, T., Allen, C., Arora, M., Barber, R.M., Bhutta, Z.A., Brown, A., Carter, A., Casey, D.C., Charlson, F.J., and Chen, A.Z. (2016). Global, regional, and national incidence, prevalence, and years lived with disability for 310 diseases and injuries, 1990–2015: a systematic analysis for the Global Burden of Disease Study 2015. Lancet *388*, 1545-1602.
177. Vrhovski, B., Jensen, S., and Weiss, A.S. (1997). Coacervation characteristics of recombinant human tropoelastin. FEBS Journal *250*, 92-98.
178. Wachi, H., Nonaka, R., Sato, F., Shibata-Sato, K., Ishida, M., Iketani, S., Maeda, I., Okamoto, K., Urban, Z., and Onoue, S. (2008). Characterization of the molecular interaction between tropoelastin and DANCE/fibulin-5. Journal of Biochemistry *143*, 633-639.
179. Wang, B.., König, K., and Halbhuber, K. (2010). Two-photon microscopy of deep intravital tissues and its merits in clinical research. Journal of microscopy *238*, 1-20.
180. Wang, H., Naghavi, M., Allen, C., Barber, R., Carter, A., Casey, D., Charlson, F., Chen, A., Coates, M., and Coggeshall, M. (2016). Global, regional, and national life expectancy, all-cause mortality, and cause-specific mortality for 249 causes of death, 1980–2015: a systematic analysis for the Global Burden of Disease Study 2015. Lancet *388*, 1459-1544.
181. Weinberg, C.B., and Bell, E. (1986). A blood vessel model constructed from collagen and cultured vascular cells. Science *231*, 397-400.
182. Wilson, C.L., and Schwarzbauer, J.E. (1992). The alternatively spliced V region contributes to the differential incorporation of plasma and cellular fibronectins into fibrin clots. Journal of Cell Biology *119*, 923-933.

183. Wolfinbarger Jr, L., Lange, P., Linhurst, A., Moore, E., and Nolf, B. (2009) US20090041729A1 - Process for Decellularizing Soft-Tissue Engineered Medical Implants, and Decellularized Soft-Tissue Medical Implants Produced. (2009, February 12). Retrieved March 27, 2018, from https://patents.google.com/patent/US20090041729
184. Yanagisawa, H., and Davis, E.C. (2010). Unraveling the mechanism of elastic fiber assembly: the roles of short fibulins. International Journal of Biochemistry & Cell Biology *42*, 1084-1093.
185. Ye, Q., Zund, G., Jockenhoevel, S., Schoeberlein, A., Hoerstrup, S.P., Grunenfelder, J., Benedikt, P., and Turina, M. (2000). Scaffold precoating with human autologous extracellular matrix for improved cell attachment in cardiovascular tissue engineering. ASAIO Journal *46*, 730-733.
186. Yeo, G.C., Keeley, F.W., and Weiss, A.S. (2011). Coacervation of tropoelastin. Advances in Colloid and Interface Science *167*, 94-103.
187. Yousif, L. F., Di Russo, J., & Sorokin, L. (2013). Laminin isoforms in endothelial and perivascular basement membranes. Cell Adhesion & Migration *7*, 101-110.
188. Yow, K.H., Ingram, J., Korossis, S., Ingham, E., and Homer-Vanniasinkam, S. (2006). Tissue engineering of vascular conduits. British Journal of Surgery *93*, 652-661.
189. Zanetti, M., Braghetta, P., Sabatelli, P., Mura, I., Doliana, R., Colombatti, A., Volpin, D., Bonaldo, P., and Bressan, G.M. (2004). EMILIN-1 deficiency induces elastogenesis and vascular cell defects. Molecular and Cellular Biology *24*, 638-650.
190. Zerlauth, G., and Wolf, G. (1984). Plasma fibronectin as a marker for cancer and other diseases. American Journal of Medicine *77*, 685-689.
191. Zhang, H., Apfelroth, S.D., Hu, W., Davis, E.C., Sanguineti, C., Bonadio, J., Mecham, R.P., and Ramirez, F. (1994). Structure and expression of fibrillin-2, a novel microfibrillar component preferentially located in elastic matrices. Journal of Cell Biology *124*, 855-863.
192. Zhang, M.-C., Giro, M., Quaglino, D., and Davidson, J.M. (1995). Transforming growth factor-beta reverses a posttranscriptional defect in elastin synthesis in a cutis laxa skin fibroblast strain. Journal of Clinical Investigation *95*, 986-994.
193. Zhang, M., Pierce, R.A., Wachi, H., Mecham, R.P., and Parks, W.C. (1999). An open reading frame element mediates posttranscriptional regulation of tropoelastin and

responsiveness to transforming growth factor β1. Molecular and Cellular Biology *19*, 7314-7326.

194. Zhang, W.J., Liu, W., Cui, L., and Cao, Y. (2007). Tissue engineering of blood vessel. Journal of Cellular and Molecular Medicine *11*, 945-957.

8 APPENDIX – PRELIMINARY DATA

8.1 Abstract

Wound healing is a multi-step process involving the coordination of many cell types, including immune cells, epithelial cells, fibroblasts, and myofibroblasts. Fibronectin plays several important roles during the process of wound healing. During the earliest stage of hemostasis, plasma FN participates in thrombus formation. In the middle stages of wound healing, cellular FN is produced and secreted by both fibroblasts and myofibroblasts, allowing for these cells to anchor to the extracellular matrix and migrate into the wounded tissue. During the late stages of wound healing, cellular fibronectin plays an important role in scar contraction, providing myofibroblasts with the necessary anchors to exert force on the collagen-rich extracellular matrix within the scar. Despite the breadth of knowledge surrounding the role of FN in wound healing, further fundamental research is required to determine its role in wound healing in different contexts.

The objective of this project was to verify that FN could be deleted in mice expressing Cre recombinase-ERT2 under the α-smooth muscle actin promoter with the FN gene flanked by LoxP sites (FN(fl/fl); αSMA-CreERt2/+). The hypothesis is that FN can be deleted in cells expressing αSMA, such as activated fibroblasts and myofibroblasts. In order to test this hypothesis, mouse skin fibroblasts were isolated from mouse skin explants, treated with TGF-β1 to induce transdifferentiation to myofibroblasts and hence expression of αSMA, and treated with tamoxifen to cause deletion of the flanked FN gene. To verify deletion of the FN gene, immunofluorescence and deletion PCR experiments were employed.

Results showed that mouse skin fibroblasts can be transdifferentiated into myofibroblasts and FN can be deleted in these cells, indicating the potential use of this mouse line in wound healing experiments and the determination of the precise role FN plays in the process of wound healing in various contexts.

8.2 Résumé

La cicatrisation des plaies est un processus complexe qui se réalise en plusieurs étapes et nécessite la participation de différents types de cellules dont les cellules immunitaires, les cellules épithéliales, les fibroblastes, et les myofibroblastes. La fibronectine (FN), une protéine de la matrice extracellulaire, joue un rôle crucial en participant a différentes étapes de ce processus. En effet, durant la phase initiale d'hémostase, la FN plasmique participe à la formation du thrombus. Par la suite, durant les phases intermédiaires de guérison, la FN cellulaire secrétée par les fibroblastes et les myofibroblstes , permettent à ces dernières de s'adhérer à la matrice extracellulaire et de migrer dans les tissus endommagés. Enfin et durant la phase terminale , la fibronectine cellulaire joue un rôle important dans la contraction des plaies, tout en fournissant les sites d'ancrage des myofibroblastes afin d'exercer des forces contractiles sur la matrice extracellulaire riche en collagène. . Malgré les connaissances déjà acquises sur le rôle de la FN dans le processus de guérison des plaies, de la recherche fondamentale reste encore nécessaire pour déterminer le rôle de la FN dans divers contextes.

Notre hypothèse est que le gène codant la fibronectine FN peut être délété des cellules exprimant αSMA, comme les fibroblastes et myofibroblastes activés. Pour tester cette hypothèse, des fibroblastes cutanés de souris ont été isolés à partir d'explants de peau de souris, traités avec TGF-β1 pour induire leur transdifférenciation en myofibroblastes et par conséquent l'expression de αSMA. Ces explants sont également traités avec tamoxifen pour causer la délétion du gène FN ???. Des expériences d'immunofluorescence et de réaction de polymérisation en chaine PCR ont été réalisées afin de vérifier la délétion du gène de la FN.

Les résultats obtenus montrent que les fibroblastes cutanés de souris sont capables de se transdifférencier en myofibroblastes et que le gène de la FN peut être délété dans ces cellules. Ces résultats encourageant indiquent l'importance de ces lignées murines dans les expériences de réparation des plaies et élucide le rôle précis que joue la fibronectine dans différents contextes de cette réparation.

8.3 Dermal Wound Healing

8.3.1 Process

Wound healing is an important process which can be subdivided into four overlapping steps: rapid hemostasis, or fibrin clot formation; appropriate inflammation characterized by leukocyte and phagocyte infiltration; fibroblast proliferation and migration into the wound; and tissue remodelling by fibroblasts and myofibroblasts within the wound (Figure 19) (Mathieu et al., 2006). The first stage of wound healing takes place in mere seconds and is characterized by the formation of a fibrin clot which prevents further hemorrhaging and blocks infiltration of external debris and infectious agents. During this stage, platelets leave the bloodstream and bind each other via fibrinogen, the precursor to fibrin, and integrins. Upon cleavage by thrombin, fibrin is released and bound to plasma fibronectin by the clotting protein Factor XIII, creating a more stable clot. During this time, cells surrounding the wound secrete growth factors and pro-inflammatory cytokines such as transforming growth factor-β (TGF-β), fibroblast growth factor (FGF), platelet-derived growth factor (PDGF) (Gosain and DiPietro, 2004), interleukins 1β and 6 (IL-1β, IL-6), and tumor necrosis factor-α (TNFα) (Dinarello, 2000; Maynard, 2015).

Next, immune cells invade the wounded tissue in the following order: neutrophils, which clear debris and microbes, macrophages, which produce more cytokines and clear apoptotic cells, and lymphocytes. While the macrophages do their work, they produce and secrete factors which aid in the transition from the inflammatory stage to the proliferative stage by stimulating endothelial cells, keratinocytes, and fibroblasts to become regenerative and triggering the onset of the proliferative phase of wound healing (Maynard, 2015; Mosser and Edwards, 2008).

During the proliferative phase of wound healing, the constituent cells in the epithelium and dermis undergo focal adhesion-dependent migration similar to the immune cells from the inflammatory stage. Once in the wound, endothelial cells, keratinocytes, and fibroblasts begin to proliferate, resulting in capillary bed formation, reepithelialisation of the wound, and fibroblast repopulation of the wound. As they proliferate, some fibroblasts remain in the wound bed and begin to produce ECM proteins such as EDA fibronectin and collagen, while others migrate to the apical portion of

the wound, where the matrix is stiffer and unorganized. Triggered by the presence of TGF-β and EDA fibronectin and sensing of the stiffness of the ECM through FAs, these fibroblasts begin to undergo the phenotypic changes necessary to become myofibroblasts (Guo and DiPietro, 2010; Hinz and Gabbiani, 2003; Maynard, 2015).

The final stage of wound healing is the remodelling stage, which can take up to several years. At this stage, the fibroblasts and myofibroblasts within the wound are anchored to the ECM and are actively modifying it to develop an architecture similar to the native, unwounded tissue. During this phase of wound healing, myofibroblasts contract the surrounding matrix to completely close the wound and compact the newly formed scar tissue. Once their task is completed, the myofibroblasts are cleared from the healed wound by apoptosis (Desmouliere et al., 1995; Guo and DiPietro, 2010; Maynard, 2015).

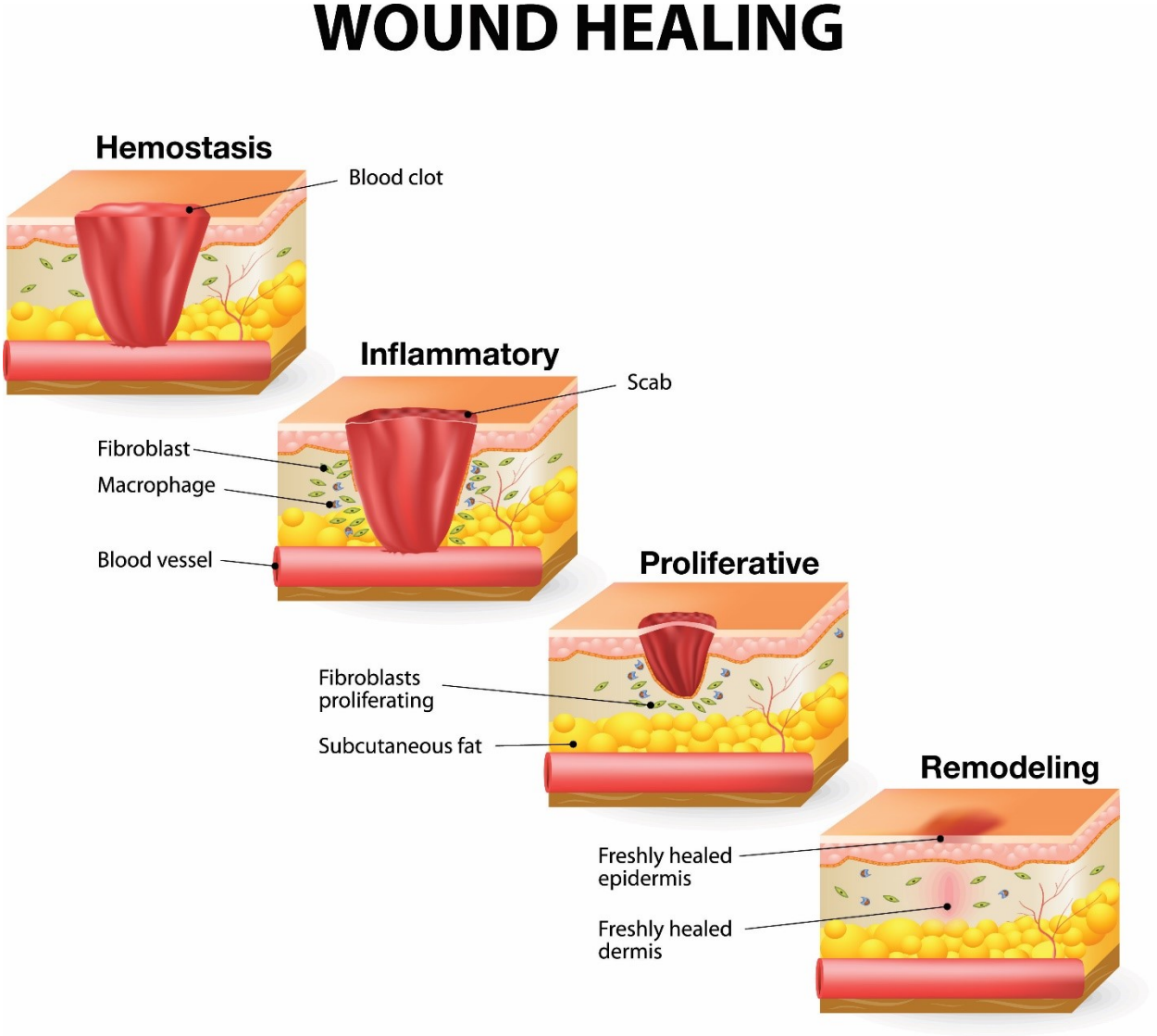

Figure 19. Schematic of the process of dermal wound healing.

Dermal wound healing is a complex, multi-stage process comprising four main phases: hemostasis, inflammation, proliferation, and remodeling. During the hemostasis stage, thrombus formation prevents blood loss and infection by plugging the injured tissue. During the inflammatory stage, immune cells infiltrate the wound, clear debris, and secrete cytokines. During the proliferative stage, fibroblasts, endothelial cells, and keratinocytes proliferate and infiltrate the wound; fibroblasts and endothelial cells form highly vascularized granulation tissue, while keratinocytes seal the wound in a process called reepithelialisation. The final stage is remodeling, where fibroblasts continuously degrade and reform the ECM to return the wound to a near-physiological state. Figure adapted from Maynard, 2015.

8.3.2 Role of Fibronectin in Wound Healing

Fibronectin plays several important roles throughout the wound healing process, with plasma fibronectin working primarily in the early stages of wound healing and cellular fibronectin isoforms working in the later stages of wound healing. During the initial thrombogenic stage of wound healing, circulating plasma fibronectin is incorporated into the fibrin clot via noncovalent interactions with fibrin and via covalent crosslinking to fibrin by activated transglutaminase (Pankov and Yamada, 2002; Wilson and Schwarzbauer, 1992). Within this provisional matrix, the interactions of fibrin and fibronectin allow fibronectin to develop an extended conformation, revealing cryptic cell binding domains required for fibroblast activation by platelet derived growth factor (Clark et al., 2003). Furthermore, incorporation of fibronectin within the provisional matrix is important for platelet aggregation, migration, and adhesion (Wilson and Schwarzbauer, 1992).

Cellular fibronectin has several important roles during the later stages of wound healing. During the proliferative stage of wound healing, cellular fibronectin is produced and secreted by fibroblasts and endothelial cells, which incorporate it into the granulation tissue of the wound (Repesh et al., 1982). Cellular fibronectin is incorporated into a thick fibrous network around fibroblasts within the wound bed, which then bind the fibronectin matrix and align themselves parallel to the epidermis, revealing cellular fibronectin's important roles in cell adhesion and maintenance of tissue architecture (Repesh et al., 1982; Sottile and Mosher, 1997). Cellular fibronectin acts as an important cue for angiogenesis within the granulation tissue, and expression isoforms containing both of the alternatively spliced EDA and EDB domains is greatly upregulated in cells within sprouting capillaries and developed capillaries within the granulation tissue (Fernandez-Sauze et al., 2009). Cellular fibronectin also retains the roles it has in normal ECM, being responsible for the regulation of ECM formation and composition (e.g. collagen I and III fibrillogenesis, deposition and assembly of fibrillin microfibrils, elastogenesis, etc.), cell migration, adhesion, spreading, proliferation, and apoptosis, and the availability of such growth factors as bone morphogenic protein, TGF-β1, and vascular endothelial growth factor (Clark et al., 1982; George et al., 1993; Lee et al., 2017; Liao et al., 2002; Plow et al., 2000; Sabatier et al., 2009).

Additionally, EDA fibronectin, along with TGF- β1, is required for fibroblast transdifferentiation into myofibroblasts within healing wounds (Serini et al., 1998; Tomasek et al., 2002). Myofibroblasts are fibroblasts bearing a contractile phenotype similar to smooth muscle cells. They can be differentiated from typical fibroblasts by the expression of certain marker proteins, including α-smooth muscle actin and smooth muscle protein 22α (Tomasek et al., 2002). EDA fibronectin within the matrix can be bound by actin-linked super-mature FAs on the cell surface of myofibroblasts, which myofibroblasts utilize to test the mechanical tension of the surrounding ECM. Myofibroblasts may also use matrix-bound EDA fibronectin to contract the wound, a major step in the process of wound healing (Hinz and Gabbiani, 2003; Tomasek et al., 2002).

In vivo experiments have supported the separate roles that plasma and cellular fibronectin play in wound healing. For instance, plasma fibronectin plays an essential role in the protection of neuronal and non-neuronal cells after traumatic brain injury and transient local brain tissue ischemia (Sakai et al., 2001; Tate et al., 2007). Furthermore, mice expressing EDA-null cellular fibronectin showed delayed wound reepithelialisation, reduced cell compactness, and ulcerative processes at newly formed epidermis (Muro et al., 2003). Despite their distinct roles during non-overlapping stages of wound healing, plasma and cellular fibronectin have been shown to be capable of carrying out some of each other's roles. In support of this, further studies showed that conditional knockout of plasma fibronectin in mice had no effect on the processes of hemostasis and wound healing (Sakai et al., 2001). Important experiments even demonstrated that plasma fibronectin, independent of the species of origin, can be incorporated into assembling and established cellular fibronectin matrices (Hayman and Ruoslahti, 1979).

8.4 *Cre* Recombinase *LoxP* System

The *Cre* recombinase *LoxP* system is a site specific DNA recombination technique which was developed in the late 1980s and early 1990s (Orban et al., 1992; Sauer and Henderson, 1988). The *Cre-LoxP* system is one of the most widely utilized techniques for studying the effect of genotype on phenotype in transgenic animal models. The system consists of the DNA recombinase enzyme

Cre, which is expressed under a cell type specific promoter sequence chosen by the researcher, and 34bp *LoxP* sequences which flank the gene of interest (Figure 26). Only when both the *Cre* recombinase and *LoxP* sites exist within the same cell can DNA recombination occur, making the technique useful for observing the effect of gene deletion within specific tissues and preventing issues related to systemic deletion of a gene, including embryonic lethality. Furthermore, the system can be made to be inducible by fusing the *Cre* recombinase with a targetable receptor, allowing for both tissue-specific and temporal control of gene deletion (Feil et al., 2009).

When the recombinase enzyme is expressed within a cell whose genome contains *LoxP* sequences flanking a gene of interest, the recombinase can cause a DNA recombination event between *LoxP* sites on the same and on separate chromosomes. First, two *Cre* recombinase proteins bind to the first and last 13bp sequences on the *LoxP* sites. Once the recombinase proteins have bound to the *LoxP* sites, they bind each other and form a tetrameric structure. Next, the doubles stranded DNA is cleaved by *Cre* and subsequently ligated by DNA ligase. Since *LoxP* sites are directional, the result of DNA recombination is dependent upon their orientation within the DNA: If the sites are in the same direction, the DNA between the sites is excised; if the sites are in opposite directions, the DNA between the sites is inverted (Orban et al., 1992).

In the inducible *Cre-LoxP* system, the recombinase enzyme will only be expressed in cells bearing the gene after treatment of the cells with a specific compound. The most common inducible *Cre-LoxP* system utilizes a specifically engineered copy of the estrogen receptor fused to the *Cre* protein. This modified estrogen receptor is specific for the breast cancer drug tamoxifen, and its fusion to *Cre* causes the recombinase to be shuttled to and sequestered in the cytoplasm, preventing it from binding to the *LoxP* sites within the genome. Upon binding of tamoxifen to the modified estrogen receptor, the *CreER* complex translocates to the nucleus and cleaves DNA at the *LoxP* sites (Feil et al., 1997; Feil et al., 2009).

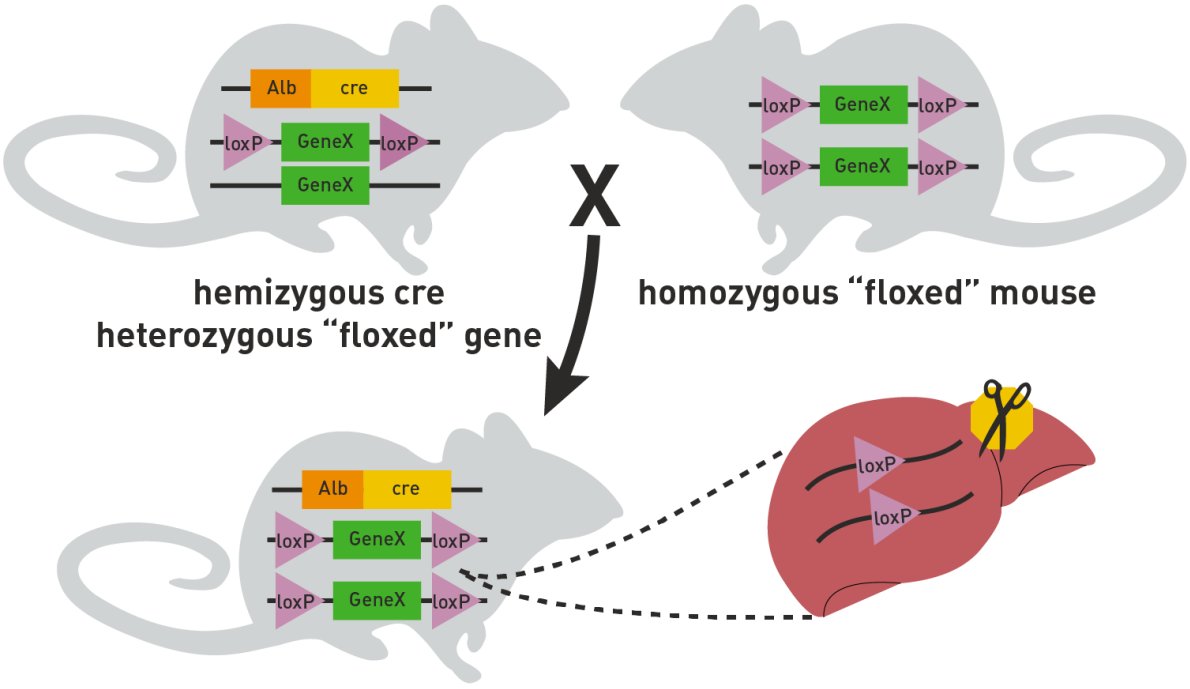

Figure 20. *Cre-LoxP* Tissue-specific gene knockout.

The above figure represents an example of tissue-specific gene knockout in transgenic mice expressing *Cre* recombinase under the liver-specific promoter for albumin. In this example, the crossing of a hemizygous *Cre* mouse heterozygous for the "floxed" (flanked by *LoxP*) gene of interest with a homozygous floxed mouse results in 50% progeny hemizygous for *Cre* and homozygous for the floxed gene of interest. If the system is non-inducible, all cell types expressing albumin will also express *Cre*, resulting in excision of the floxed gene. If the system is inducible, the floxed gene will be excised in all cell types expressing albumin only after the proper inducing agent has been administered to the model organism (K, 2011).

8.5 Objectives

Wound healing is a critical process the body employs to repair damaged tissues, and errors in wound healing regulation can result in complications such as hypertrophic scarring and keloid formation. There are many cell types and proteins which are critical to proper wound healing, including cellular fibronectin. Although the role of cellular fibronectin in wound healing is partially understood, there remains more to be discovered. Using a Cre-LoxP transgenic mouse model with a floxed cellular fibronectin gene and Cre recombinase expression under the α-smooth muscle actin promoter, this study seeks to elucidate the exact role cellular fibronectin plays in wound healing by deleting it in mouse skin fibroblasts and myofibroblasts.

The specific objectives of this study are:

1. To establish whether mouse skin fibroblasts express myofibroblast markers upon treatment with transforming growth factor β1.
2. To determine whether cellular fibronectin can be deleted in mouse skin fibroblasts obtained from P3-P8 αSMA-CreERt2/+ mouse pups.

8.6 RESULTS

8.6.1 Cultured Mouse Skin Fibroblast express myofibroblast markers

To determine whether cellular FN could be deleted in mouse skin fibroblasts obtained from P3-P8 αSMA-Cre^{ERt2}/+ mouse pups, we attempted to induce their transdifferentiation into myofibroblasts. To do this, the cells were incubated in plastic cell culture flasks for 3 days with 5ng/mL of TGF-β1 or nothing. After the incubation was completed, the cells were seeded on glass 8-well chamber slides (75,000 cells per well) and left to expand for 2 days. After the 2 day incubation period, the cells were fixed with 70:30 methanol:acetone solution and prepared for immunofluorescence analysis. The cells were stained with antibodies against two myofibroblast markers, αSMA and SM22α. Results showed that mouse skin fibroblasts used in the experiment clearly express both markers extensively, indicating a myofibroblastic phenotype and that it is possible to induce deletion of cellular FN from mouse skin fibroblasts in αSMA-CreERt2/+ mice (Figure 21).

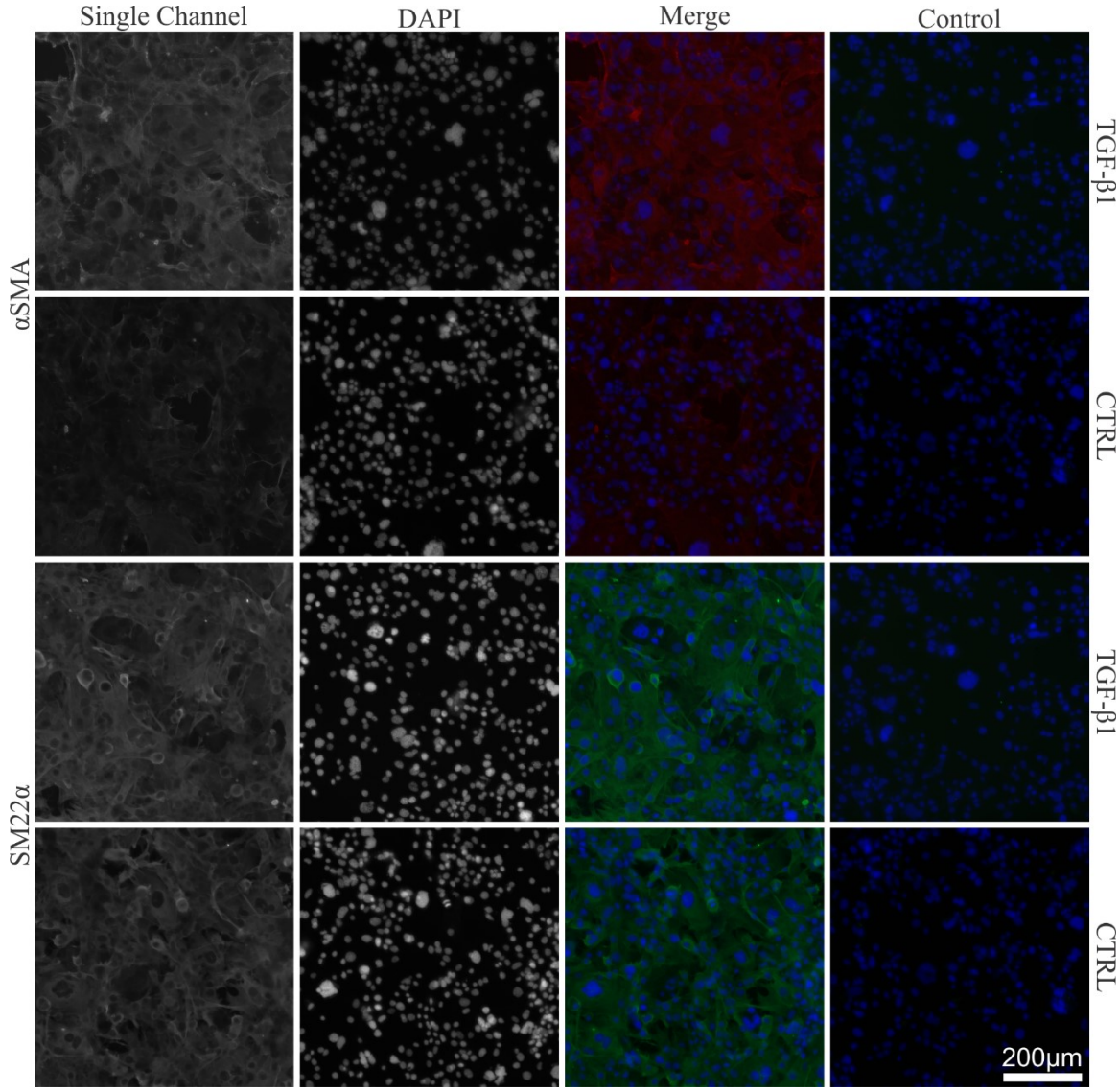

Figure 21. Immunofluorescence analysis of myofibroblast marker expression in Mouse Skin Fibroblasts treated with TGF- β1**.** Mouse Skin Fibroblasts cultured on plastic were treated with or without (CTRL) 5ng/mL of TGF-β1 for 3 days (TGF-β1). Cells were seeded in 8-well chamber slides (75,000 per well) and grown for 2 days. Immunofluorescence staining was accomplished using antibodies against the myofibroblast markers αSMA (red channel) and SM22α (green channel). Nuclear staining was accomplished using DAPI. The control column represents secondary antibody control. Image magnification is 200x and the scale bar represents 200μm for all images.

8.6.2 Cellular FN can be deleted from cultured Mouse Skin Fibroblasts originating from P3-P8 $FN^{(fl/fl)}$; αSMA-Cre^{ERt2}/+ mouse pups

Next, we attempted to induce deletion of cellular FN in αSMA-Cre^{ERt2}/+ mouse skin fibroblasts by incubating them for 3 days with either 5ng/mL of ethanol or with 5ng/mL of tamoxifen, a drug which binds a modified estrogen receptor fused to *Cre* recombinase, causing translocation of the complex from the cytosol to the nucleus where *Cre* can work. After incubation, the cells were seeded in glass 8-well chamber slides (75,000 cell per well) and incubated for 2 days in FN-depleted serum-containing medium. After incubation, the cells were fixed using 70:30 methanol:acetone solution, prepared for immunofluorescence, and stained for total FN and cellular FN. Results showed clear deletion of cellular FN, indicating that αSMA-Cre^{ERt2}/+ mice can have cellular FN deleted in myofibroblasts. The results also showed that cellular FN was deleted in cells treated with ethanol, which should not happen (Figure 22).

To be sure that cellular FN was deleted in these cell, deletion PCR was employed. Genomic DNA was isolated from cells used in both experiments above (5×10^6 cells per condition), resulting in 4 conditions: untreated MSFs, TGF-β1 treated MSFs, TGF-β1 + ethanol treated MSFs, and TGF-β1 + tamoxifen treated MSFs. Next, the DNA was used in a PCR reaction and subsequently loaded onto a 1.7% agarose gel. The expected band size for the deleted cellular FN gene was 380bp while the expected band size for the intact gene was 1200bp. Results showed that cellular FN was deleted in all MSFs, corroborating the immunofluorescence analysis in figure 10, while the control 3T3 cells showed an intact cellular FN gene, indicating that the primers and PCR reaction worked (Figure 23). Importantly, the results indicated that cellular FN was deleted in αSMA-Cre^{ERt2}/+ MSFs and that these mice could be used in cellular FN knockout wound healing experiments, though further work must be done to determine why all cells showed deletion.

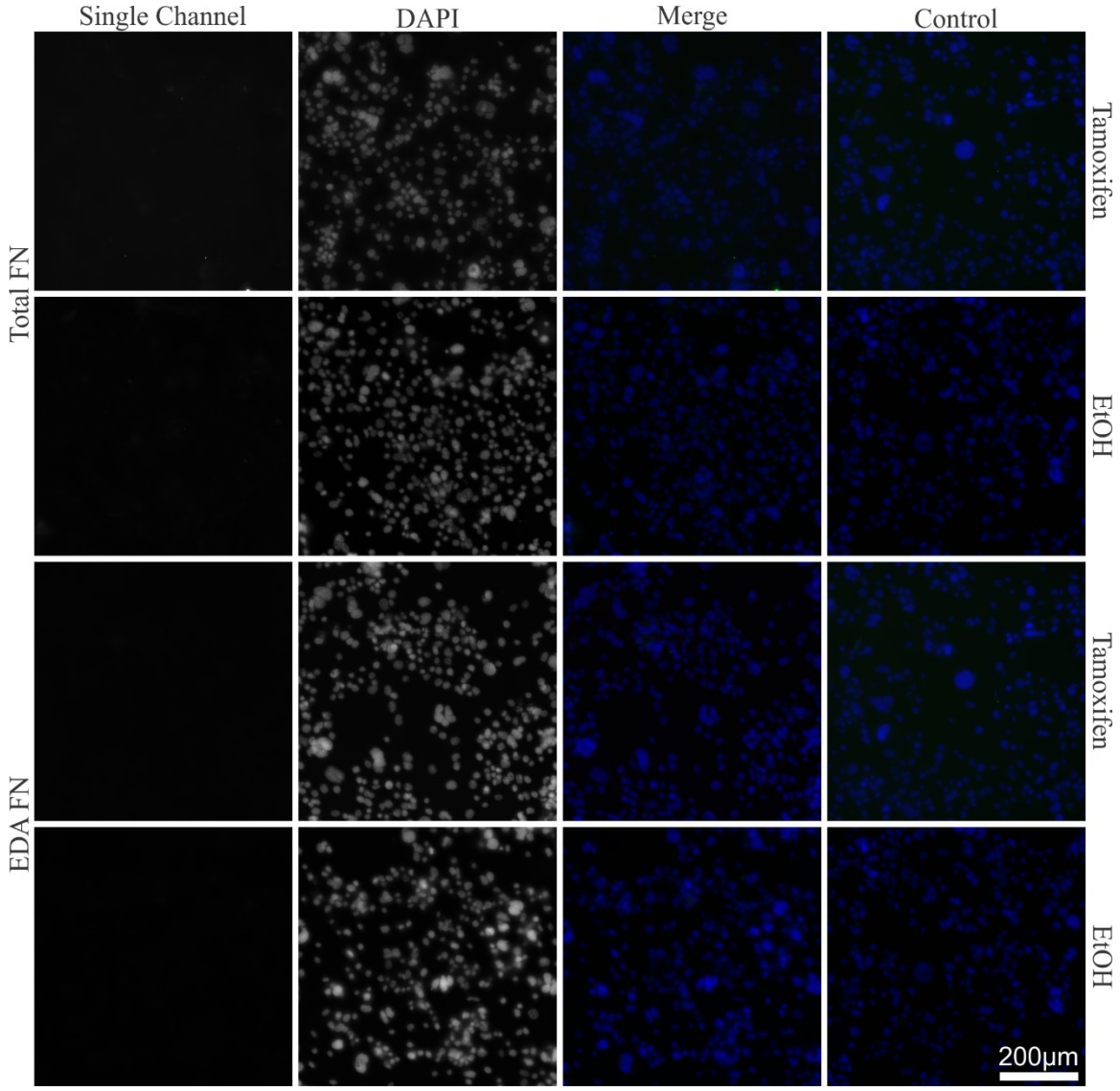

Figure 22. Immunofluorescence analysis of myofibroblast marker expression in Mouse Skin Fibroblasts. Mouse Skin Fibroblasts cultured on plastic and treated with or without 5ng/mL of TGF-β1 for 3 days followed by 5ng/mL of Tamoxifen or ethanol for 3 days. Cells were seeded in 8-well chamber slides (75,000 per well) and grown for 2 days. Immunofluorescence staining was accomplished using antibodies against total FN (green channel) and EDA FN (red channel). Nuclear staining was accomplished using DAPI. The control column represents secondary antibody control. Image magnification is 200x and the scale bar represents 200µm for all images.

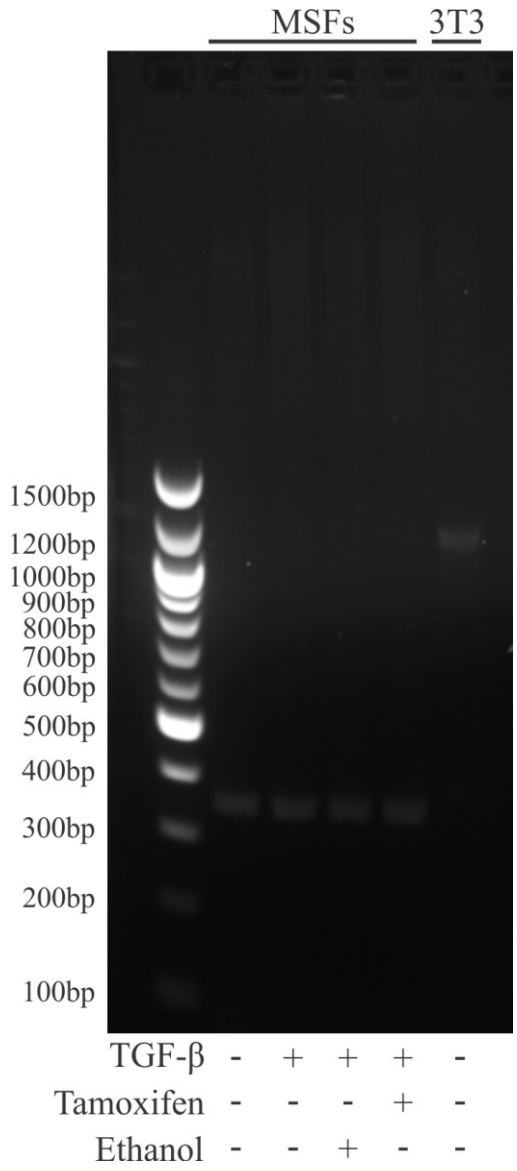

Figure 23. PCR analysis of cellular FN deletion in mouse skin fibroblasts. Mouse Skin Fibroblasts cultured in plastic culture flasks were treated with or without 5ng/mL of TGF-β1 for 3 days. Cells treated with TGF-β1 were subsequently incubated with 5ng/mL of Tamoxifen or ethanol for 3 days. Genomic DNA was isolated from 5×10^6 MSFs per condition and from an equal number of 3T3 cells. A 1.7% agarose gel and 100 base pair DNA ladder were used to visualize results. Expected band sizes: 380bp (cellular FN gene deleted) and 1200bp (intact cellular FN gene).

8.7 Rationale, Discussion, and Conclusions

8.7.1 Rationale

Up to now, experiments attempting to elucidate the role of fibronectin isoforms on wound healing have focused on the individual isoforms, cellular and plasma fibronectin, and have yielded important results. However, several attempts have shown some compensatory mechanism for fibronectin, indicating overlapping functions and obscuring some functions that fibronectin may have in the process of wound healing; however, no experiments have been conducted in the context of a fibronectin double knockout (Sakai et al., 2001; Tan et al., 2004). Considering this and the fact that our lab possesses a tamoxifen-inducible plasma and cellular fibronectin double knockout mouse strain, we sought to determine whether it would be possible to use these mice for wound healing experiments despite the facts that the *Cre* recombinase is under control of the αSMA promoter, a protein expressed in myofibroblasts and smooth muscle cells. To make this determination, we employed cell culture immunofluorescence experiments and deletion PCR experiments.

8.7.2 Discussion

Mouse skin fibroblast phenotype in cell culture

Mouse skin fibroblasts obtained from mouse skin explants expressed the myofibroblast markers αSMA and SM22α, indicating a myofibroblast phenotype. Previous studies have shown that cells change their phenotype based on the substrate they are grown on (van Putten et al., 2016).These cells were cultured on plastic, a much harder substrate than the connective tissues of the body, which likely caused this phenotypic change. Furthermore, our results showed an increase in the number of cells expressing the aforementioned myofibroblast markers upon incubation of the cells with the growth factor TGF-β1 (data not shown). This result also agrees with the literature (Hinz, 2009). Taken together, these data indicate that deletion of cellular fibronectin within these cells is more than possible, especially considering the tissue microenvironment within wounds, which contains active TGF-β1 as well as myofibroblasts.

Cellular fibronectin deletion in mouse skin fibroblasts

Previous studies conducted to elucidate the role of fibronectin and its splice variants in wound healing have used knockout mouse models (Muro et al., 2003; Sakai et al., 2001). Our results showed no production of cellular fibronectin in tamoxifen-treated cells in cell culture, however there was also deletion in ethanol-treated cells. Considering that ethanol acts as a control for tamoxifen, this result indicates some issue with cellular fibronectin deletion in these cells or with the experiment itself. To determine the origin of the issue, we conducted deletion PCR, and results indicated that fibronectin had indeed been deleted. Yet again, however, results showed deletion in our controls (cells treated with nothing, TGF-β1 only, or TGF-β1 + ethanol), indicating an issue. One possibility is spontaneous activity of the *CreERT2* recombinase, as outlined in a 2017 study investigating the phenomenon (Kristianto et al., 2017). Although further experiments are required to determine the cause of these odd results, our results showed clear deletion of cellular fibronectin in cells obtained from αSMA-Cre^{ERt2}/+ mouse skin, paving the way for future *in vivo* experiments attempting to knockout both plasma and cellular fibronectin and investigate the effects on wound healing.

8.7.2 Conclusions

This study aimed to determine whether cellular fibronectin could be effectively deleted in transgenic mice using the *Cre-LoxP* technique with the *Cre* recombinase under control of the promoter for the α-smooth muscle actin gene. Our results showed that mouse skin fibroblasts obtained from transgenic mouse pups express α-smooth muscle actin, indicating that they have a myofibroblast phenotype. Results from deletion experiments revealed that cellular fibronectin was deleted at both the protein and genomic level, indicating that the transgenic mouse line could be effectively used for future study of the effect of fibronectin deletion on wound healing.